VŠB – TECHNICAL UNIVERSITY OF OSTRAVA

FACULTY OF METALLURGY AND MATERIALS ENGINEERING

Department of Metallurgy and Foundry

Doctoral thesis

STUDY OF GRAIN REFINEMENT OF HYPEREUTECTIC ALUMINUM SILICON ALLOYS

Study program: **Metallurgical Technology.**

Supervisor: **Prof. Ing. Tomáš Elbel, CSc.**

PhD student: **M.Sc. Nguyen Hong Hai.**

Ostrava 2012

Acknowledgements

Foremost, I would like to express my sincere gratitude to my supervisor Prof. Ing. Tomáš Elbel, CSc for the support of my Ph.D study and research, for his patience, motivation, enthusiasm, and immense knowledge. His guidance helped me in all the time of research and writing of this thesis. I could not have imagined having a better supervisor and mentor for my Ph.D study.

Besides my supervisor, I would like to thank to Prof. Nguyen Van Thai, Dr. Sc. and Assoc. Prof. Nguyen Huu Dung, Dr., their useful advices and comments helped me to orient the ideas in this thesis.

My sincere thanks also goes to Doc. Ing. Rudolf Kořený, CSc., who helped me so much when I began studying in Czech Republic.

Finally, I wish to thank my colleagues in departerment, my parents, and my family for providing a loving environment for me.

Preface

Hypereutectic aluminum silicon alloys is aluminum silicon alloys with silicon content is more than 12.5 wt%. In industry, aluminum silicon alloys was used with silicon content from 17 wt%. to 25 wt%. During crystallization process, the first phase which was crystalized from liquid alloy is primary silicon particles. Microstructure of hyper-eutectic aluminum silicon alloys is coarse-grained primary silicon particles on the eutectic matrix. The grain size of primary silicon could be reached 100 – 250 μm. Therefore, they could have a significant effect on mold filling, toughness and mechanical properties of casting. After liquid temperature reaches solid-line, primary silicon crystallization finishes. Then, eutectic (α + Si) could be formed. Microstructure of eutectic phase is brittle silicon particles on α-Al matrix. Refinement of hyper-eutectic aluminum silicon alloys is widely used to obtain increasing mechanical properties, especially fracture toughness.

To refine primary silicon, phosphorus addition has been adopted as the most popular method which utilizes heterogeneous nucleation as a way to increase the number of primary silicon particles and, thus, reduces its average size. Phosphorus was used in the kind of Al-CuP master alloy or CuP master alloys. The refinement mechanism is well accepted that dissolved phosphorus combines with aluminum and forms aluminum phosphide (AlP) crystals. Aluminum phosphide crystals in the melt increase the amount of nucleation sites for silicon which solidifies later. The previous studies show that, refinement effects depend on phosphorus solubility and retained phosphorus. The particle size of primary silicon also depends on refinement temperature and refinement time.

Sodium and sodium compound are used to refine the brittle silicon particles which were formed in eutectic phase. It acts as an adsorption on the surface of silicon particles. Morphology and size of the silicon in eutectic phase were also affected.

Using both of phosphorus and sodium compound could be established. They maybe have a reciprocal influence, for example sodium not only adsorbs on surface of silicon particles in eutectic phase but also adsorbs on surface of nucleation sites (AlP). Follow thermodynamic of crystallization process, crystallization process of silicon in eutectic phase only begins after crystallization process of primary silicon already finishes. Thus, the time for refiner addition into the melt is very important.

The present study is to provide a description of hyper-eutectic aluminum silicon alloys refinement, enabling a better understanding relation between phosphorus solubility and refinement mechanism.

Keywords: Hypereutectic, aluminum silicon alloys, grain refinement; refinement mechanism, primary silicon.

List of figures

List of tables

Contents

1. Introduction to aluminum silicon alloys

1.1 Introduction

Aluminum casting alloys are generally of interest because of their high specific strengths compared to other casting alloys such as cast irons or steels. Furthermore, aluminum casting alloys have good castability, good fluidity, and comparably low melting points. Of the various elements commonly alloyed with aluminum for casting purpose, silicon is among the most popular, and aluminum silicon alloys constitute approximately 80 % of the aluminum casting alloys.

1.1.1 Phase diagram and structure of aluminum silicon alloys

Hypereutectic Al-Si alloys are widely used in the automobile and aerospace industries because they exhibit several specific and interesting properties, such as excellent wear resistance, high strength-to-weight ratio, and low coefficient of thermal expansion, good corrosion resistance, excellent fluidity, and good castability. They are used in various applications such as liner-less engine block, automotive pistons, compressor bodies, and pumps. Hypereutectic Al-Si alloys are used to produce engine block without cylinder liners, automotive pistons because of their high wear resistance resulting from a large volume fraction of the silicon phase. [1,3]

Aluminum silicon alloys can be divided into two types. These are simply and complex Al-Si alloys. The composition of simply Al-Si alloys consist only Al and Si. And complex Al-Si alloys are the simply that be added by other alloying elements. In industry, aluminum silicon alloys are used with 5-20 wt% silicon content. The eutectic and hypoeutectic aluminum silicon alloys are widely used. Because these alloys are good castability and corrosion resistance, but mechanical properties are not high. Some properties of aluminum and silicon crystal are showed in table 1.1.

The simplest model of microstructure of aluminum silicon alloys can be presented in figure 1.1. The maximum solubility of silicon in aluminum is 1.65 wt% at 577 ^{0}C. Amount of dissolved silicon decreases with temperature (0.8 wt% silicon at 500 ^{0}C, and 0.3 wt% silicon at 400 ^{0}C). But this value is negligible at room temperature. Aluminum and silicon form a simple binary system with a eutectic at 12.6 wt.% silicon and a temperature of 577 ^{0}C. According to the diagram, the structures of aluminum silicon alloys are as follow:

- α : Aluminum solid solution.

- Eutectic (α + Si): A soft continuous matrix (α – aluminum solid solution) containing hard precipitates of silicon of different morphology.
- α + (α +Si): Hypoeutectic structure.
- Si_I + (α + Si): Hypereutectic structure. Where, primary silicon crystal (Si_I) is the first phase which is formed from liquid during solidification process.

Eutectic aluminum silicon alloys has higher strengthen than α – aluminum solid solution, but less flexibility. Their structure consist plate-like silicon particles. These particles are distributed on the soft matrix that like stress cracks, resulting in poor mechanical properties. It can be solved by using modification methods. Then, plate-like silicon particles are refined.

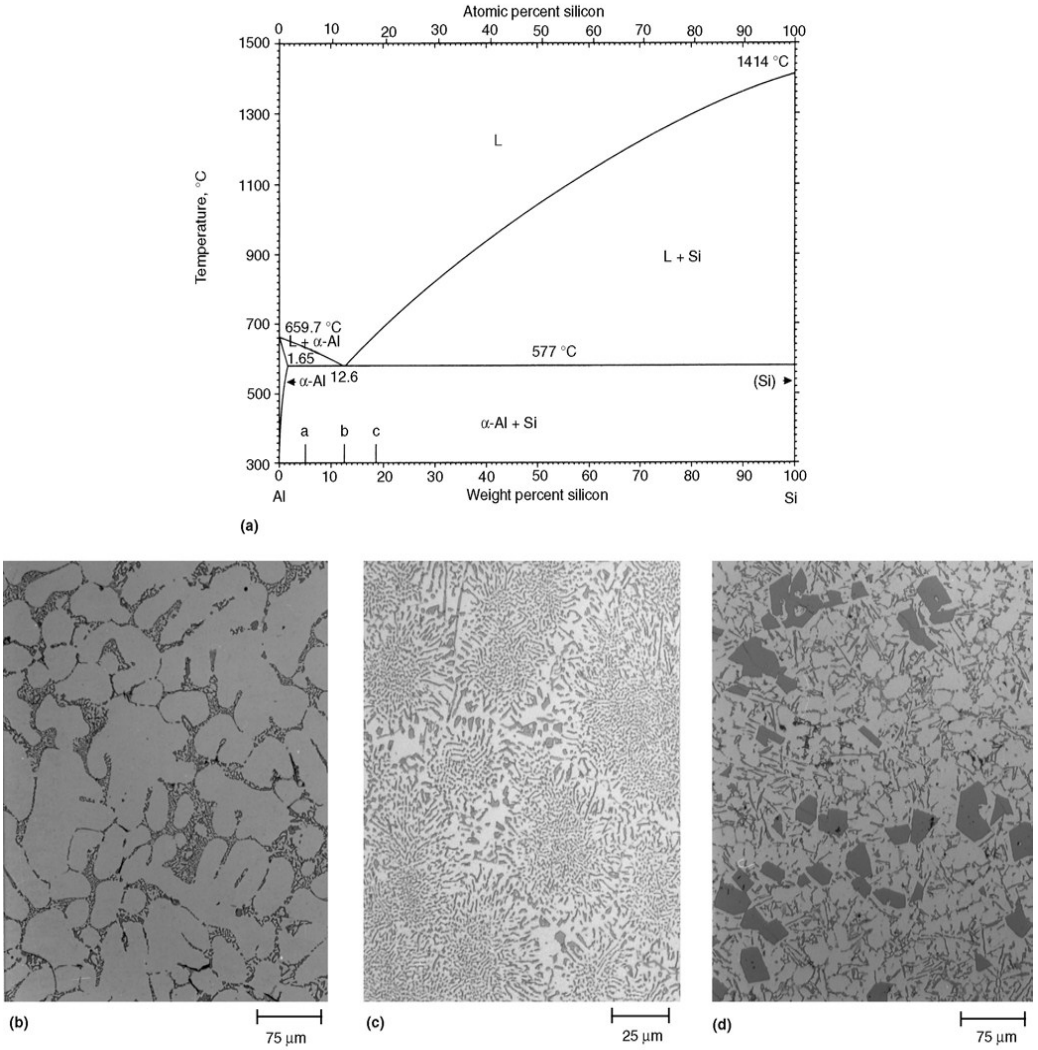

Figure 1.1 Cast aluminum silicon alloys. (a) Al-Si equilibrium diagram. (b) Microstructure of hypoeutectic alloy (1.65 – 12.6 wt% Si). 150x. (c) Microstructure of eutectic alloy (12.6 wt% Si). 400x. (d) Microstructure of hypereutectic alloy (> 12.6 wt% Si). 150x. [4]

Table 1.1 Properties of aluminum and silicon crystals [4].

Element	Lattice type	Specific weight,g/cm^3	Melting temperature,^{0}C	Elastic modulus, GPa	Thermal expansion,$10^{-6}K^{-1}$	Thermal coefficient, W/cmK
Al	A1	2.693	660	72	23.5	2.38 (0^0C)
Si	A4	2.3263	1430	162.9	2.92	0.8 (30^0C)

Due to the high silicon content of hypereutectic aluminum silicon alloys, their properties are improved, such as good wear resistance, low thermal expansion coefficient, good castability. However, all of the aforementioned desirable properties of hypereutectic aluminum silicon alloys depend on the characteristics of their cast microstructure, and the size, morphology (or shape), and distribution of eutectic and primary silicon particles. The morphology of primary silicon particles can be rather complex, such as plate-like, star-shape, polygonal, blocky, and feathery varying with solidification conditions, chemical composition, and alloying elements.

In these forms, primary silicon particles compromise the machinability, wear resistance, and mechanical properties of the alloy castings. Grain refinement and control of the eutectic and primary silicon particles is an effective way of improving the properties of the hypereutectic aluminum silicon alloys. For examples, hypereutectic aluminum silicon alloys with a uniform distribution of fine primary silicon particles have higher strength and better wear resistance.

Table 1.2 Composition of hypereutectic aluminum silicon alloys (American Standard)

	Composition, %						
	Si	**Fe**	**Cu**	**Mg**	**Mn**	**Ti**	**V**
A 390-1	16-18	0.6-1.0	4.0-5.0	0.5-0.65			
A 390-2	16-18	< 1.0	4.0-5.0				
B 390-1	16-18	< 1.1	4.0-5.0	0.5-0.65	< 0.5		
B 393-1	18-20	< 0.18	0.4-0.8	0.9-1.2	0.2-0.6		
B 393-2	21-23	< 0.4	0.7-1.1	0.8-1.3	< 0.1	0.1-0.2	0.08-0.15

Table 1.3 Composition of aluminum silicon alloys (German Standard)

Composition, %										
	Si	**Cu**	**Mg**	**Zn**	**Sn**	**Fe**	**Mn**	**Ni**	**Ti**	**Pb**
AlSi	4,5-6	0,1	0,1	0,1	0,05	0,6	0,5	0,1	0,2	0,1
AlSi	12-13.5	0,1	0,1	0,1	-	0,7	0,4	-	0,15	
AlSiMg	5.0-6.0	0,05	0,4-0,8	0,1	0,05	0,5	0,4	-	0,2	0,05
AlSiMg	6,5-7	0,1	0,2-0,4	0,1	0,05	0,5	0,5	0,5	0,1-0,2	0,03
AlSiMgFe	9,0-11	0,1	0,2-0,5	0,1	0,05	1	0,4	0,05	0,15	0,05
AlSiCu	4,5-5,5	1-1,5	0,4-0,6	0,1	0,05	0,6	0,5	0,25	0,2	0,1
AlSiCuZn	5-7,5	3.0-5.0	0,1-0,3	2	0,1	1	0,3-0,6	0,3	0,15	0,3
AlSiCuNiMg	9,5-10,5	2-2,5	1,2-1,5	0,1	-	0,8	0,1	0,8-1,2	0,1	
AlSiCuMgNiCrCo	17-20	1,3-1,8	0,8-1,5	0,2	0,1	0,7	0,6	0,8-1,5	0,2	0,1

1.1.2 Influence of alloying elements and impurities to structure and properties of hypereutectic aluminum silicon alloys [36].

The important alloying elements and impurities are listed here as a concise review of major effects. Some of the effects, particularly with respect to impurities, are not well documented and are specific to particular alloys or conditions.

Silicon is the basic alloying element of hypereutectic aluminum silicon alloys. It makes alloys have good fluidity, good castability and good forge ability. Low thermal expansion coefficient of hypereutectic aluminum silicon alloys is suitable for industry production of piston. The maximum amount of silicon content in hypereutectic aluminum silicon alloys are between 22-24 wt%. However, it can be approximately 40-50 wt% if using powder metallurgy method. In addition, the high hardness of silicon particles makes these alloys have good wear resistance.

Alkali elements or titanium, zirconium, boron are used in aluminum silicon alloys as a grain refine and improve conductivity. Boron can be used alone (at levels of 0.005 to 0.1%) as a grain refiner during solidification, but becomes more effective when used with an excess of titanium. Commercial grain refiners commonly contain titanium and boron in a 5-to-l ratio. Sodium and strontium can make silicon crystals refiner and well distribute.

Calcium has very low solubility in aluminum and forms the intermetallic $CaAl_4$. An interesting group of alloys containing about 5% Ca and 5% Zn have superplastic properties. Calcium combines with silicon to form CaSi2, which is almost insoluble in aluminum and therefore will increase the conductivity of commercial-grade metal slightly. In aluminum-magnesium-silicon alloys, calcium will decrease age hardening. Its effect on aluminum-silicon alloys is to increase strength and decrease elongation, but it does not make these alloys heat treatable.

Iron is the most common impurity found in aluminum. It has a high solubility in molten aluminum and is therefore easily dissolved at all molten stages of production. The solubility of iron in the solid state is very low (~0.04%) and therefore, most of the iron present in aluminum over this amount appears as an intermetallic second phase in combination with aluminum and often other elements.

Cobalt is not a common addition to aluminum alloys. It has been added to some aluminum-silicon alloys containing iron, where it transforms the acicular ß (aluminum-iron-silicon) into a more rounded aluminum-cobalt-iron phase, thus improving strength and elongation. Aluminum-zinc-magnesium-copper alloys containing 0.2 to 1.9% Co are produced by powder metallurgy.

Copper. Aluminum-copper alloys containing 2 to 10% Cu, generally with other additions, form important families of alloys. Both cast and wrought aluminum-copper alloys respond to solution heat treatment and subsequent aging with an increase in strength and hardness and a decrease in elongation. The strengthening is maximum between 4 and 6% Cu, depending upon the influence of other constituents present.

Copper-magnesium. The main benefit of adding magnesium to aluminum-copper alloys is the increased strength possible following solution heat treatment and quenching. In wrought material of certain alloys of this type, an increase in strength accompanied by high ductility occurs on aging at room temperature. On artificial aging, a further increase in strength, especially in yield strength can be obtained, but at a substantial sacrifice in tensile elongation.

Magnesium is the major alloying element in the 5xxx series of alloys. Its maximum solid solubility in aluminum is 17.4%, but the magnesium content in current wrought alloys does not exceed 5.5%. The addition of magnesium markedly increases the strength of aluminum without unduly decreasing the ductility. Corrosion resistance and weldability are good.

Magnesium-Manganese. In wrought alloys, this system has high strength in the work-hardened condition, high resistance to corrosion, and good welding characteristics. Increasing amounts of either magnesium or manganese intensify the difficulty of fabrication and increase the tendency toward cracking during hot rolling, particularly if traces of sodium are present.

Manganese is a common impurity in primary aluminum, in which its concentration normally ranges from 5 to 50 ppm. It decreases resistivity. Manganese increases strength either in solid solution or as a finely precipitated intermetallic phase. It has no adverse effect on corrosion resistance. Manganese has a very limited solid solubility in aluminum in the presence of normal impurities but remains in solution when chill cast so that most of the manganese added is substantially retained in solution, even in large ingots.

Molybdenum is a very low level (0.1 to 1.0 ppm) impurity in aluminum. It has been used at a concentration of 0.3% as a grain refiner, because the aluminum end of the equilibrium diagram is peritectic, and also as a modifier for the iron constituents, but it is not in current use for these purposes.

Nickel. The solid solubility of nickel in aluminum does not exceed 0.04%. Over this amount, it is present as an insoluble intermetallic, usually in combination with iron. Nickel (up to 2%) increases the strength of high-purity aluminum but reduces ductility. Binary aluminum-nickel alloys are no longer in use but nickel is added to aluminum-copper and to aluminum-silicon alloys to improve hardness and strength at elevated temperatures and to reduce the coefficient of expansion.

Phosphorus is a minor impurity (1 to 10 ppm) in commercial-grade aluminum. Its solubility in molten aluminum is very low (~0.01% at 660^{o}C) and considerably smaller in the solid.

Zinc. The aluminum-zinc alloys have been known for many years, but hot cracking of the casting alloys and the susceptibility to stress-corrosion cracking of the wrought alloys curtailed their use. Aluminum-zinc alloys containing other elements offer the highest combination of tensile properties in wrought aluminum alloys.

Hydrogen has a higher solubility in the liquid state at the melting point than in the solid at the same temperature. Because of this, gas porosity can form during solidification. Hydrogen is produced by the reduction of water vapor in the atmosphere by aluminum and by the decomposition of hydrocarbons. In addition to causing primary porosity in casting, hydrogen causes secondary porosity, blistering, and high-temperature deterioration (advanced

internal gas precipitation) during heat treating. It probably plays a role in grain-boundary decohesion during stress-corrosion cracking. Its level in melts is controlled by fluxing with hydrogen-free gases or by vacuum degassing.

1.1.3 Properties of hypereutectic aluminum silicon alloys.

The optimum structure of hypereutectic aluminum silicon alloys must consist of fine, uniformly distributed primary silicon crystals in a eutectic matrix. This alloy does not require heat treatment, which may eliminate internal stresses that may cause fatigue failure.

Castability – For alloy B390.0, the diecastability rating is good, and relatively thin and intricate sections can be produced. Pressure tightness and resistance to hot cracking are good. Resistance to die soldering is excellent. For A 390.0, permanent mold castability is good. Sand castability is only good because the slower cooling rates adversely affect casting microstructure. Pressure tightness and resistance to hot cracking are good. Gating designs for proper directional solidification and feeding are essential for sound castings. Pressure tightness is rated good.

Machinability – tool life when machining these alloys is at its best with adequate refinement of primary silicon crystals. Cutting tools of cast iron cutting grade carbide and M-7 tool steel may be acceptable, but the recommend cutting material is polycrystalline diamond. These alloys require a cutting fluid in most operations. Many of the commercial water-emulsion cutting fluid are satisfactory. Aside from tool wearing, these alloys have excellent machining characteristics. Chips are short and easy to remove, and high-quality surface finishes are generated easily.

Weldability – Weldability is fair. The best processes are inert gas arc or oxyacetylene welding. Brazing is not recommended.

Corrosion Resistance – Resistance to corrosion is good to great, depending on the alloys' intended environments. Chemical conversion coatings increase corrosion resistance.

Mechanical properties – Mechanical properties of these alloys depend on composition of alloying elements, especially silicon content. If the silicon content increases, mechanical properties decrease relatively. [5]

The hypereutectic aluminum-silicon alloys have outstanding fluidity and excellent machinability in terms of surface finish and chip characteristics. Also, the recent introductions of polycrystalline diamond cutting tools have done much to alleviate previous problem of

poor life when these alloys are machined. To guarantee the best machinability, mechanical properties, and performance of parts cast from hypereutectic aluminum-silicon alloys, the melt must be treated to control primary silicon size. This treatment, termed refinement, is accomplished by adding a few hundredths of percent phosphorus to the melt. Phosphorus from this addition nucleates the primary silicon particles during solidification. Properly refined primary silicon is only 8 to 10% the size of unrefined silicon.

When hypereutectic aluminum silicon alloys are conventionally high-pressure die cast, refinement is not needed; rapid solidification and turbulence result in a fine structure even when the melt is not treated with phosphorus. Removal of sodium by fluxing is essential prior to the phosphorus addition, because sodium forms sodium phosphide. In this compound, phosphorus loses its nucleating effect on the primary silicon. [6]

Physical properties – Physical properties of these alloys depend on the silicon content. Thermal conductivity and thermal expansion reduce when silicon content increases. Magnesium addition tends to increase a little thermal expansion. Electric conductivity mainly depends on amount of silicon in solid solution. Copper and magnesium also affect to electric conductivity.

Table 1.4 Typical mechanical properties of aluminum permanent mold casting alloys. [6]

AA No.	**A356.0**	**A390.0**				**443.0**	**A444.0**	
Temper	T61	F	T5	T6	T7	F	F	T4
Tensile strength, MPa	283	200	200	310	262	159	165	159
Tensile yield strength, MPA	207	200	200	310	262	62	76	69
Elongation in 50 mm, %	10.0	< 1.0	< 1.0	< 1.0	< 1.0	10.0	13.0	21.0
Hardness, HB	90	110	110	145	120	45	44	45
Compressive yield strength, MPa	221	…	…	414	359	62	…	76
Shear strength, MPa	193	…	…	…	…	110	…	110
Endurance limit, MPa	13	…	…	17	14.5	8	…	8
Mudulus elasticity, kPa.10^6	72	82	…	…	…	71	…	

Table 1.5 Typical mechanical properties of aluminum sand casting alloys [6].

AA No.	**A356.0**	**A390.0**				**443.0**	**A444.0**	
Temper	T6	F	T5	T6	T7	F	F	T4
Tensile strength, MPa	228	179	179	278	250	131	145	159
Tensile yield strength, MPA	164	…	…	…	…	55	62	62
Elongation in 50 mm, %	3.5	< 1.0	< 1.0	< 1.0	< 1.0	8	9	12
Hardness, HB	70	100	100	140	115	40	…	…
Compressive yield strength, MPa	172	…	…	…	…	62	…	…
Shear strength, MPa	179	…	…	…	…	97	55	71
Endurance limit, MPa	59	…	…	90	…	55	…	…
Mudulus elasticity, kPa.10^6	72	82	…	…	…	71	…	…

1.2 Research objectives.

This study has been performed to determine the effects on cast mechanical properties microstructure, if any, of the application of grain refinement during solidification of hypereutectic aluminum silicon alloys. In order to accomplish this, the following major objectives are identified:

a) Produce AlCuP master alloy that would allow the effective application of grain refinement to a solidifying molten material. The effect of this master alloy will be compared with previous master alloy in needed working condition.
b) Using AlCuP master alloy to refine hypereutectic aluminum silicon alloys with 20 wt% of silicon content. Quantitatively determine the effect of an applied method on the mechanical properties and the characteristics of the microstructure of these alloys, namely: thermal expansion, tensile strength, hardness, wear resistance and the primary silicon particle size and distribution.

c) From the results, a final grain refinement method of hypereutectic aluminum silicon alloys can be provided. Thus, the relation between phosphorus solubility and mechanism of grain refinement can be described.

The focus of this study is on the application of AlCuP master alloy during manufacture process of piston of Kamaz automobile in the reality conditions of Vietnam industry. The alloys was used with 18-20 wt.% silicon content.

1.3 Technical approach

Hypereutectic aluminum silicon alloys are technological interest because of the advantageous properties imparted to them by the high volume fraction of hard eutectic and primary silicon particles. However, the morphology of the eutectic silicon particles is generally needle or plate-like and the primary silicon particles are large and faceted, producing stress concentrations that degrade the mechanical properties of the material. Therefore, it is necessary to refine the size of these particles and to modify their morphologies.

Refinement of hypereutectic aluminum silicon alloys is widely used to obtain increasing mechanical properties, especially fracture toughness. Refinement and modification can be accomplished with increased cooling rates, but this approach is difficult to control and not practical for some casting processes or casting with thin sections. Besides, physical methods for refinement have been designed as an alternative to chemical modification. These include mechanical and electromagnetic vibration, mechanical and electromagnetic stirring, semi-solid processing, and intensive melt shearing. But, the equipment for these processes is generally complex and expensive, and these methods have yet to be widely implemented by the casting industry. An additional technique for refinement is the application of an electric current to the casting during solidification. Previous study have shown that this process is effective for variety of metals, including cast iron [10], pure aluminum, and Al 7050 alloy [11], but few studies have been performed using this technique on Al-Si alloys, and fewer yet on hypereutectic aluminum silicon alloys [12].

Therefore, chemical modification is often used. It is well established that sodium or strontium can be used to refine the eutectic silicon from a plate like to a fibrous morphology [7]. To refine primary silicon particles, phosphorus addition has been adopted as the most popular method which utilizes heterogenerous nucleation as a way to increase the number of

primary silicon crystals, reduces its average size, and improves its morphology. The refinement mechanism is well accepted that dissolved phosphorus combines with aluminum and form aluminum-phosphide (AlP) crystals. AlP crystals in the melt increase the amount of heterogenerous nucleation sites for silicon which solidifies later. Higher adding temperature and longer adding time prove more dissolved phosphorus which necessary for silicon refinement [8].

The current study performed casting of aluminum silicon alloys of 18-20 wt.% silicon content with the refinement of master alloys (AlCuP). This master alloy was used to investigate the effects of the aluminum-phosphide on the primary silicon practices. For the modifiers were melted completely, the melts must be fully stirred. A columned metallurgical samples and tensile sample billets were performed using a permanent mold machine from mild steel that had been preheated at 250 ^{0}C. And the alloys of interest were melted using an electric furnace and poured manually. In order to reveal the refinement effect of primary silicon in the tested alloys, two kind of metallurgical sample were used respectively. The tensile tests were carried out using MTS 809 Axia-Torsion Test System. Microstructure of the tested alloys was observed and quantitatively analyzed using Axiovert 100A microscope and Leica DM 4000M microscope with an image collection and analysis system.

2. Grain Refinement of Hypereutectic Aluminum Silicon Alloys

2.1 Basic knowledge of refinement process

Grain refinement plays a vital role in cast and wrought aluminum alloys. There are number of reasons why the control of grain size is important in aluminum cast alloys. Firstly, reduced mechanical properties have been noted in plate products for structural application when a uniform as cast grain size is not achieved [13,15]. Twinned columnar grains have been reported to reduce fabricability, yield strength and tensile elongation to fracture. Secondly, a coarse grained structure may result in a variety of surface defects in alloys used in rolled or extruded form for architectural applications [14]. Thirdly, hot cracking in the shell zone is more severe if the grain structure is not equiaxed. An equiaxed structure allows a higher casting rate to be achieved before hot cracking is produced.

Apart from wrought alloys grain refinement has several benefits in cast alloys like improved mechanical properties that are uniform throughout the casting, distribution of phase

and microporosity, improved ability to achieve a uniform anodized surface, better strength and fatigue life [16, 17]

In this study, grain refinement can be understood to be directly related to the nucleation and growth process of primary silicon alloys. The theory involves heterogeneous nucleation in alloy solidifying.

2.1.1 The nucleation

A small crystal can be called nucleation site during solidification if it was formed from the melt and capable of continued growth. From a thermodynamic point of view the establishment of a solid-liquid interface is not easy. A small solid particle is not necessarily stable although this phase has a lower free energy than the liquid phase below melting temperature because of the free energy associated with the solid-liquid interface. The change in free energy corresponding to the liquid-solid transition must therefore include not only the change in free energy between the two phases but also the free energy of the solid-liquid interface. From a kinetic point of view it is possible to arrive at the same result on the basis that the atoms at the surface of a very small crystal have a higher energy than the surface atoms of a larger crystal [18]. Therefore, the equilibrium temperature at which atoms arrive and leave at the same rate is lower for a very small crystal than for a larger one. Consequently for each temperature below melting temperature, a solid particle can be in equilibrium with the liquid when its radius of curvature has a particular value, known as the *critical radius*. Because at higher supercooling there is more bulk free energy to compensate for the surface free energy, the critical radius decreases with increasing supercooling.

On the other hand, at any supercooling, there exists within the melt a statistical distribution of atom clusters or embryos of different sizes having the character of the solid phase. The probability of finding an *embryo* of a given size increases as the temperature decreases. *Nucleation* occurs when the supercooling is such that there are sufficient embryos with a radius larger than the *critical radius* [19].

The unlikelihood that statistical fluctuations in the melt can create crystals with a large radius is the reason why nucleation is so difficult at small values of the super- cooling. Thus, homogeneous nucleation is only possible for high supercooling (on the order of 0.25 Tm) according to [19]. However small contamination particles in the melt, oxides on the melt surface or contact with the walls of a mould may catalyze nucleation at a much smaller

supercooling and with fewer atoms required to form the critical nucleus. This is known as *heterogeneous nucleation.*

2.1.2 Calculation of the critical radius and energy barrier

Assume that there is a solid particle inside liquid metal. The change in the free energy per unit volume, ΔG, to form a solid embryo of spherical shape of radius, r, involves the variation of the volume free energy and the surface free energy associated with the solid-liquid interface and is given by

$$\Delta G = \Delta G_v + \Delta G_i = -\frac{4\pi.r^3}{3}\frac{L\Delta T}{T_m} + 4\pi\gamma_{SL}.r^2 \qquad (1)$$

Where ΔG_v is the change in free energy on solidification associated with the volume.

ΔG_i is the free energy associated with the interface.

γ_{SL} is the solid-liquid interfacial free energy.

L is the latent heat per unit volume.

ΔT is the supercooling.

The critical radius, r*, occurs when ΔG has a maximum given by the condition, $\frac{d(\Delta G)}{dr} = 0$, as

$$r^* = \frac{-2\gamma_{SL}}{\Delta G_v} = \frac{2\gamma_{SL}T_m}{L}\frac{1}{\Delta T} \qquad (2)$$

Figure 2.1, due to [20], gives a comprehensive picture of the variation of the free energy of an embryo as a function of its radius and ΔT:

a. At temperatures T greater than T_m both ΔG_v and ΔG_i increase with r. Therefore the sum ΔG, increases monotonically with r.
b. At the melting point, ΔG_v=0 but ΔG_i still increases monotonically.
c. Below the equilibrium temperature the sign of ΔG_v is negative because the liquid is metastable while the behavior of ΔG_i is the same as in (a) and (b).

At large values of r, the cubic dependence of ΔG_v dominates over ΔG_i and AG passes through a maximum at the critical radius, r^*. When a thermal fluctuation causes an embryo to

become larger than r*, growth will occur as a result of the decrease in the total free energy. And the *critical energy of activation* for an embryo of radius r* is given by

$$\Delta G^* = \frac{16}{3}\pi \frac{\gamma_{SL}^3 T_m^2}{L^2 \Delta T^2} \tag{3}$$

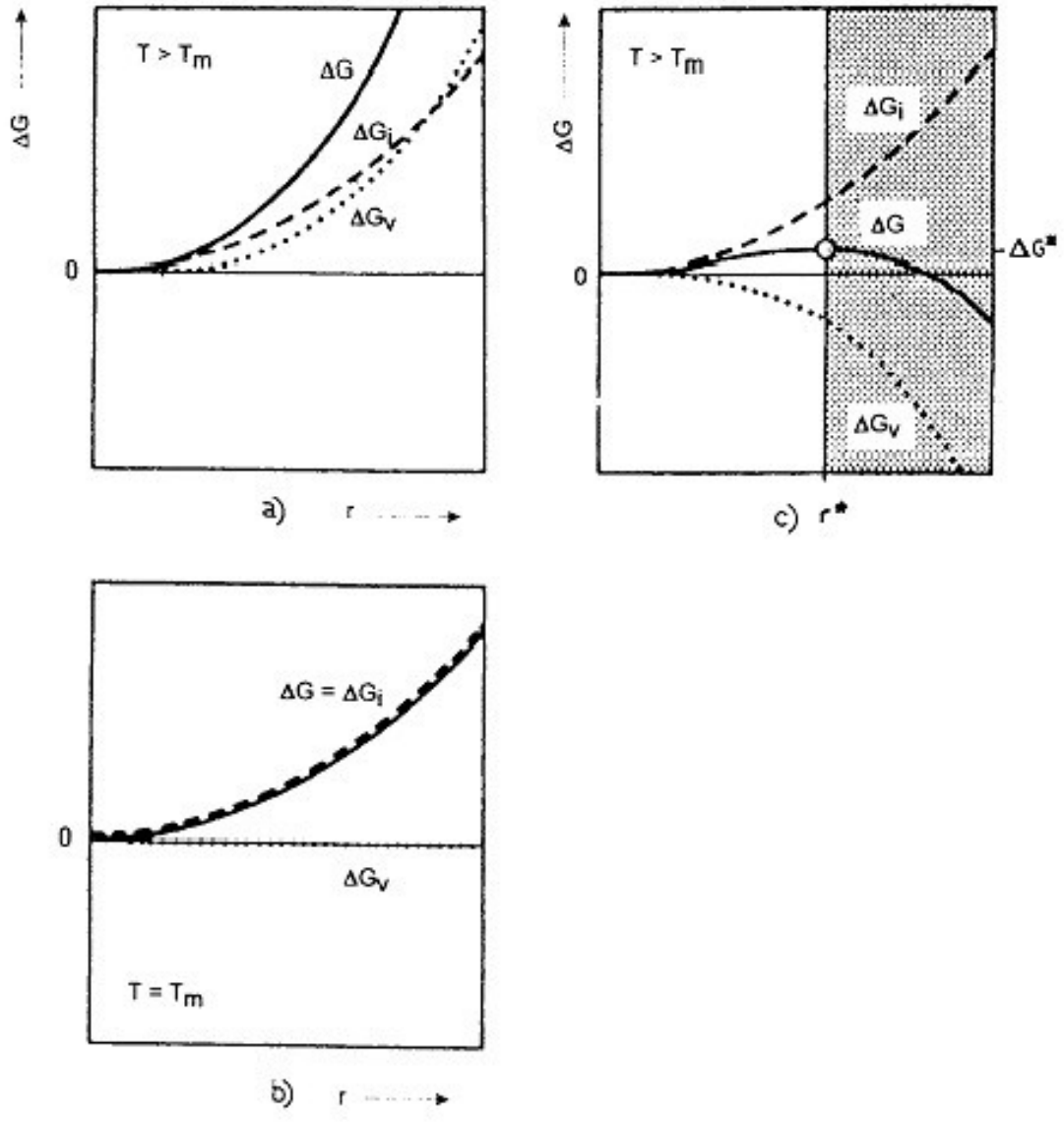

Figure 2.1 Volume, surface and total values of the free energy of a crystal cluster as a function of radius, r, at three temperatures: (a) T> Tm, (b) T= Tm , and (c) T<Tm [20].

Figure 2.2 shows the solid nucleating on a substrate in a liquid. For this simple case, the nucleation is a spherical cap that makes an angle θ with the substrate given by

$$\gamma_{cL} - \gamma_{cS} = \gamma_{SL} \cos\theta \tag{4}$$

Where γ_{cL} is the catalyst-liquid interfacial free energy and γ_{cS} is the catalyst-solid interfacial free energy. Thus, the thermodynamic barrier to nucleation is reduced to

$$\Delta G^* = \frac{16}{3}\pi \frac{\gamma_{SL}^3 T_m^2}{L^2 \Delta T^2} = \frac{16\pi\gamma_{SL}^3}{3\Delta G_v} f(\theta) \tag{5}$$

Where $f(\theta)$ is a function of the contact angle on the substrate on which nucleation takes place [21].

$$f(\theta) = \frac{(2+\cos\theta)(1-\cos\theta)^2}{4} = \frac{2-3\cos\theta+\cos^3\theta}{4} \tag{6}$$

If nucleation occurs in a scratch or a cavity of the catalytic substrate, the number of atoms in a critical nucleus and the value of AG* can be reduced even more. From the classical heterogeneous nucleation point of view, a good nucleant corresponds to a small contact angle between the nucleating particle and the growing solid.

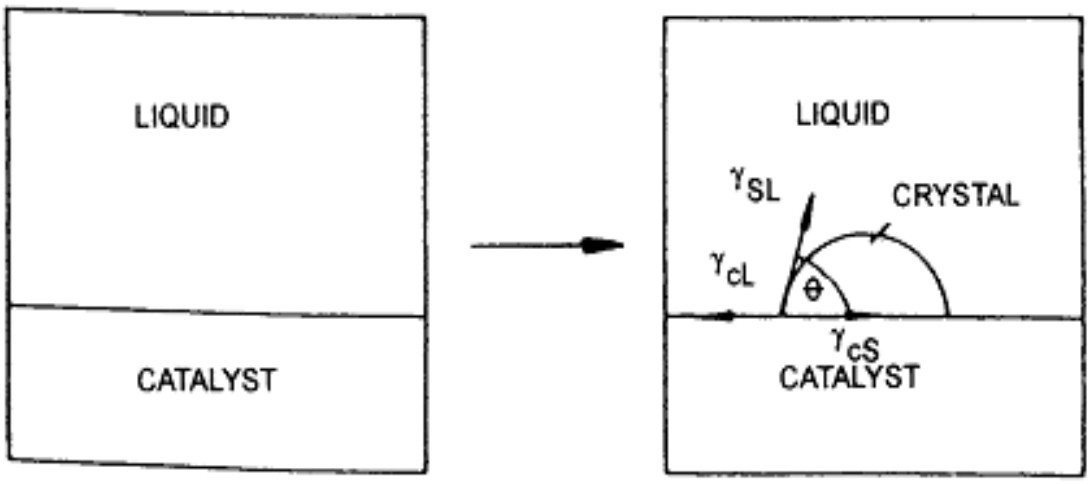

Figure 2.2 Schematic representation showing the formation of spherical cap of solid (s) on a substrate, contact angle and surface tension forces [21]

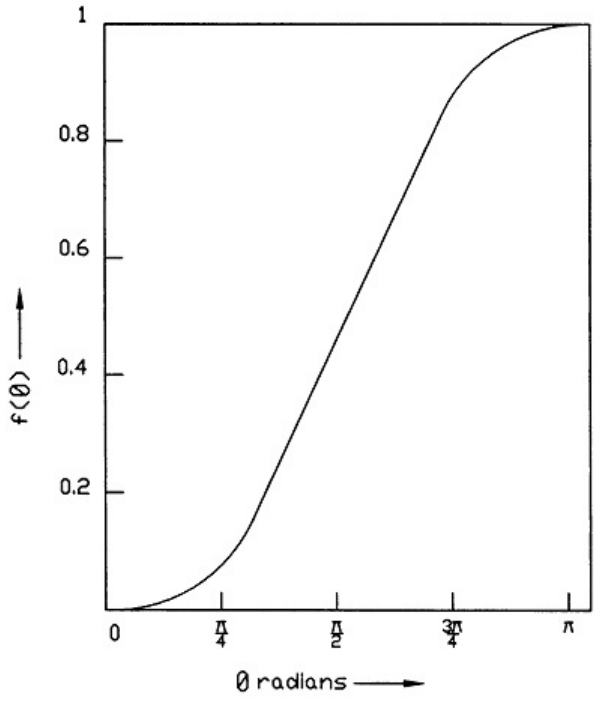

Figure 2.3 Showing the variation of $f(\theta)$, where $f(\theta)$ is equal to $(2-3\cos\theta+\cos^3\theta)/4$ [21]

2.1.3 Nucleation rate

The heterogeneous nucleation rate is considered per unit area of active catalytic site. To determine the rate of nucleation, it is necessary to find expression for the number of embryos that have critical size and the rate at which atoms or molecules attach to the critical nucleus. Figure 2.3 shows the variation of $f(\theta)$ and since $f(\theta)$ is always less than 1, the critical free energy for heterogenerous nucleation is always less than or equal to that for homogenerous nucleation. However, it is clear that potent heterogeneous substrates are those with θ close to zero [21].

The values of supercooling, ΔT is of the order 1-2K for observable nucleation rates in commercial aluminum alloys with grain refiners. Therefore, clearly heterogeneous nucleation is taking place. The following simplified expression for heterogeneous nucleation rate per unit volume in $m^{-3}s^{-1}$ is

$$I^V = 10^{18} N_V^P \exp\left[\frac{-16\pi\gamma_{sL}^3 f(\theta)}{3K_B \Delta G_V^2}\right] \qquad (7)$$

Where, K_B is the Boltzmann's constant, J/K; N_V^P is the number of nuclei/m^3, and I^V is the heterogeneous nucleation rate, number of nuclei/m^3.sec.

Therefore, it can be seen that if contact angle is close to zero, wetting of substrate for nucleation is promoted and nucleation rate increases.

2.1.4 Growth of nuclei

Once nucleation takes place, more importantly heterogeneous nucleation, the growth front of the nuclei is seldom planar. The well-known constitutional supercooling occurs as solute is rejected at the interface and the criterion is given by [20].

$$\frac{G_L}{R} \geq \frac{-m_L C_0 (1-k)}{k D_L} \qquad (8)$$

Where, G_L is the temperature gradient in the liquid ahead of the solid–liquid interface (K/m), R is the growth rate of solid liquid interface (m/sec), m_L is the liquidus slope of phase diagram (K/wt%), C_0 is the bulk alloy composition in the liquid (wt%), k the partition coefficient between solid and liquid, and D_L is the diffusion coefficient of the solute in the liquid (m^2/sec).

Normally in a casting we have a columnar zone and a central portion of equiaxed crystals [31]. The columnar dendrites grow in [1 0 0] directions in the cubic system and growth direction is antiparallel to the heat flow direction. The equiaxed dendrites grow in the same direction of heat flow i.e. radially outward. The formation of equiaxed crystals is due to dendrite arm melt off which provides nuclei for equiaxed crystals.

2.1.5 Grain refinement effects.

In industry, most of cast aluminum alloys are grain refined before casting. The commonly used grain refiners are available nucleants or master alloys, such as CuP, Al-10Ti, Sr, RE and so on. The efficiency of a grain refiner is assessed by the grain refining curves.

Figure 2.4 shows the effect of phosphorus content on primary silicon size of Al-17SiCu4Mg [33]. The influence of phosphorus on the primary silicon is obvious. The size of primary silicon particles in the alloys is decreased with the increasing of phosphorus content. When adding content of phosphorus to the alloys is 60 ppm, the refinement of primary silicon particles is optimal.

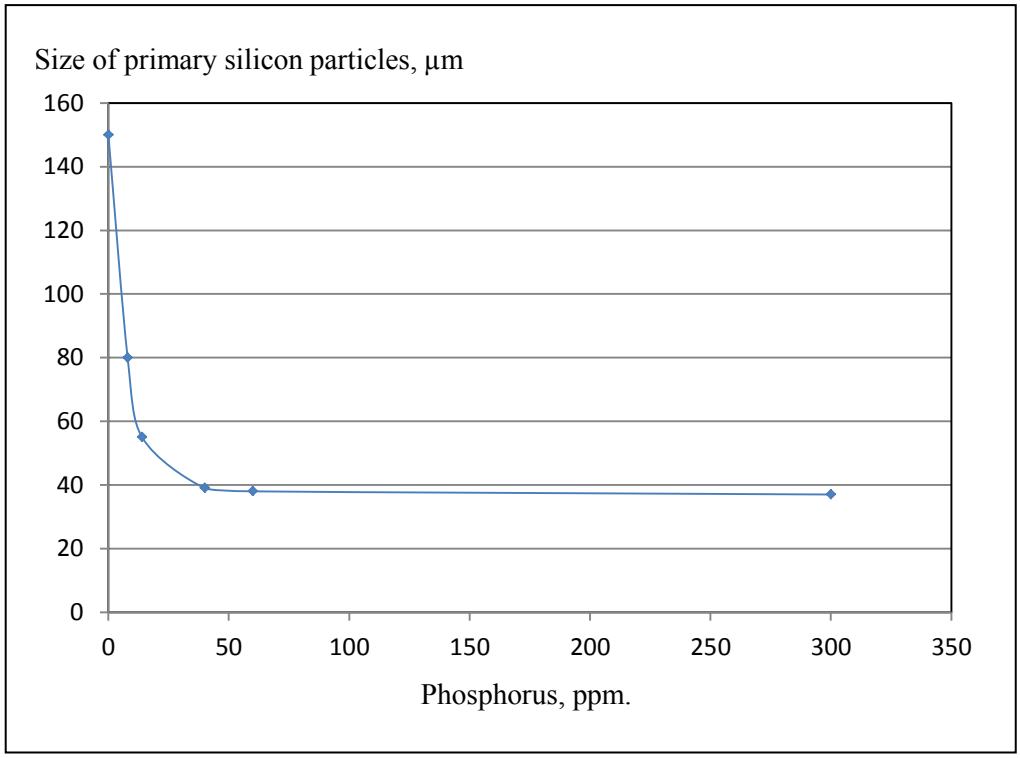

Figure 2.4 Influence of phosphorus content on primary silicon particles [33].

The effect of phosphorus on the primary silicon of the hypereutectic AI-20Si alloys is shown in figures 2.5(a)-(d). Many coarse block and stripe primary silicon can be found in the unmodified alloy (shown in Fig.2.5(a)). The addition of phosphorus refines obviously the primary silicon. The size of primary silicon decreases with increasing phosphorus content. And their edges and angles are passivated (as shown in Figs. 2.5(b)-(d)). The optimal refinement effect of primary silicon is obtained when the alloy contains 0.08% phosphorus. Increasing continuously the phosphorus content can coarsen the primary silicon of the tested alloys, which means that excess phosphorus is unfavorable to the refinement of primary silicon [30].

The effect of refinement time also plays an extremely important role in improving microstructure of hypereutectic alloys [7]. Each various refinement temperature always has a unique refinement time. This time is enough for master alloys dissolving into the melt. Refinement time depends not only on temperature but also alloys and master alloys. If this time is short, master alloys cannot be completely dissolved to the melt. The effect of refinement decreases. Besides, if this time is long, the size of primary silicon particles is not significantly reduced.

Refinement temperature is crucial to solubility and loss by burning of master alloys. The solubility of phosphorus in the melt increases with increasing temperature. When the efficacy variables were fully archived, increasing temperature does not solve anything [7].

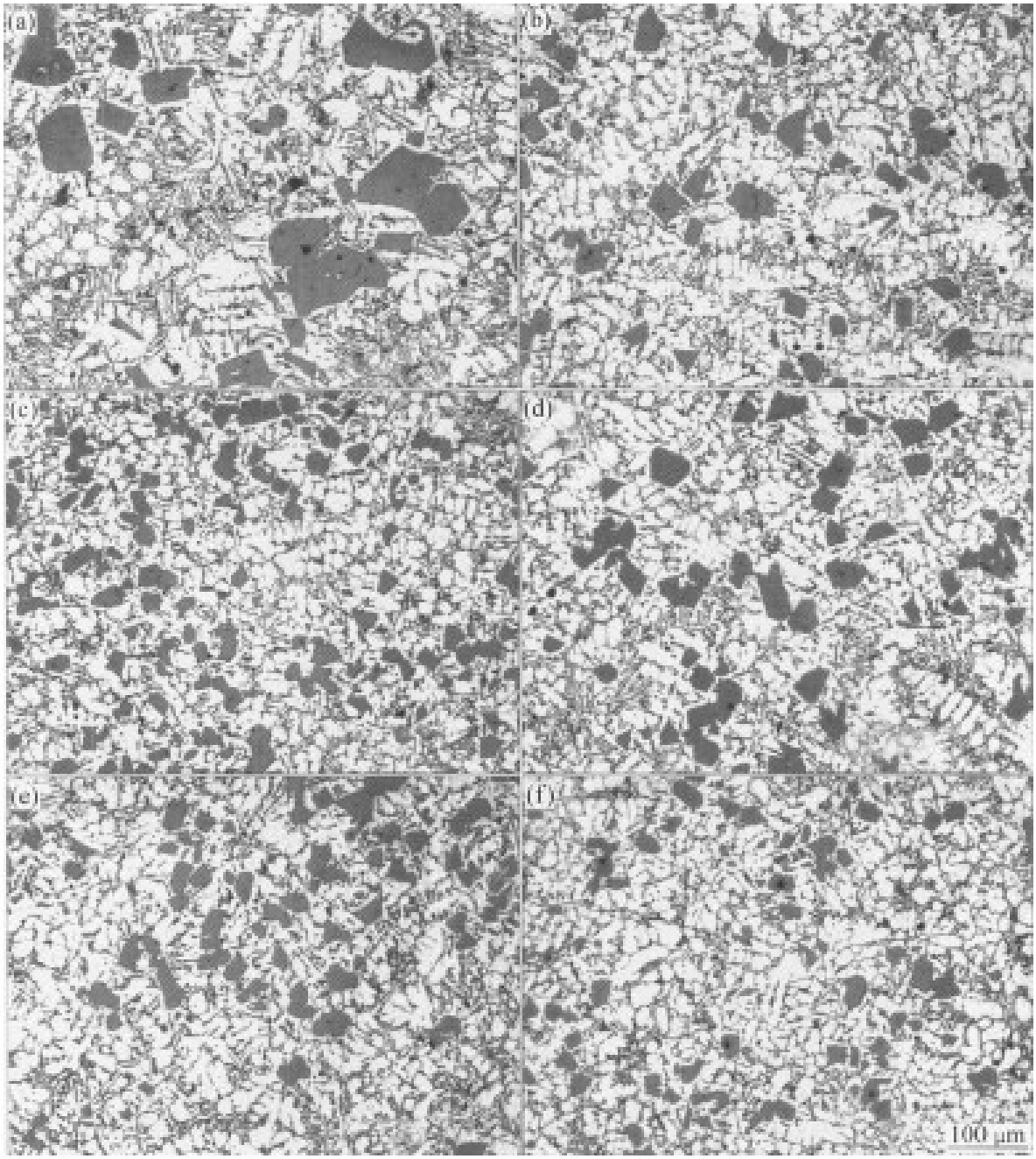

Figure 2.5 Primary silicon morphologies of AI-20Si alloys modified with different modifiers: (a) P and RE free; (b) 0.06% P and 0.6% RE; (c) 0.08% P and 0.6% RE; (d) 0.1% P and 0.6% RE; e)0.08% P and 0.3% RE; (0.08% P and 0.9% RE [30].

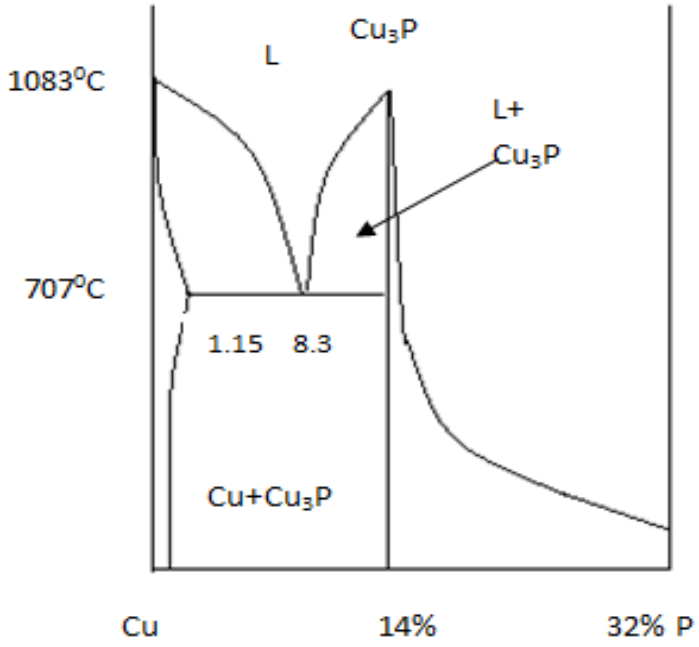

Figure 2.6 Cu-P phase diagram.

From the previous studies [3,7,8,9,16,23,26,30,33, 34], the most effective master alloys of hypereutectic aluminum silicon alloys is CuP master alloys. The amount of copper content has to be investigated. Increased copper concentration shifts temperature of primary solidification to higher temperature. Also high copper contributed to good mechanical properties [8, 32]. Figure 2.6 show that, refinement temperature of Cu-P master alloys is high, so losses by burning of elements in melt were increased [35]. The effect of refinement seems to be low [24].

2.2 Grain refinement of primary silicon.

In hypereutectic aluminum silicon alloys, the first phase which was form from liquid during cooling process is coarse and faceted primary silicon crystal. Depending on silicon content and cooling condition during solidification, the structure of these alloys contains α-Al particles, primary silicon crystals, (α+Si) eutectic and intermetallic phases, such as Mg_2Si, $CuAl_2$. In these alloys, the formation of nucleation site for silicon is very important. It can control structure and properties of casting. Many methods were applied. But, chemical

method using phosphorus and its master alloys has been considered as the most important refining element for primary silicon particles [8].

As such, it is of interest to refine both of the eutectic and primary silicon particles. Grain refinement is a common route to achieving significant improvement in the size and morphology of primary silicon particles. However, the same chemical modifiers are not commonly used for both purposes. Simultaneous modification of both the eutectic and primary silicon particles in hypereutectic alloys is particularly difficult.

Table 2.1 Comparison of mechanical properties of hypo and hypereutectic Al-Si alloys in as-cast conditions, and in hot extruded condition for hypereutectic composition [7]

Material	0.2% YS (MPa)	UTS (MPa)	Ductility (%)	Microhardness (HV)
Al–7Si	55.3±2.1	141.7±2.1	12.2±0.5	38.5±1.2
Al–10Si	75.4±1.6	154.7±3.4	10.3±0.8	39.2±0.4
Al–19Si	80.8±3.2	129.6±8.7	2.3±1.9	43.4±2.1
Al–19Si(Ext)	82.7±3.1	189.0±12.1	21.4±8.8	59.2±0.5

Table 2.1 shows a comparison of several mechanical properties for hypoeutectic and hypereutectic aluminum silicon alloys [7]. The ultimate tensile strength and ductility decreased for the hypereutectic case, but hot extruding the hypereutectic alloy increased these properties to levels superior to that of the hypoeutectic alloys, as show in the last row of Table 2.1, by reducing the size and increasing the uniformity of the primary silicon particles.

2.2.1 Chemical refinement of primary silicon.

Refinement of hypereutectic aluminum silicon alloys is widely used to obtain increasing mechanical properties. To refine primary silicon, phosphorus addition has been adopted as the most popular method which utilizes heterogeneous nucleation as a way to increase the number of primary silicon crystals, thus, reduces its average size. The refinement mechanism is well accepted that dissolved phosphorus combines with aluminum and forms aluminum phosphide (AlP) crystals which is crystallographically similar to silicon and promotes epitaxial growth [8,27,29]. AlP crystals in the melt increase the amount of heterogenerous nucleation sites for silicon which solidifies later. Form the results of [8], phosphorus addition, higher adding temperature and longer adding time provide more

dissolved phosphorus which is necessary for silicon refinement. It is concluded that increasing the adding temperature does not affect on the size of primary silicon when the primary silicon is sufficiently refined. Morphology and size of the primary silicon in phosphorus-refined alloys were also affected by the amount of phosphorus addition. Increasing the amount of phosphorus addition changed the shape of most primary silicon crystals to polyhedral one. Beside, solubility of phosphorus in the melt is evaluated as a function of two variables: temperature and silicon content. Phosphorus solubility in hypereutectic aluminum silicon melts increases with increasing temperature and decreases with increasing silicon content. The retained phosphorus increases with the amount of added phosphorus and the adding temperature. However, increasing the retained phosphorus is saturated to the maximum value which is assumed to be the phosphorus solubility in the liquid alloy. When the primary silicon is completely refined, average size is 20 μm, more retained phosphorus cannot promote the refinement. In another way, effective phosphorus denote the minimum amount of the retained phosphorus which results in the completely refinement.

Crystallization, examined as a complex of transformations that take place during the transition of a body from liquid into crystalline state, is the result of simultaneous occurrence of a number of different physic-chemical phenomena [37]. In cast alloys, crystallization takes place within the range of temperatures marking the beginning (T_{lid}) and end (T_{sol}) of the solidification process. The kinetics of crystallization is reflected in the shape of the cooling curve, which enables evaluating the quality of molten metal and the consequences of its refining and modification treatment. From the run of this curve one can judge about the characteristic arrests and inflexion points that occur on the temperature derivative in function of time. The arrests are caused by the effect of external heat sources. Their value depends on the thermal effects originating from the crystallization of compounds, eutectics and intermetallic phases [38].

From the data comprised in table 2.2 it follows that the exothermic effect of proeutectic crystallization (T_{efekt}) occurs only in alloys after modification with phosphorus, or with an addition of complex master alloys of the Al-CuP-Me (Me= Cr, Co, Mo, Nb, TiB, W, Zr) type. The temperature range of the crystallization is from 653 to 682^0C, a thermodynamic consequence of which is the exothermic heat effect distinctly visible on a cooling curve [34].

Very important in the formation of primary structure during the solidification of silumins are also the conditions of heat transfer. Slow crystallization results in coarse-grain structure. Increasing the rate of heat transfer results in microstructure. The thermodynamic

aspects of the crystallization process affect also the formation of silicon crystals, aluminum dendrites and intermetallic phases [39,40].

Table 2.2 Characteristic temperature values at the initial stage of AlSi20 silumin solidification after refinement with phosphorus and Al-CuP-Me master alloys [34].

Sample type	Solidification temperature, °C				
	$T_{zal.}$	$T_{liq.}$	$\mathbf{T_{efekt}}$	$T_{min.}$	T_E
AlSi	777	642	-	569	570
AlSi+P	780	691	**671**	567	569
CuP+AlCo	776	687	**670**	565	569
CuP+AlCr	789	689	**680**	565	568
CuP+AlMo	769	692	**671**	568	570
CuP+AlNb	776	667	**653**	569	571
CuP+AlNi	774	668	**661**	564	565
CuP+AlSr	775	713	**664**	567	569
CuP+AlTi	780	695	**671**	570	571
CuP+AlTiB	780	728	**682**	571	572
CuP+AlW	766	692	**666**	568	571
CuP+AlZr	778	691	**663**	569	571

Where, T_{zal} is pouring temperature; T_E is eutectic temperature; $T_{liq.}$ Is liquid temperature.

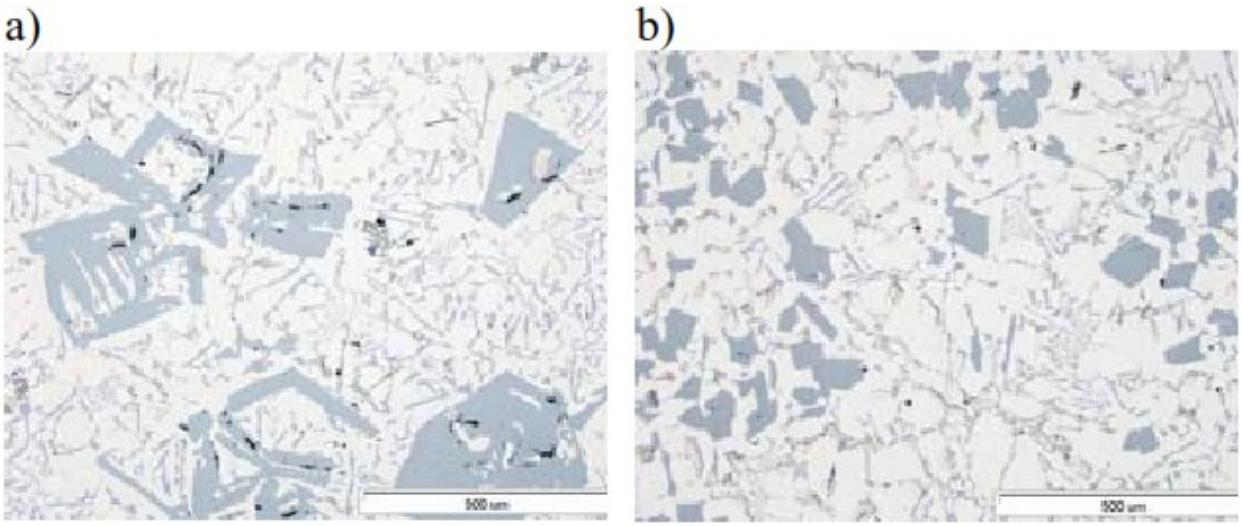

Figure 2.7 Microstructure of AlSi20 alloy; a) before modification; b) after modification with 0,05%P master alloy [34].

The problem of modifying both the eutectic and primary silicon particles in hypereutectic alloys is more difficult. While phosphorus is effectively refines the primary particles, it does not refine or modify the eutectic particles. Additions of both phosphorus and sodium, to refine primary and modify eutectic particles, respectively, are both much less

effective than when added in isolation. This is presumably because they can react to form Na_3P[28]. Following the CT theory [25], there seems no doubt that silicon in aluminum silicon alloys nucleates on an aluminum phosphide, possibly AlP, as review recently [26]. For hypereutectic aluminum silicon alloys, with sufficient phosphorus addition, it seems that aluminum phosphide may nucleate freely in the melt, forming a nucleus around which silicon can wrap completely around and so develop into a compact crystal. However, hypereutectic alloys have sufficient aluminum phosphide nuclei to create a mix of nucleation on free aluminum phosphide particles and aluminum phosphide already nucleated on oxide bifirms. In the presence of oxide bifirms, with their unique properties of a central unbounded interface, during the cooling of the melt some aluminum phosphide is likely to nucleate on one or more of outer surfaces. This is assumed since in studies so far, it seems that most if not all intermetallics nucleate on bifilm suspended in the melt [25].

Figure 2.8 indicates that, when silicon in turn nucleates on the aluminum phosphide particle, it is unable to wrap completely around. Instead, it clearly finds the oxide bifilm to be a tolerably favorable substrate, and so will extend outward, away from the aluminum phosphide nucleus, spreading across the bifilm.

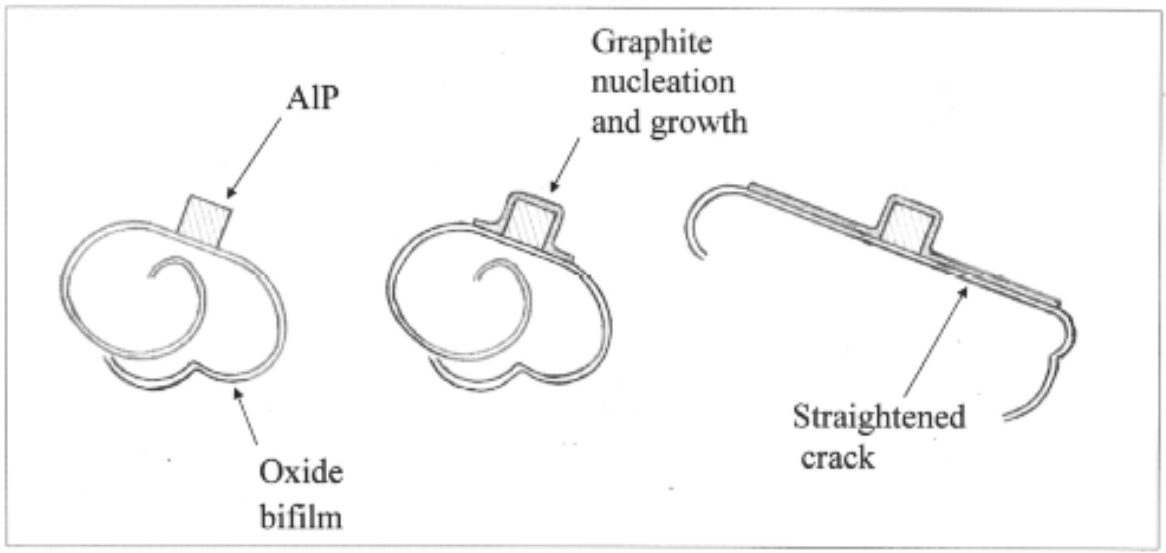

Figure 2.8 Nucleation and growth of silicon on aluminum phosphide particle in turn nucleates on a bifilm [24].

The structure of the hypereutectic aluminum silicon alloys is therefore a mixture of compact silicon particles that have nucleated on aluminum phosphide in suspension in the melt, together with platelet silicon that has grown on bifilms. This dual nature of hypereutectic alloys seemd to have been generally overlooked in the casting literature [24].

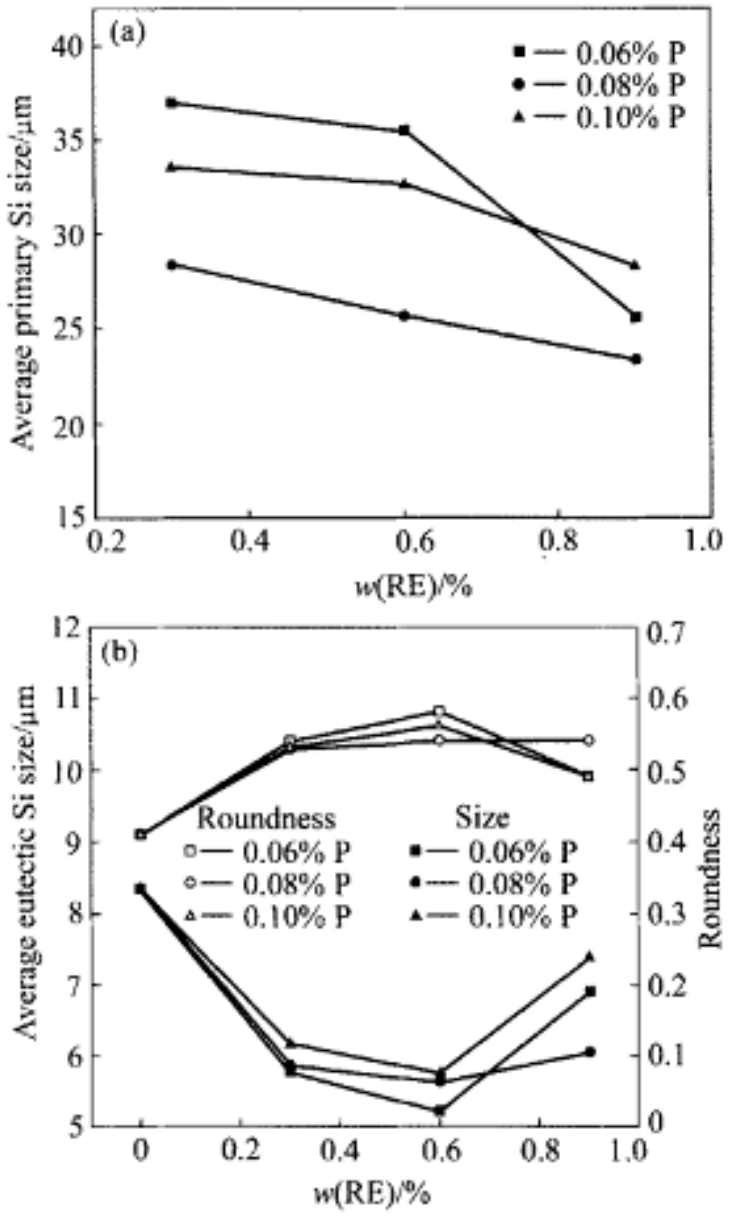

Figure 2.9 Effect of RE content on microstructure parameters of primary Si and eutectic Si of Al-20% alloys: (a) Primary Si; (b) Eutectic Si [30].

From figure 2.9, rare earth metals have been found to refine the primary silicon particles. The complex modification of phosphorus and rare earth metals can obviously modify the primary silicon and the refinement effect of phosphorus on the primary silicon is more distinct. The size of primary silicon decreases with increasing phosphorus content. The edges and angles of silicon are passivated. The optimal refinement effect of primary silicon is obtained when the alloy contains 0.08% phosphorus under the 0.90% rare earth metals condition. The primary silicon particles are refined to 23.3 μm from 66.4 μm of the unmodified alloys. Excess phosphorus is unfavorable to the refinement of primary silicon.

Rare earth metals can obviously modify the eutectic silicon particles. The large needle eutectic silicon particles are modified to the fine fiber or lamella ones with increasing rare earth metals content. The size of the eutectic silicon decreases obviously with the addition of rare earth metals. The best modification effect on the eutectic silicon particles can be obtained with the addition of 0.60% rare earth metals and 0.06% phosphorus. The size of eutectic silicon particles decreases to 5.2 μm from 8.3 μm. Phosphorus decreases the modification of rare earth metals on the eutectic silicon.

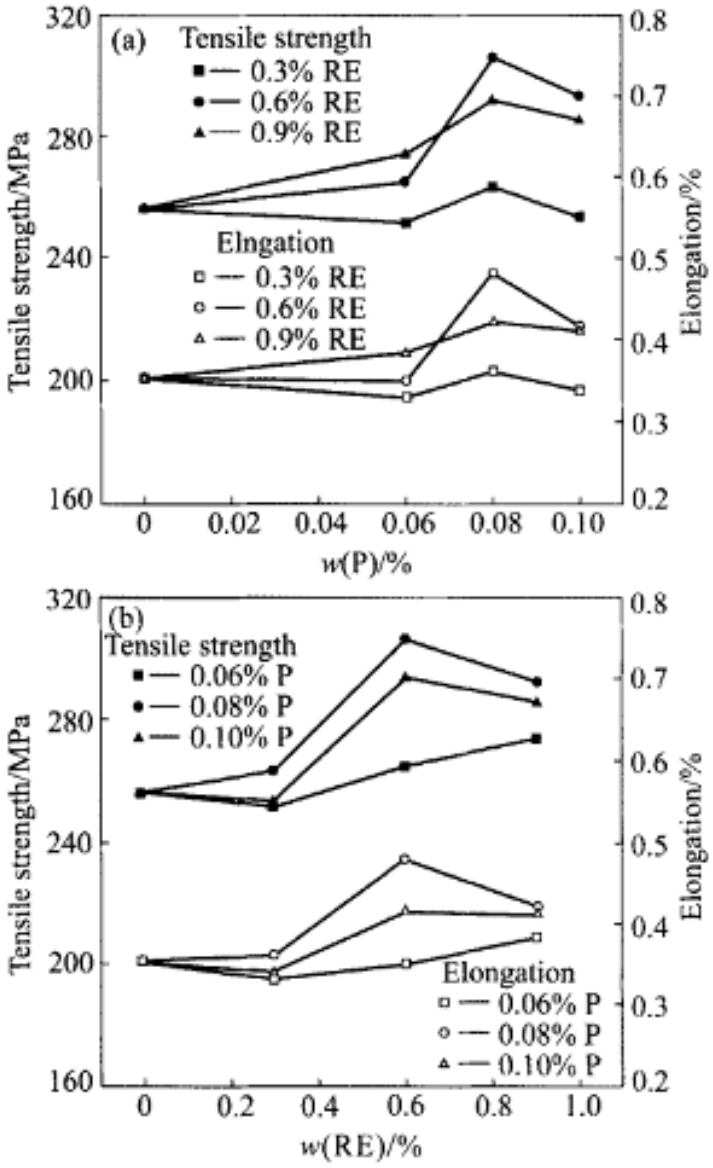

Figure 2.10 Effect of P and RE content on mechanical properties of Al-20Si alloys; (a) P content; (b) RE content [30].

Figure 2.10 shows that, the mechanical properties of hypereutectic Al-20Si alloys are improved obviously with the addition of phosphorus and rare earth metals. When the tested

alloys are modified with 0.08% phosphorus and 0.60% rare earth metals, the optimal combination of strength and plasticity is obtained. The tensile strength is improved to 306 MPa from 256 MPa of the unmodified alloy, increased by 20%. The elongation is improved to 0.48% from *0.35%,* increased by 40% [30].

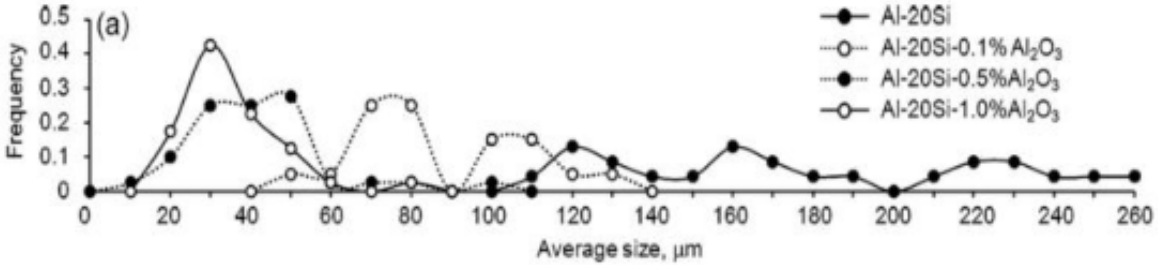

Figure 2.11 Histogram showing refinement of primary silicon particles in Al-20 wt.% Si alloys using Al2O3 nanoparticles [49].

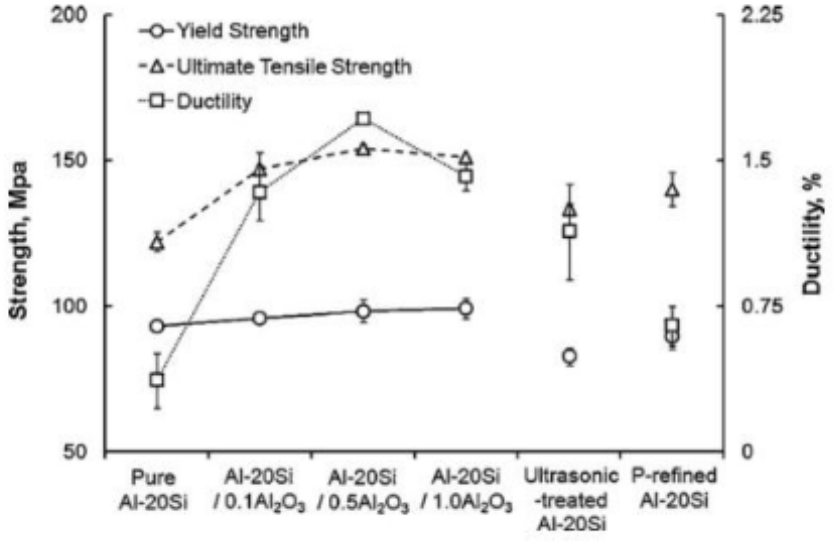

Figure 2.12 Effect of Al2O3 nanoparticles on mechanical properties of Al-20 wt.% Si alloys compared to ultrasonic and phosphorus modified conditions [49].

Choi et al [49]. demonstrated that modification of both the eutectic and primary silicon particles in hypereutectic Al-Si alloys can be achieved with the addition of γ-Al_2O_3 nanoparticles [49]. Figure 2.11 shows histograms of primary silicon particles size in Al-20 wt.% Si alloys treated with various amounts of Al_2O_3 nanoparticles additions. Furthermore, it was also found that these nanoparticles reinforced the metal matrix, leading to higher

ductility, yield strength, and ultimate tensile strength, than is found using traditional refinement techniques. These results are demonstrated in Figure 2.12 as compared to ultrasonic treated, phosphorus modified, and unmodified Al-20 wt.% Si.

2.2.2 Physical methods of refinement of cast microstructure of hypereutectic aluminum silicon alloys.

It is well known that increased solidification rate generally leads to the refinement of cast microstructures. In the case of Al-Si alloys, rapid solidification refines both the primary [50] and eutectic [41] silicon particles and also decreases the secondary dendrite arm spacing [50]. Unfortunately, in many industrial applications, achieving the desired solidification rate is neither physically, nor economically practical. A number of other methods for physically refining the microstructure of Al-Si alloys have been developed.

One method for physical refinement is electromagnetic vibration has been used as a method for microstructural refinement that does not involve contacting the mold. Instead, the vibration is induced by applying orthogonal static magnetic and alternating electric fields [42]. Radjai et al. [46] studied the effect of such a vibration on the refinement of Al - 17 wt.% Si and concluded that electromagnetic vibration caused a cavitation effect that crushed the primary silicon particles into smaller pieces. Similarly, Yu et al. [45] found significant refinement of the primary silicon particles with the application of this technique. Figure 2.13 shows the change in equivalent diameter of the primary silicon particles as a function of current density and magnetic flux used to create the electromagnetic vibrations. Unfortunately, electromagnetic vibration faces many of the same problems for implementation as mechanical vibration in that it is not well suited for large molds or sand casting, and that the equipment is expensive [42].

If a variable magnetic field is applied to the melt, a corresponding electric field is induced in the fluid, and the Lorentz force caused fluid motion to occur [51]. These currents break off dendrite arms and increase nucleation in the same way as mechanical vibration or stirring. This technique is called electromagnetic stirring. Lu et al. [44] found that in hypereutectic Al-Si alloys, electromagnetic stirring implemented at current levels above 12 amps caused the primary silicon particles to congregate, leading to heterogeneity in the microstructure. They found that moderate currents, between 8 and 12 amps, are optimal for refinement. While this refinement of the primary silicon particles is significant, electromagnetic stirring has negligible effects on the eutectic silicon particles. Jung et al. [43]

demonstrated this fact in aluminum alloy A356, but also showed that this method could be effectively used in conjunction with chemical modification using strontium to refine both the eutectic particles and the α-Al dendrites.

Another physical method of refinement is the intensive melt shearing process, in which the liquid metal is subjected to intense shearing via a twin screw mechanism prior to use in a high pressure die casting process, as shown schematically in Figure 2.14 [48]. It has been found that this process leads a greater refinement of the primary silicon particles than does chemical modification using phosphorus [47,48]. Zhang et al. [47] speculated that the mechanism of this refinement is the distribution of oxide films as well dispersed nanoscale particles that act as substrates for heterogeneous nucleation.

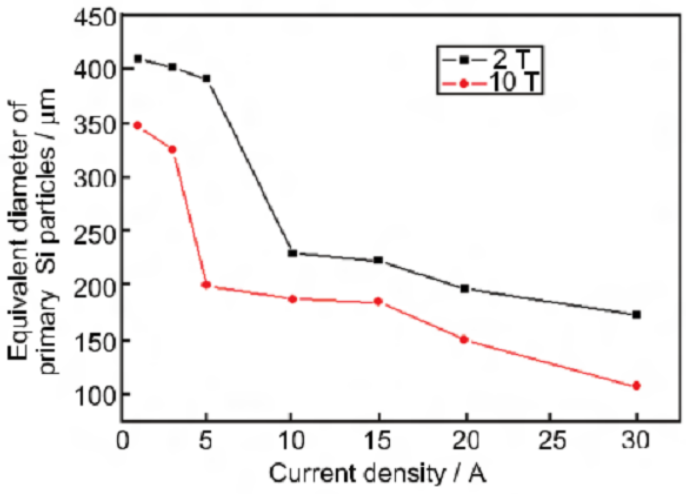

Figure 2.13 Change in equivalent diameter of primary silicon particles in Al-18 wt.% Si alloy using electromagnetic vibration with different electric current densities and magnetic fluxes [45].

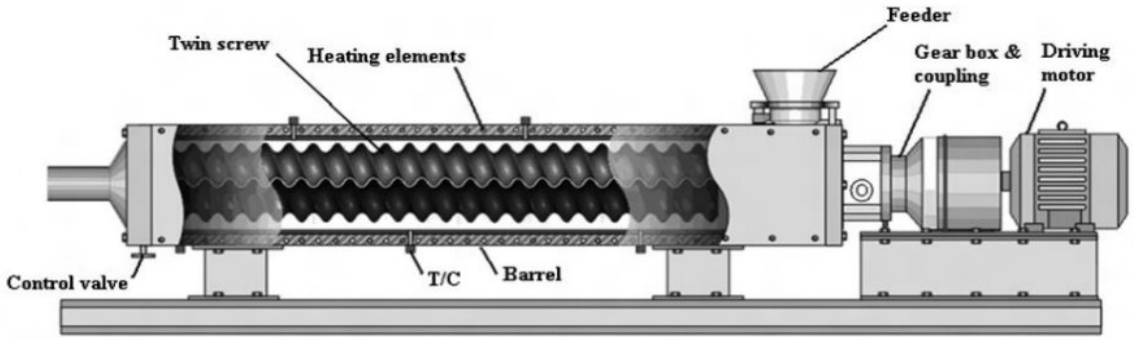

Figure 2.14 Schematic of intensive melt shearing apparatus [48].

2.2.3 Refinement of hypereutectic microstructure by an applied electric current.

An alternative method for the refinement of cast microstructures is the application of an electric current during solidification. Several early studies theoretically [52] and experimentally [53] investigated the effect of an applied electric current on the segregation and redistribution of solute atoms at a freezing interface during solidification.

These studies concluded that electro transport created by high current densities has a purifying effect on the material and improves segregation. Additionally, because the resistivity of most solid metals is about half that of the liquid phase, significant joule heat. These early studies created an interest in the effect of an applied electric current on the cast microstructure of various materials, and resulted in experimentation being performed by a number of researchers. Among these studies, two distinct regimes of high and low current density can be identified. High current density studies involved the use of generated by the electric current would have the effect of reducing the growth of dendrite arms, with the result of increasing the interfacial stability.

These early studies created an interest in the effect of an applied electric current on the cast microstructure of various materials, and resulted in experimentation being performed by a number of researchers. Among these studies, two distinct regimes of high and low current density can be identified. High current density studies involved the use of capacitor banks to discharge pulsed current, and low current density studies involved the use of power supplies to apply current in a steady or pulsed manner.

Hongsheng et al. [55] conducted a study on hypoeutectic, eutectic, and hypereutectic composition Al-Si piston alloys, and compared the results directly with chemical modification. The charge material was melted using an electric resistance furnace and the current was supplied by a capacitor bank, with a pulsed frequency of 4 Hz, using steel electrodes. Although it was stated that a voltage of 2000V was used, the current density was not discussed. They reported that pulsed electric current refined the α-Al grains as effectively as chemical modification using sodium salt, although their method for grain size measurement was not discussed. In particular, it was shown that the electric current application had a much greater effect when applied at a higher melt temperature, translating to the nucleation rather than the growth stage of solidification, which agrees with the finding of Liao et al. [54]. It was reported that the eutectic silicon particles in the samples treated with the pulsed current were smaller and more uniform.

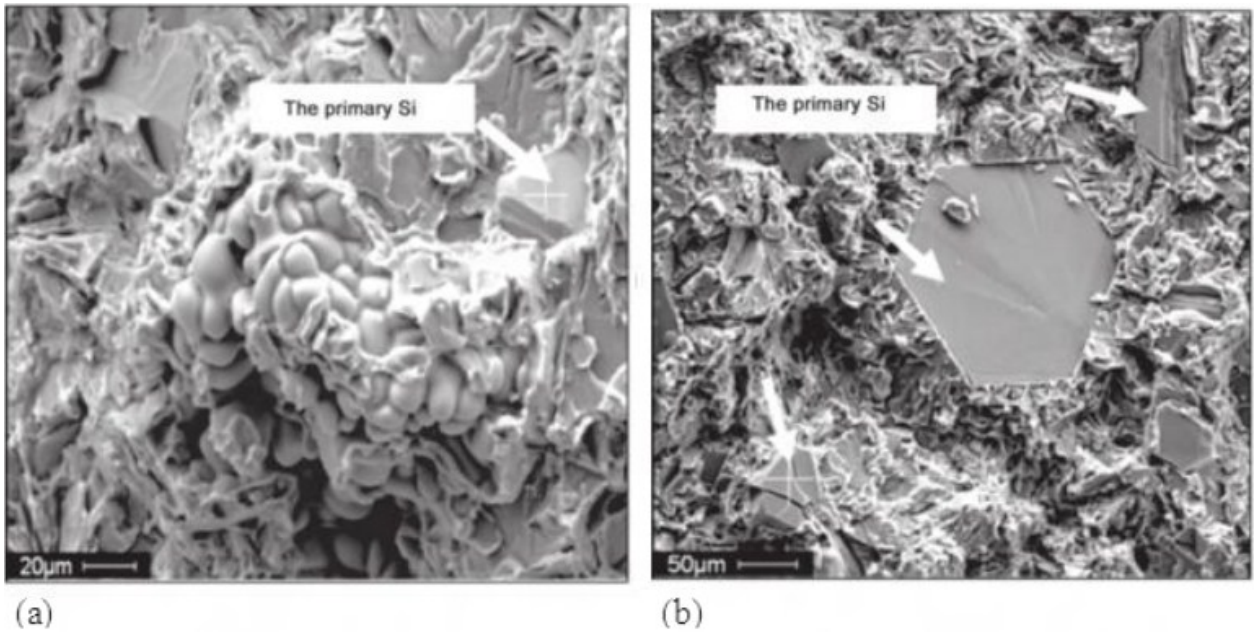

Figure 2.15 SEM photomicrographs showing difference in size of primary silicon particles with applied electric current (a), and without applied electric current (b) [55].

Figure 2.15 shows SEM photomicrographs of the difference in size of the primary silicon particles with and without the application of the pulsed electric current. Hongsheng et al. concluded that the effect of the electric current on the primary silicon particles was more significant than on the eutectic silicon particles. The effects of the pulsed electric current were more pronounced on alloys with higher silicon content.

The tensile strength and micro hardness of the alloys were uniformly increased with the application of the electric current.

The results obtained in [45] have demonstrated the application of an electric current of approximately 500mA/cm^2 during solidification has the following effects on the cast microstructure of hypereutectic Al-Si alloys:

(i) The average dendrite cell size was reduced in all cases except the for the at the bottom of the Al-20 wt.% Si alloy.

(ii) The applied electric current did not change the size of the largest primary silicon particles, but it appeared to have qualitatively increased the population of relatively smaller sized primary silicon particles in the Al-20 wt.% Si alloy.

(iii) Qualitatively, the applied electric current did not change the size or size distribution of the primary silicon particles in the Al-13 wt.% Si alloy.

(iii) The size, size distribution, and morphology of the eutectic silicon particles were not altered by the applied electric current during solidification.

For Al-20 wt.% Si alloy, the application of 465-518 mA/cm^2 steady electric current during solidification did not reduce the size of the largest primary silicon particles, but it appeared to have qualitatively increased the population of relatively smaller size primary silicon particles. The application of electric current during solidification did not appear to have any effect on the size or size distribution of primary silicon particles in the Al-13 wt.% Si alloy [45].

The application of a steady electric current during solidification did not appear to have any effect on the size or morphology of the eutectic silicon particles in both the Al-13 wt.% Si and Al-20 wt.% Si alloys.

2.3 Conclusion.

Hypereutectic Al-Si alloys have been investigated because of their excellent properties, which include excellent wear and corrosion resistance, high temperature strength, low coefficient of thermal expansion, good cast performance, and high specific strength. Therefore, the hypereutectic Al-Si alloys are used with advantage in aeronautic, astronautic, and auto- mobile industries. It has been documented extensively that the microstructure of hypereutectic Al-Si alloys, prepared by conventional casting routines, usually consist of a coarse primary silicon phase in a fibrous eutectic matrix. The brittleness of coarse Si crystals (both eutectic and primary silicon) is the main reason responsible for the poor properties of AI-Si alloys because coarse silicon crystals lead to premature crack initiation and fracture in tension. In order to refine the primary silicon, many methods have been carried into execution, such as high-pressure casting, rapid solidification technique, and melt overheating treatment.

However, these processes are complex and difficult to control. The desired properties cannot be obtained or may even become worse. The microstructure control using minor element addition is the most popular method due to its simplicity and effectiveness. Phosphor is the most effective refinement element of primary silicon in hypereutectic A1-Si alloy. The size of primary silicon particles can be refined to 20-30 pm by adding minor phosphorus.

Because the phosphorus has not any refinement effect on the eutectic silicon, the eutectic silicon can still keep the large needle shape. Recently, attention has been given to the

complex modification of primary and eutectic silicon in order to significantly enhance the mechanical properties of hypereutectic AI-Si alloys. It has been documented that RE, Ti, Sr and so on can modify the eutectic silicon in the hypereutectic AI-Si alloys. The refinement of primary silicon crystals was also found with addition of these elements. If combining with P and these elements to complexly alloy the hypereutectic Al-Si alloys, both the primary and eutectic silicon in alloys may be modified and the mechanical properties may be improved.

In the present study, the grain refinement of hypereutectic Al-20% alloys with AlCuP master alloys was conducted. The influences of phosphorus content on the microstructure and mechanical properties of hypereutectic Al-20% alloy were investigated.

3. Experimental Work

3.1 Methodology of experiment

Purpose of present study is finding out the complete grain refinement method and its mechanism of hypereutectic aluminum silicon alloys, especially the alloys with 18-20 wt. % silicon. Thereby apply to produce the piston of high-powered diesel engine of truck and bus in Vietnam, in order to replace the imported products, hence, to contribute to Vietnam automotive industry.

The main subject of present study is piston which was made by hypereutectic aluminum silicon alloys with 18-20 wt. % silicon. It was refined by using AlCuP master alloy with 0.5-1 wt. % phosphorus.

3.2 Study methodology

3.2.1 Reaction chamber, experimental system and mold design.

Reaction chamber: Operation principle of reaction chamber is indicated on figure 3.1. Aluminum and grinded CuP were melted in resistance electric furnace, raising the temperature till to melting temperature was reached. This molten was poured into the reaction chamber. Under stirring, Al, CuP and phosphorus release together. The master alloy has to be cooled as fast as possible.

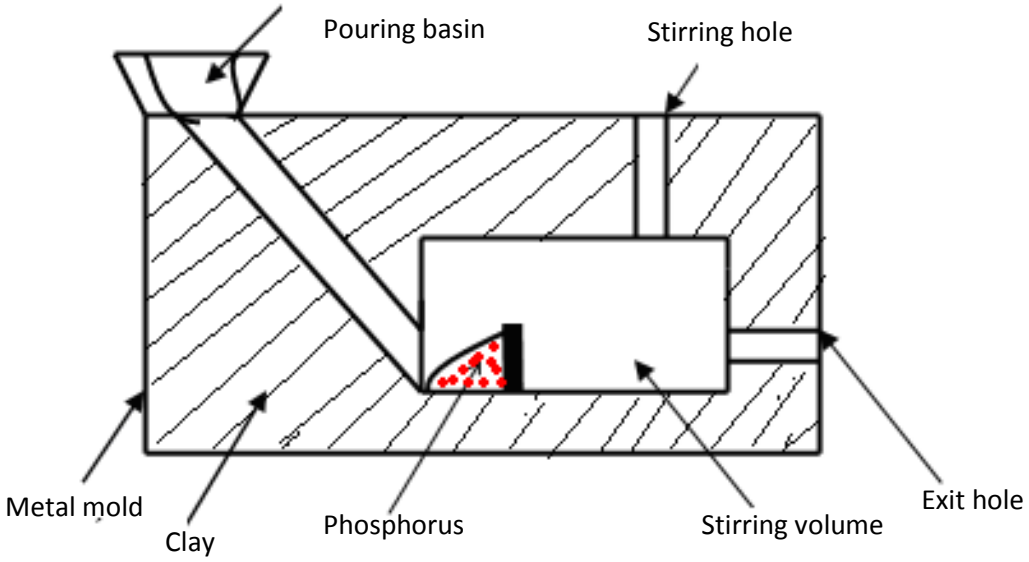

Figure 3.1 Design of reaction chamber

The stirring volume of this chamber is following the expression:

$$\Delta = \frac{G}{F \times t} \quad (9)$$

Where, Δ is the solubility of reaction chamber, kg/m^2.s.

G is amount of molten metal, kg.

F is the square area of reaction chamber, m^2.

T is pouring time, sec.

Follow formula (9), principle dimension of stirring volume is 25 centimeters in length and 10 centimeters in high.

Mold design: In designing the geometry of the mold and what material the mold should be made from, the following considerations were of primary importance:

- A mold material cannot react with tested alloys, and has thermal conductivity higher than aluminum silicon alloys to provide sufficient refinement rates.
- Ease of fabrication of the mold.
- Cost of the mold.

The first decision made was to cast flat plates, rather than a cylindrical geometry. Figure 3.2 shows the general shape of the mold including holes for two dowel pins in order to locate two halves of the mold each other.

Experimental system: Figure 3.3 shows the experimental system of this present study.

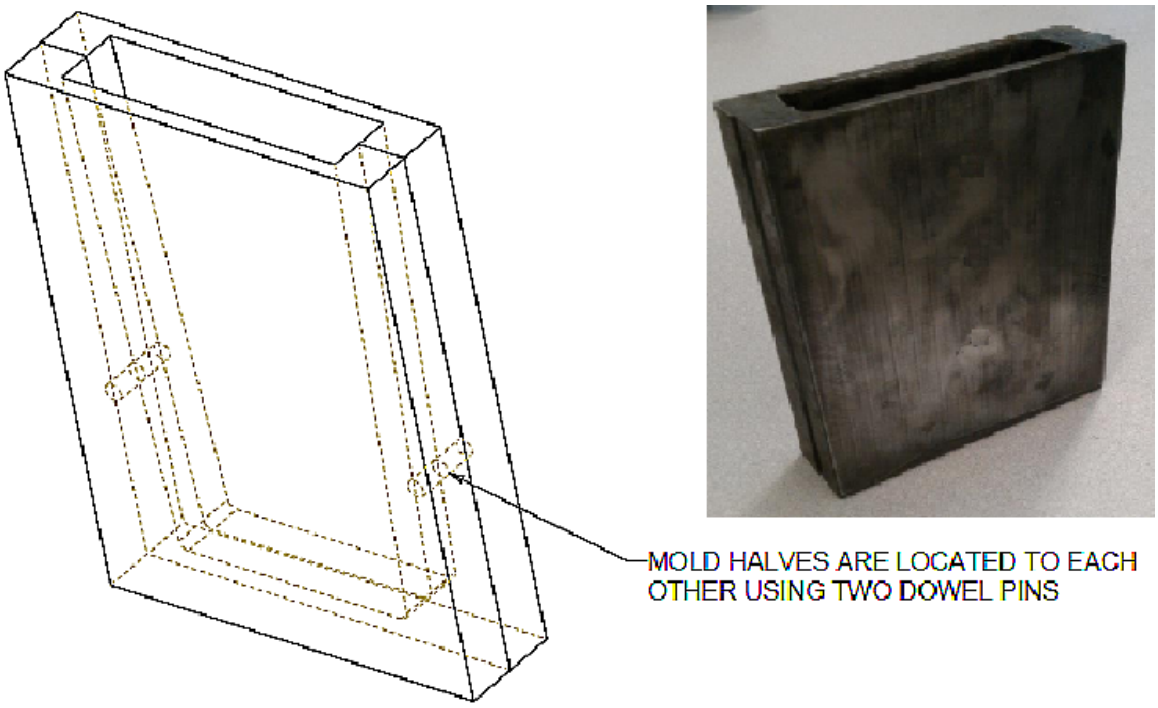

Figure 3.2 Mold machined from mild steel. The two halves of the mold were located to each other using dowel pins.

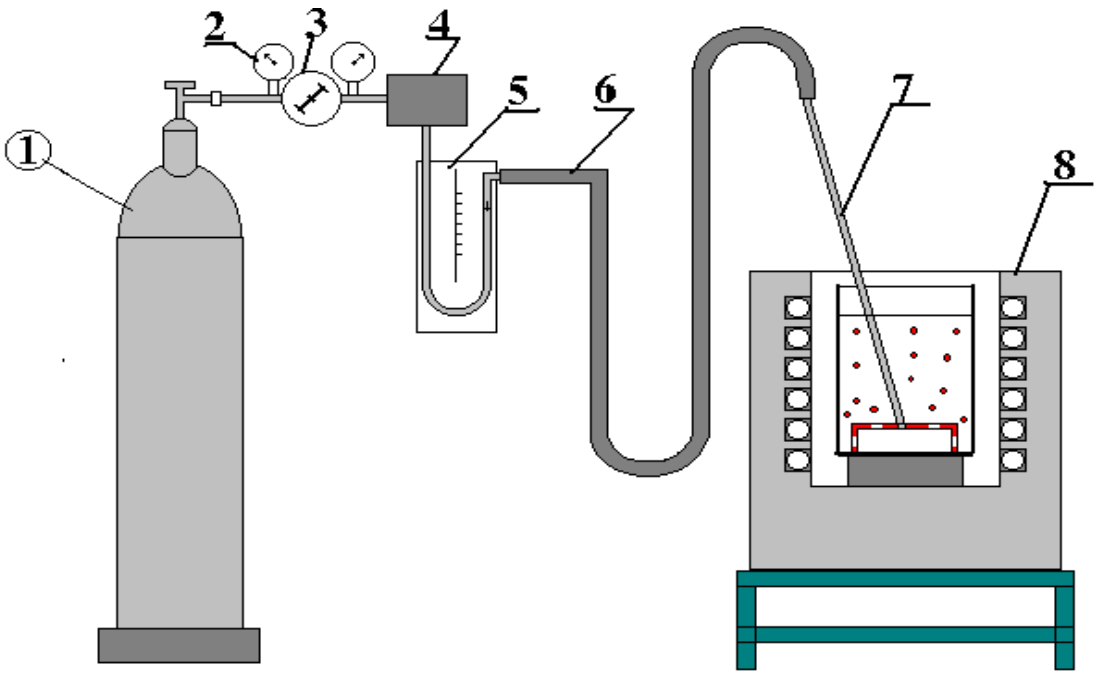

Figure 3.3 Experimental systems.

Where, 1 is argon tank; 2 is barometer; 3 is pressure reducing valve; 4 is filter of steam and deoxidize; 5 is differential pressure flow meter; 6 is pipe; 7 is blow-pipe; 8 is resistance electric furnace.

3.2.2 Manufacture process of master alloys.

The Al-CuP master alloy was produced with Cu-10P, pure phosphorus and pure aluminum respectively. The selected content of master alloy was 8 wt. % copper, phosphorus was as much as possible and aluminum for the rest. After calculating loss of burning, amount of each material is listed in table 3.1. Notice that, phosphorus was already selected without calculating because of its high loss of burning and content as much as possible.

Table 3.1 Amount of materials preparing for manufacture master alloys.

No.	Materials
1	2 kilograms of pure aluminum
2	0.4 kilograms of Cu-10P
3	0.25 kilograms of pure phosphorus

According to theory, phosphorus burns easily. And phosphorus almost does not dissolve in aluminum; it only reacts with a negligible amount of aluminum to form aluminum phosphide. Thereby it was very difficult to add phosphorus to master alloys. There were three methods to produce Al-CuP master alloys:

- Pure aluminum was melted and increases the temperature over 800 ^{0}C. Then, Cu-10P was added to the melt under covering of salt compounds. After stirring, the melt was poured in metal mold. Analyze results showed that composition of phosphorus in master alloys was only 0.56-0.84 wt %.
- Pure aluminum was melted and increases the temperature over 800 ^{0}C. Then, Cu-10P was added to the melt under covering of salt compounds. After stirring and keep temperature on the proeutectic area, the melt was poured in a metal mold. Pure phosphorus was added in the mold before. Master alloys was quick stirred and cooled by water. The results showed that composition of phosphorus in master alloys only was increased to 0.6-0.9 wt.%. Beside, this method brought about pollution of environment.
- After many experiments, present study found out a suitable method. Pure aluminum was melted and increases the temperature over 800 ^{0}C. Then, grinded Cu-10P was added to the melt under covering of salt compounds. After fully stirring, the melt was poured in a reaction chamber (figure 3.1). Pure phosphorus was added in the reaction chamber before. Master alloy was quick stirred in the reaction chamber. Then, it was

poured in a metal mold that had been preheated at 150 ^{0}C, and obligatory cooled by water. In the results, composition of master alloy was 0.72-1.05 wt. % phosphorus and approximately 18 wt. % copper. This method did not bring about of environment pollution.

3.2.3 Grain refinement process.

The tested alloys which were used in this study are hypereutectic aluminum silicon alloys with 18-20 wt. % silicon. The Al-CuP master alloys were used, and addition amount of refiner is listed in Table 3.2.

Table 3.2 Addition amount of refiner (mass fraction, %).

Group No.	Phosphorus, %	Refinement temperature, ^{0}C
1	0.001	850
2	0.002	850
3	0.004	850
4	0.005	850
5	0.006	850
6	0.015	850
7	0.02	780 850 950
8	0.02 + 0.1 AlTi5B	850
9	0.03	850

In order to study on the influence of refinement methods, this present study used three methods as follow:

a) Refining complexly the primary silicon, eutectic silicon, α-Al, sodium compounds, the Al-CuP and AlTi5B were used.
b) Using Al-CuP master alloys to refine primary silicon and sodium compounds to refine eutectic silicon. AlTi5B did not be used.
c) Only refine primary silicon using Al-CuP master alloys.

All of above methods had the same melting process.

- Before melting, furnace, ladle, gating system, materials, slag-forming constituents, mold and needed equipment must be fully preheated. Especially mold was painted with the liquid mixture of graphite and water glass at 100 ^{0}C.

- Materials, slag-forming constituent and covering flux were added to ladle. Temperature of furnace was increased to 750-800 ^{0}C. Slag-forming constituent and covering flux are sodium compound. It includes 15 wt. % cryolite (Na_3AlF_6), 25 wt. % potassium chloride (KCl) and 60 wt. % sodium chloride (NaCl). Its melting temperature was 660 ^{0}C. Added amount was 0.05-0.1 wt. % of charge.
- After alloys were melted fully, slag was removed. Degassing was applied by using argon. Degassing flow was 2 liters per minute, and degassing time was 5 minutes.
- Increasing furnace temperature to 850-870 ^{0}C, keep this temperature during 20 minutes. Master alloys were added to refine the molten. Notice that, master alloys had to cut to small pieces. For the refiners were melted completely, the melt must be stirred. Refinement time is 8 or 10 minutes. Then, the molten was poured in molds.
- For revealing the refinement effects of primary silicon, metallurgical test samples were cut directly from tested alloys. For comparison, all samples were cut from the same position. The tested samples were machined to the standard samples. Dimension of tested sample was showed in figure 3.5.

3.2.4 Evaluate methods of mechanical properties of tested alloys.

(a) Microstructure of the tested alloys was observed and quantitatively analyzed using Axiovert 100A microscope and Leica DM 4000M microscope with an image collection and analysis system.

Figure 3.4 Microstructure analysis systems.

(b) The mechanical properties tests were carried out using MTS 809 Axia-Torsion Test System (figure 3.7). A typical cylindrical tensile sample is illustrated in the sketch below.

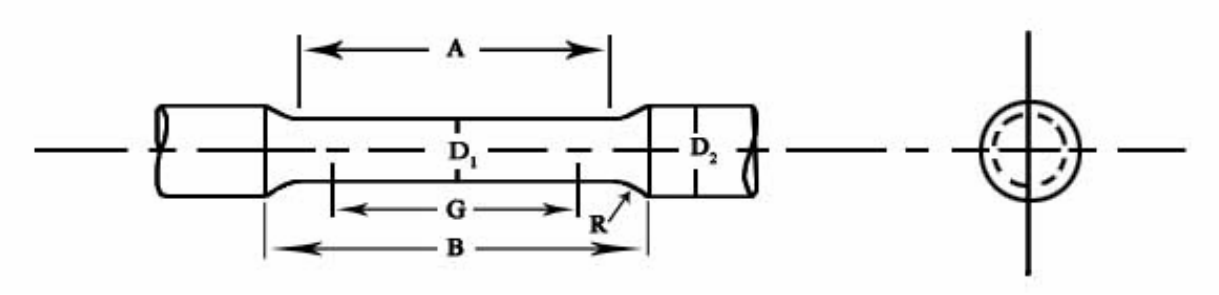

Figure 3.5 The typical tensile sample.

The important dimensions to measure prior to a tensile test are given below.

- Two marks are made within the uniform section A. The distance between these two gauge marks, denoted as G in the figure above, is called the gauge length.
- The diameter, D_1, of the gauge is measured to calculate the area of cross-section. An average several values of the diameter are taken.
- Overall, the dimensions D_1, D_2, B and R for the above tensile sample are as per some specified standard. In this present study, A = 50 mm, B = 80 mm, D_1 = 10 mm, R = 5 mm.

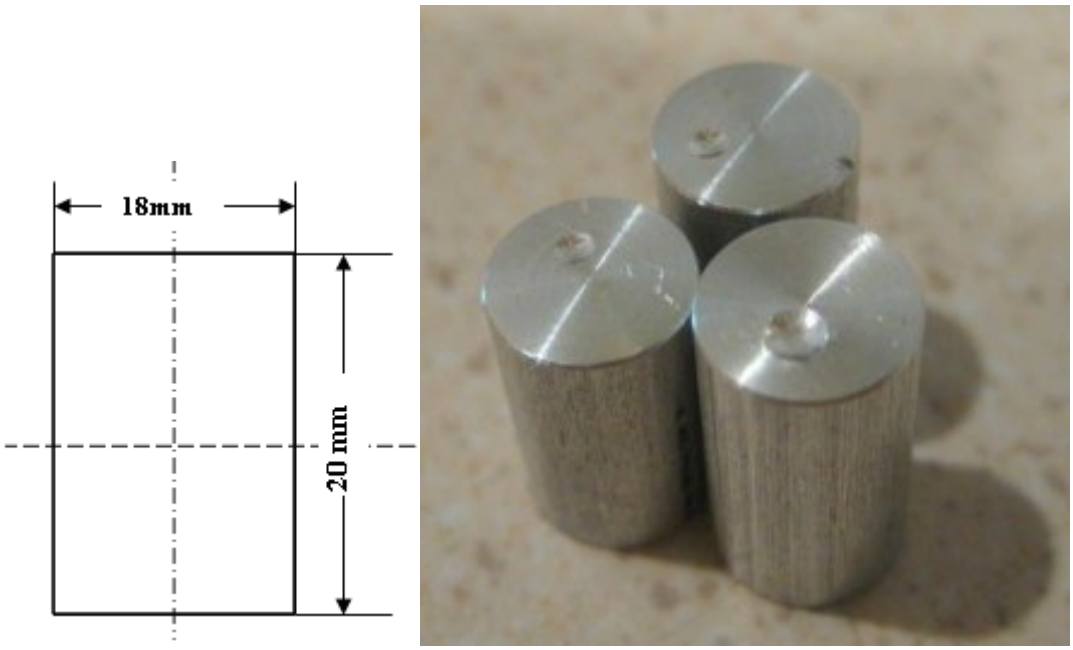

Figure 3.6 Hardness and abrasion test samples.

Figure 3.6 shows the samples of hardness test and abrasion test. In the hardness test, a hardened ball was pushed into a material sample with a known force. The diameter of the indentation is then measured. The hardness number is calculated as

$$HB = F / (\pi/2 \times D \times (D - \text{sqrt}(D \times D - I \times I))) \quad (10)$$

Where, F = Force applied, Kgf; D = ball diameter, mm; I = indentation diameter, mm; π = 3.14159

Figure 3.7 MTS 809 Axia-Torsion Test System.

4. Results and Discussion

4.1 The refinement mechanism of hypereutectic aluminum silicon alloys.

4.1.1 The formation of nucleation site.

From the theory above, dissolved phosphorus combines with aluminum and forms aluminum phosphide (AlP) crystals. AlP crystals in the melt increase the amount of hereogeneous nucleation sites for silicon which solidifies later. Equilibrium among phases was calculated using ThermoCalc version M. Solubility of phosphorus in the melt is evaluated as a function of two variables: temperature and silicon content.

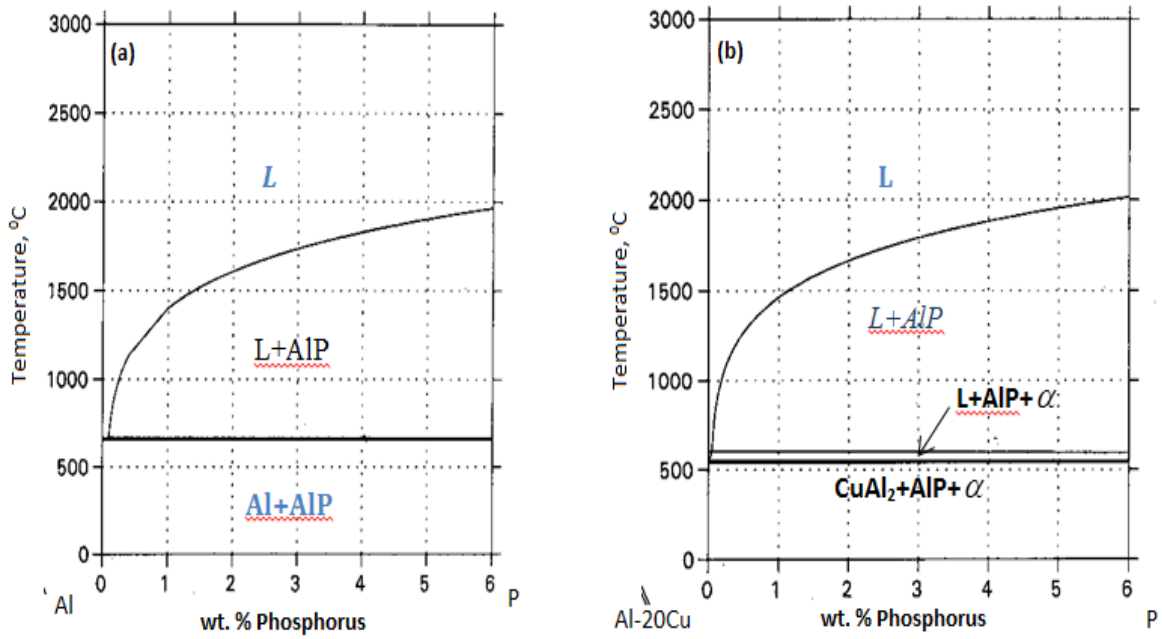

Figure 4.1 Equilibrium phases diagram of master alloys.

The problem here is the solution of phosphorus in melt. Even in theory or in fact, it is very difficult to add more than 1 wt.% of phosphorus to master alloys. Figure 4.1 indicates that aluminum phosphide was the first phase which was formed from liquid. Amount of this phase depends on phosphorus content and temperature. This amount will increases with the increasing of temperature and phosphorus content. But, amount of aluminum phosphide was small, i. e, at 100 ^{0}C, this amount is less than 0.1 wt. %.

Figure 4.1 (b) shows that the diagram of master alloys was shifted to the left because of copper effect. And, copper acted as a master role to add more phosphorus in the melt. Under low cooling rate, phosphorus seems not be dissolved in aluminum or α-Al. Follow the CuP phase diagram, copper and phosphorus can combine together to form Cu_3P. But in figure

4.1 (b), there was not any inter-metallic phase between copper and phosphorus. During production process of master alloys Al-CuP, the below reaction was happened.

$$7Al + Cu_3P = AlP + 3CuAl_2$$

However, it can say that aluminum phosphide (AlP) ready exits in master alloys. When the grain refinement process occurred, aluminum phosphide dissolves rapidly into the melt. They act as nucleation sites for primary silicon.

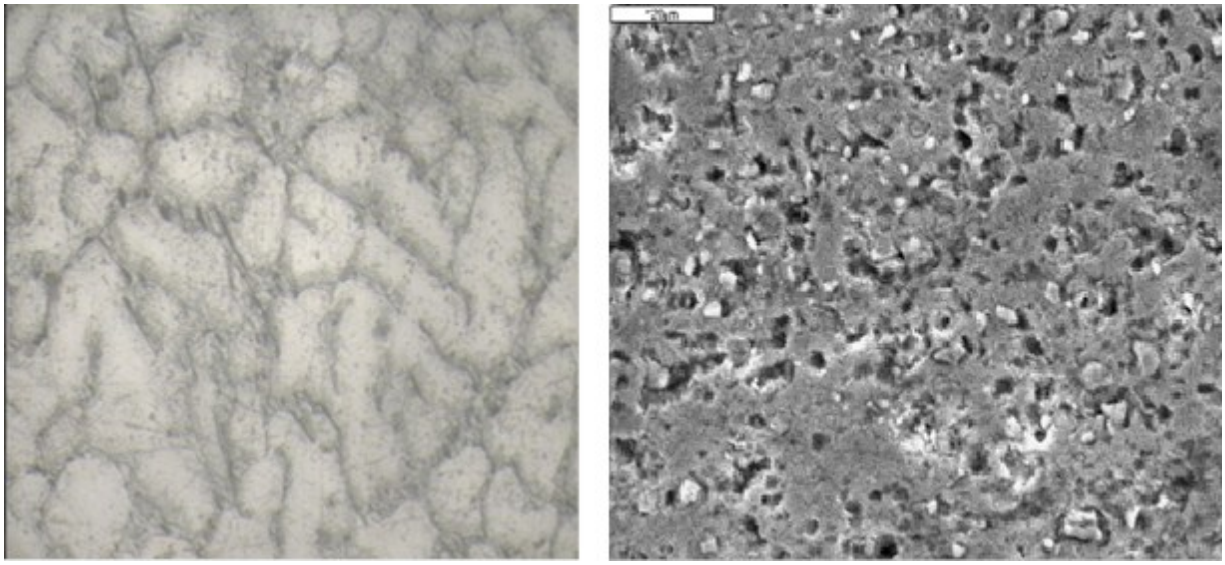

Figure 4.2 Microstructure of AlP master alloys.

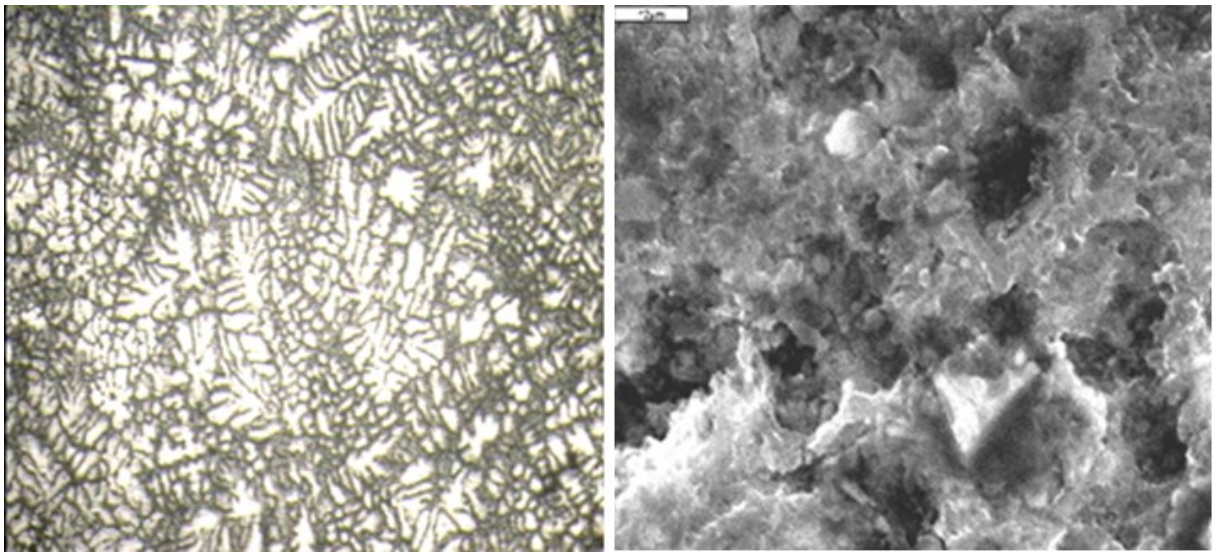

Figure 4.3 Microstructure of Al-CuP master alloys.

Figure 4.2 and 4.3 show different magnification of microstructure of Al-CuP master alloy. It can be seen that, the microstructure of master alloys includes α-Al and inter-metallic phase (Al-Cu) on the border of particles. Besides, there were dark phases. Maybe these phases were solid solution (α-Al) contenting retained phosphorus. Because, when master alloys were produced, amount of added phosphorus was saturated higher than the maximum value which

is assumed to be the phosphorus solubility in liquid alloys. After pouring in a mold, master alloys were cooled as fast as possible. Hence, phosphorus was retained in master alloys as segregations.

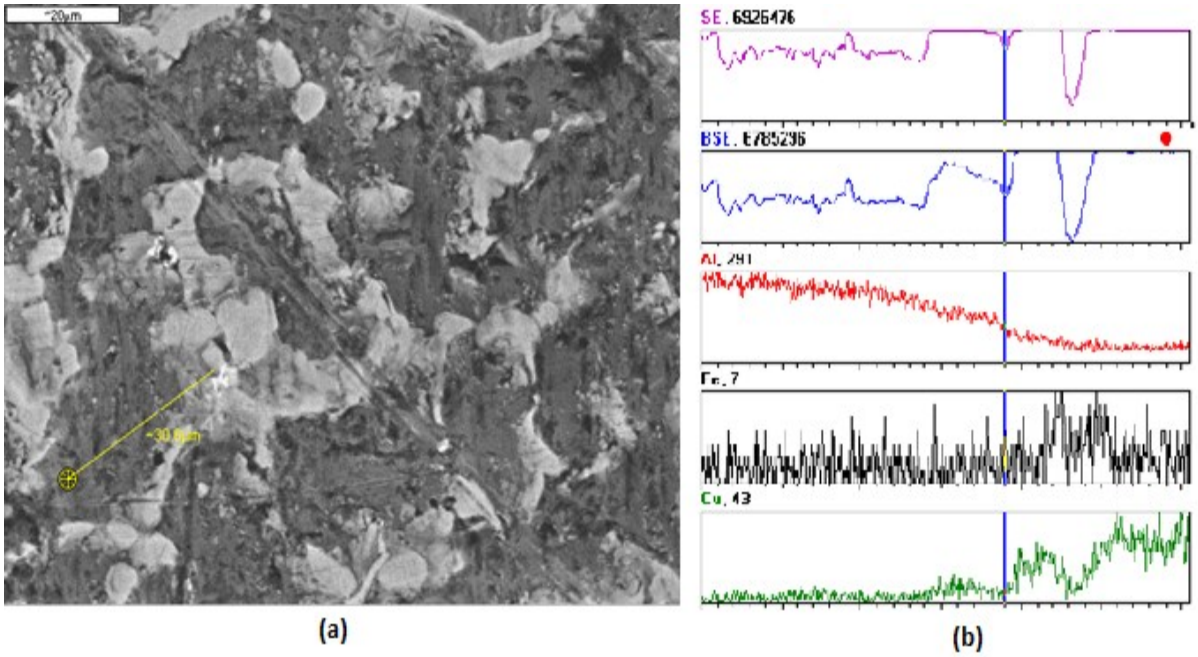

Figure 4.4 EDS analysis of Al-CuP master alloys.

The yellow line in figure 4.4 (a) shows the EDS analysis for concentrated distribution of elements that was existed in Al-CuP master alloys. The results, figure 4.4 (b), indicates that copper and iron concentrated on the border of particles, aluminum mostly existed in α-Al particles.

Table 4.1 Lattice structure and parameters of crystals in master alloys.

	Lattice structure	**Lattice parameter**					
		a	**b**	**c**	**α**	**β**	**γ**
Al	Face-centred Cubic	4.05925	4.05925	4.05925	90	90	90
Si	**Face-centred Cubic**	**5.43090**	**5.43090**	**5.43090**	**90**	**90**	**90**
Fe	Body-centred Cubic	2.86620	2.86620	2.86620	90	90	90
AlP	**Face-centred Cubic**	**5.43000**	**5.43000**	**5.43000**	**90**	**90**	**90**
Al_4Cu_9	Primitive Cubic	8.70230	8.70230	8.70230	90	90	90

Table 4.1 shows lattice structure and lattice parameters of crystals using X-Ray analysis. Master alloys were produced under cooling condition being in metal mold. Water was used as cooling medium to increase the cooling rate.

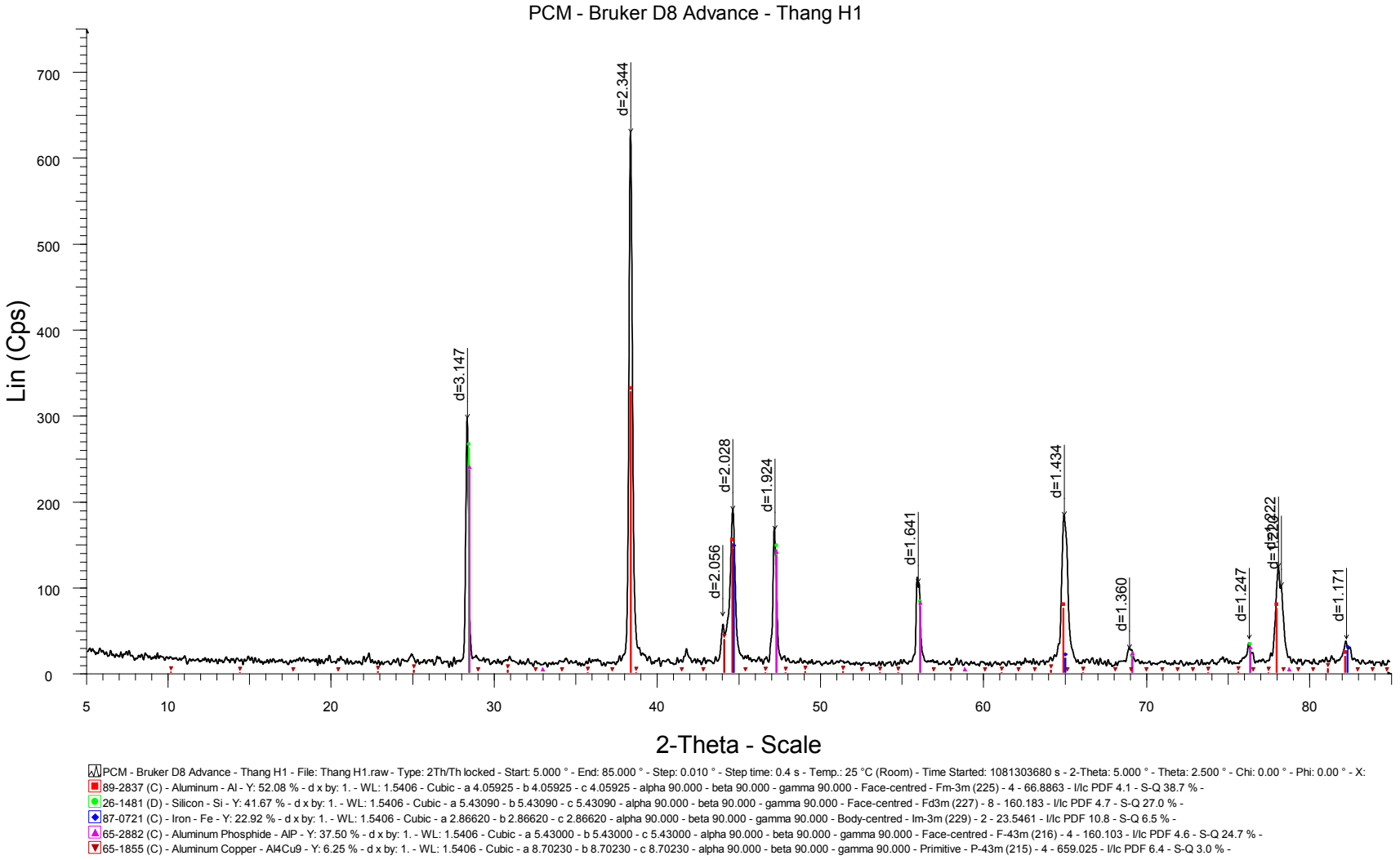

Figure 4.5 X-Ray diffraction of AlCuP master alloys

According figure 4.5, X-Ray diffraction of master alloys was showed. Only solid solution α-Al, aluminum phosphide (AlP) and inter-metallic phases (Al_4Cu_9) were formed. Besides, cause of impurities in alloys, silicon and iron also were occurred. This result completely appropriates to equilibrium phases diagram of master alloys which was showed in figure 4.1. However, there was a difference between equilibrium phases diagram and result of X-Ray diffraction. Because of low cooling rate, inter-metallic phase was Al_2Cu in diagram. But, the cooling rate, which was applied during production process of master alloys, need to be as fast as possible. Inter-metallic phase here was Al_4Cu_9.

Furthermore, table 4.1 and figure 4.5 also indicated that both of silicon crystal and aluminum phosphide had the same lattice structure (face-centred cubic). And the lattice parameters of silicon crystals and aluminum phosphide were significant difference. According to basic theory, a substrate can be a nucleation site for another if they have the same lattice structure and parameters. Thereby, aluminum phosphide absolutely can be the nucleation site for silicon which will crystalize later.

Conclusion: in order to compare with previous study [7] using CuP master alloys, phosphorus mostly existed in inter-metallic phase (Cu-P). The results of present study, using Al-CuP master alloys, indicates that phosphorus combines with aluminum and acts directly as a nucleation site for silicon. In addition, phosphorus can retain in solid solution α-Al. Retained phosphorus can be a reserved source which will creates nucleation site during refinement process.

4.1.2 The refinement mechanism.

ThermoCalc version M was applied to build equilibrium phases diagram of ternary hypereutectic Al-Si-P system. Hypereutectic alloys of three different compositions: 18 and 20 wt.% silicon were used in the experiment. Al-CuP master alloys which used as refining agent for primary silicon was produced successful in this present study.

Figure 4.6 (a) and (b) are the calculated vertical section of ternary Al-Si-P system for 18 and 20 wt. % silicon, respectively. From these figures, it can be seen that the phosphorus solubility in melt for aluminum phosphide (A-B line), increases with the elevated temperature but, decreases with the increased silicon content. The solubility in melt for silicon (B-C line) and Si + AlP (B-D line) increase with the decrease of temperature. The increased solubility is the result of phosphorus atom which cannot dissolve and will be rejected to the retained molten alloy. B point in these figures describes peritectic line of AlP-Si. The peritectic temperature is slightly higher than the liquid temperature of silicon in binary Al-Si alloy. D

point in these figures indicates an invariant ternary reaction temperature at 580 ^{0}C, slightly lower than the eutectic temperature of binary Al-Si alloy.

From figure 4.6, aluminum phosphide (AlP) was the first phase which formed from molten alloy. Follow the results above, AlP already exists in master alloys or retained phosphorus in master alloys combines with aluminum to form AlP. Silicon crystals can wrap completely around and develop follow peritectic reaction. This reaction (starts at B point and stops at D point) shows as below.

$$L + AlP \rightarrow L + AlP + Si$$

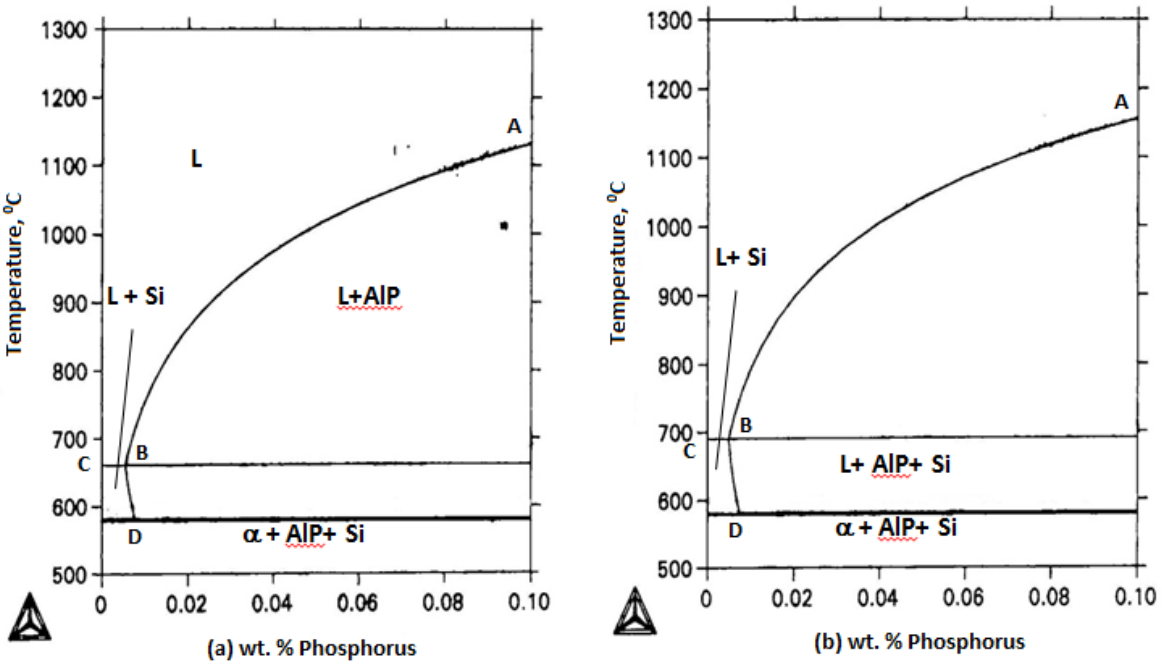

Figure 4.6 Equilibrium phases diagram of ternary hypereutectic Al-Si-P system. (a) for 18 wt.% Si; (b) for 20 wt. % Si.

When amount of aluminum phosphide in molten alloy increases, primary silicon particles becomes refiner and well distributed. Melting line of molten alloy was shifted to the left and higher temperature area with increasing amount of silicon content. It means that grain refinement effects will increase with increasing refinement temperature.

B-D line shows the influence of silicon crystallization on phosphorus saturation. Besides, amount of retained phosphorus in melt has an appropriate condition to form nucleation sites with increasing phosphorus saturation. Thereby, longer refinement time does not bad influence on size of primary silicon. Although some nucleation sites rise on the molten surface and lose effectiveness, some new nucleation sites are formed instead.

Hypereutectic Al-20Si alloys which were alloyed with 3 wt. % cooper, 1 wt. % nickel and 0.5 wt. % magnesium were investigated in figure 4.7. It can be seen that the diagram was shifted to the higher temperature and lower wt. % phosphorus area. Some inter-metallic phases, such as Al_3Ni, Al_2Cu and Mg_2Si, were formed. These phases not only made tested alloys being heat-treatable but also improve some thermal-mechanical properties, for example: wear resistant, thermal expansion as well as expansibility.

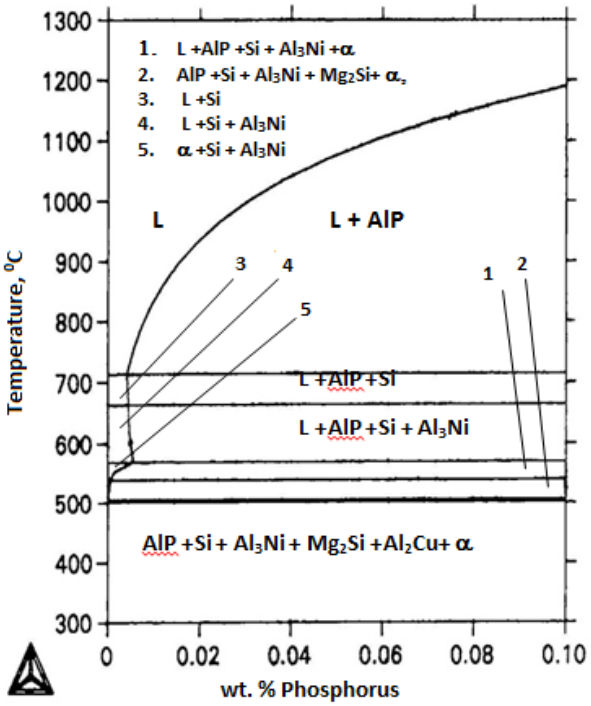

Figure 4.7 Equilibrium phases diagram of ternary hypereutectic Al-Si-P system.

As a result, present study reached the following conclusion:

- Aluminum phosphide was the main nucleation sites for primary silicon particles. These nucleation sites were formed not only during refinement process, but also during production process of master alloys.
- The refinement mechanism of primary silicon according to principle of peritectic reaction.

$$L + AlP \rightarrow L + AlP + Si$$

- The refinement effect becomes better with higher refinement temperature and appropriate refinement time.

4.2 Refinement process of hypereutectic aluminum silicon alloys.

4.2.1 Influence of refinement methods on quality of hypereutectic aluminum silicon alloys.

The experiment was applied to investigate the influence of three refinement methods. The first method was using sodium compound. It includes 15 wt. % cryolite (Na_3AlF_6), 25 wt. % potassium chloride (KCl) and 60 wt. % sodium chloride (NaCl). Added amount was 2 wt. % of charge. The second method was using mixture of Al-CuP and AlTi5B master alloys. Added amount were 0.02 wt. % phosphorus and 1.5 wt. % AlTi5B, respectively. And the third method was using Al-CuP master alloys. Added amount was 0.02 wt. % phosphorus per charge.

The negative phenomenon of sodium had to be controlled. Because sodium can adsorb on the surface of aluminum phosphide, then lose effectiveness of grain refinement. Sodium compound was added to melt before refinement using Al-CuP master alloys.

Particle size of primary silicon crystals of tested alloys were showed on table 4.2. Microstructures of tested alloys were showed on figure 4.8 and 4.9. Hardness and wear resistance were showed on figure 4.11. Where,

- **M0** is non-refined sample.
- **M1** is sample which was refined by 2 wt. % sodium compound and 0.02 wt. % phosphorus.
- **M2** is sample which was refined by 2 wt. % sodium compound, 0.02 wt. % phosphorus and 1.5 wt. % AlTi5B master alloys.
- **M3** was sample which was refined by 0.02 wt. % phosphorus.
- Tested alloys contented 21 wt. % silicon.

Table 4.2 Influence of refinement methods on particle size of primary silicon crystals.

No.	Refiner agent	Size of primary silicon, μm
M0	Non-refiner	214.7
M1	Sodium compound	17.0
M2	Sodium compound, AlCuP, AlTi5B	16.8
M3	AlCuP	28.7

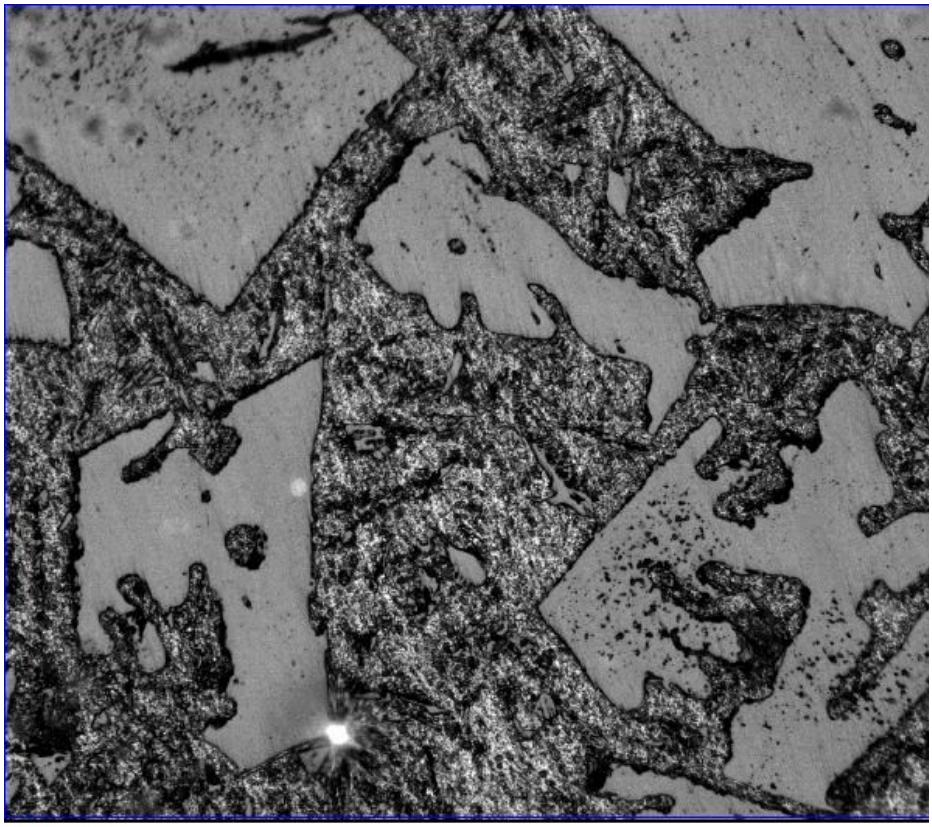

M0 x100

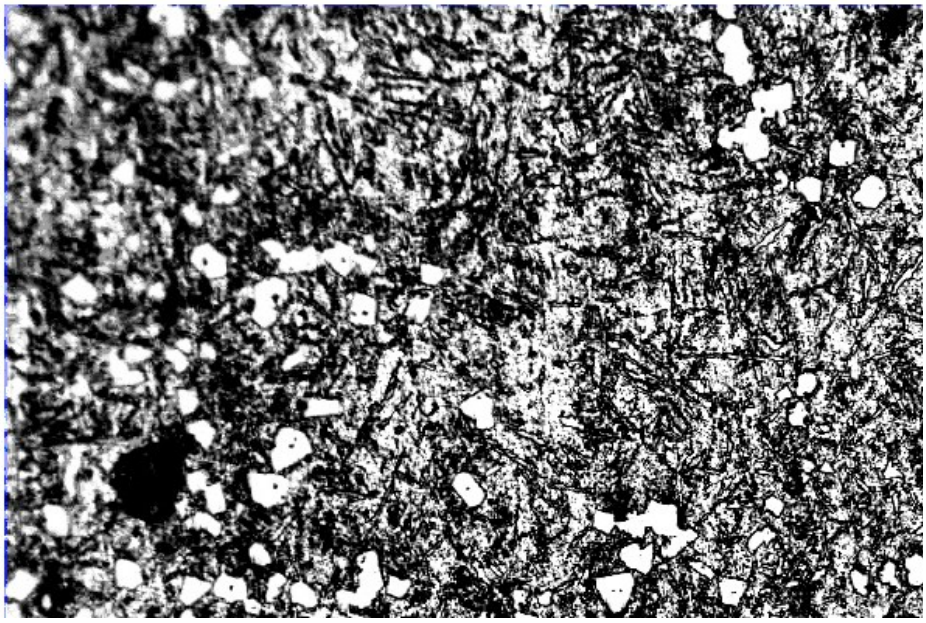

Figure 4.8 Microstructure of tested alloys; M0- non refinement; M1 – after refinement with sodium compound and phosphorus.

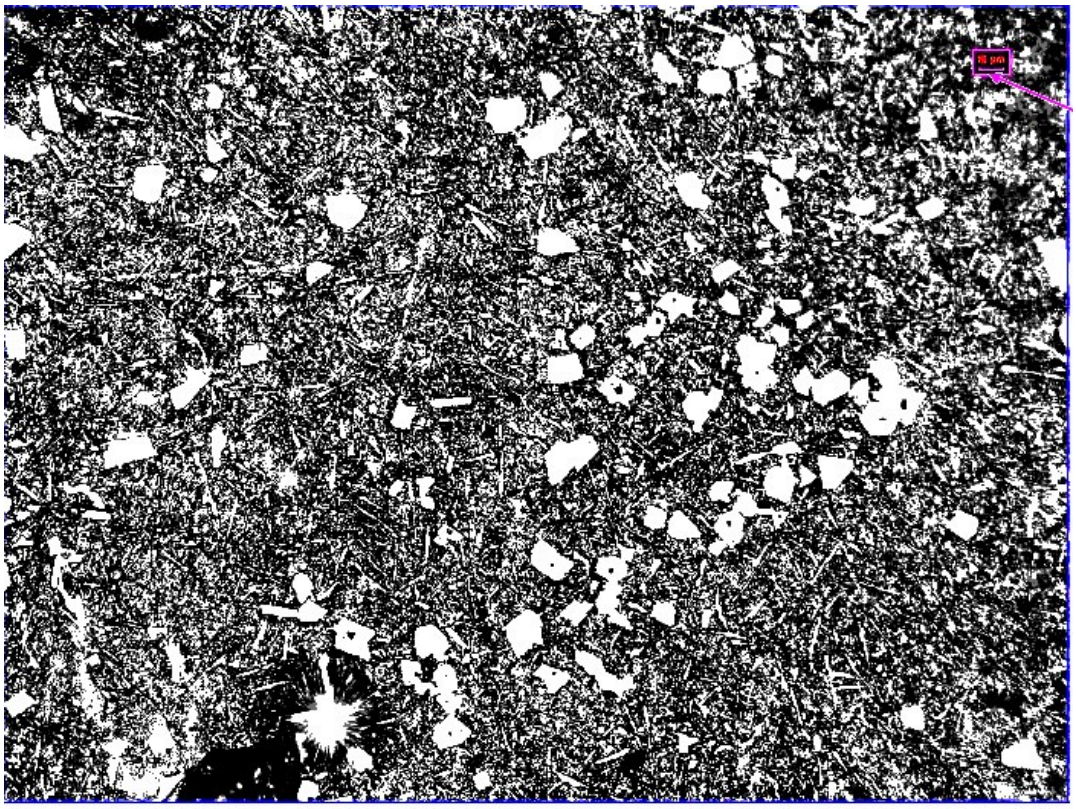

M2 x100

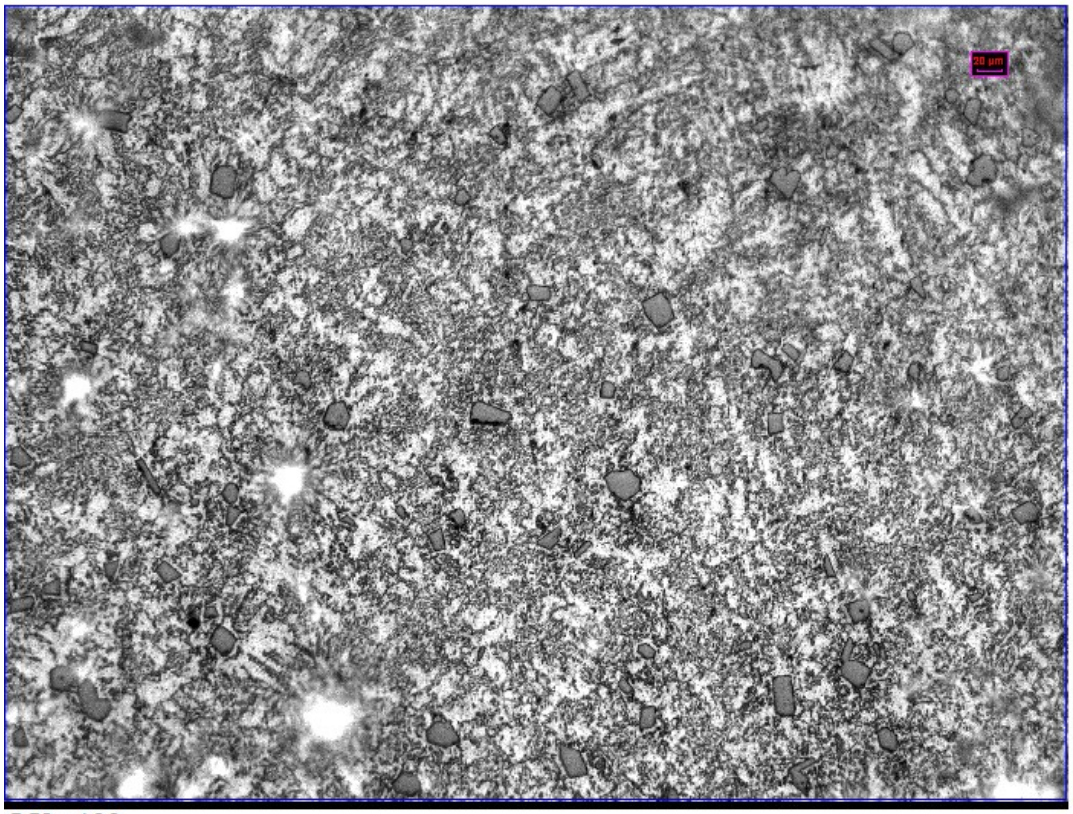

M3 x100

Figure 4.9 Microstructure of tested alloys; M2- After refinement with sodium compound, phosphorus and AlTi5B; M3 – After refinement with phosphorus.

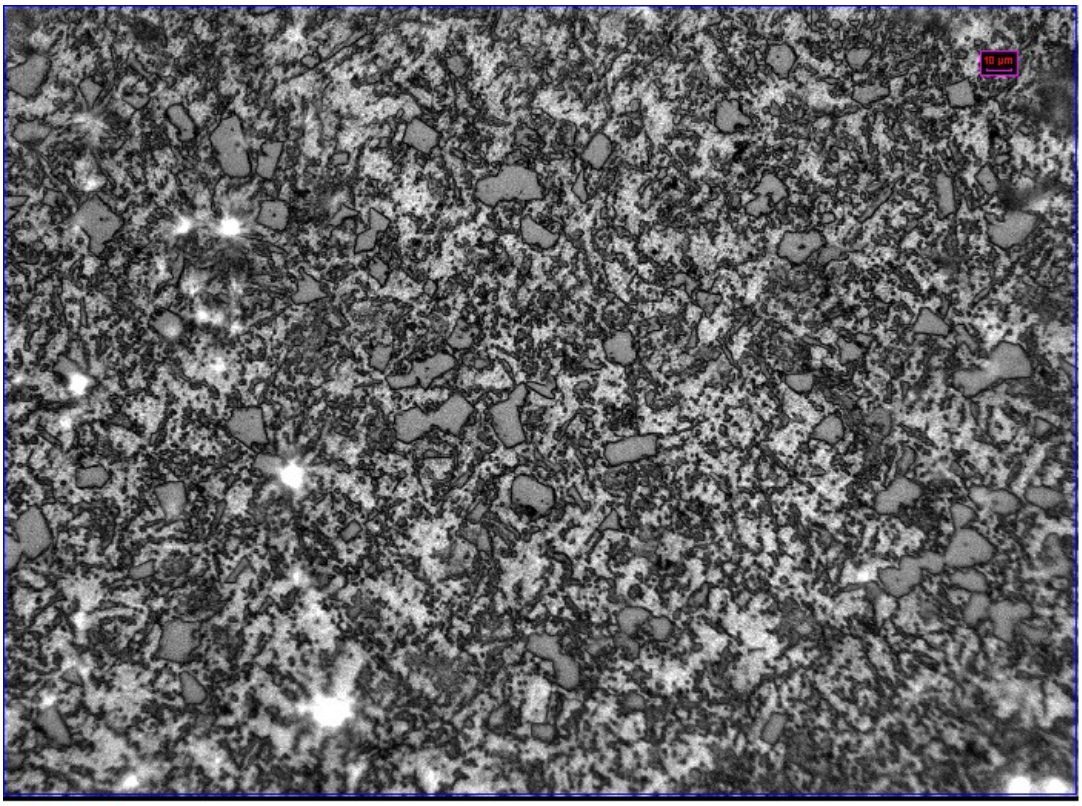

(a) x100

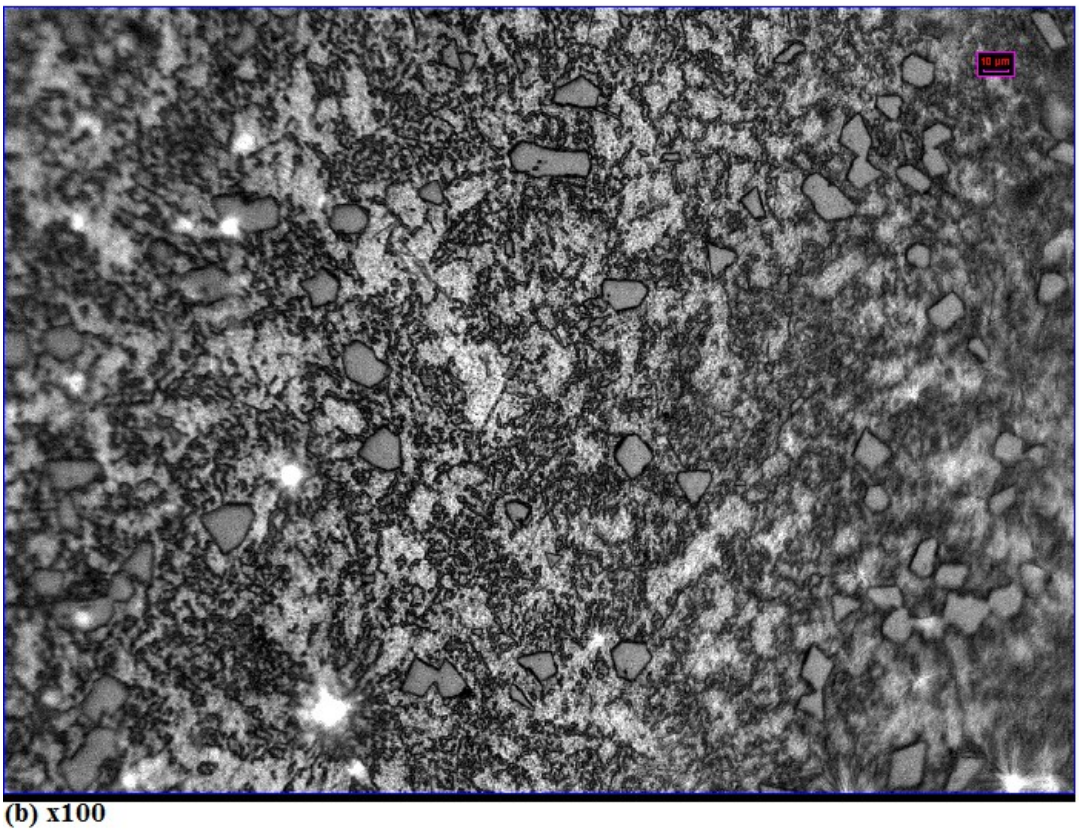

(b) x100

Figure 4.10 Comparison of microstructure using different refinement methods

From the results above, particle size of primary and eutectic silicon decreases after refinement. Furthermore, microstructures of M1, M2 and M3 indicates particle size of eutectic silicon significant decreases comparing with M3, sample does not refine using sodium compound. It shows that sodium and its compound proved their influence on refining eutectic silicon. In this experiment, sodium seems to have refinement effectiveness not only primary silicon but also eutectic silicon.

To affirm again this opinion, other experiment was used. The order of added refiner was changed. After melt temperature was overheated to 850 ^{0}C, tested alloys were refined by Al-CuP master alloys. The melt was stirring completely and slag was removed. Sodium compound was used to continue refine tested alloy. Amount of refiner which were used here and experiment above are the same. Results (figure 4.10) showed that particle sizes of primary and eutectic silicon still were similar as the case which sodium compound was first added, then Al-CuP master alloys.

Table 4.2 indicates that, after refinement, particle size of primary silicon was decreased more than ten times, from 214 μm to 18 μm. Comparison of M1 and M2 samples with M3 sample showed: particle size of primary silicon in M3 sample is larger. Particle size of M1 and M2 samples were changed insignificant. It means that Ti and B elements have no refinement effect of primary silicon. However, M1 and M2 samples were different in hardness and wear resistance significant (figure 4.11). M2 sample had the highest hardness (93 HB) and lowest wear resistance (1.8 %). From these results, Ti and B elements seem to refine aluminum particle on eutectic matrix.

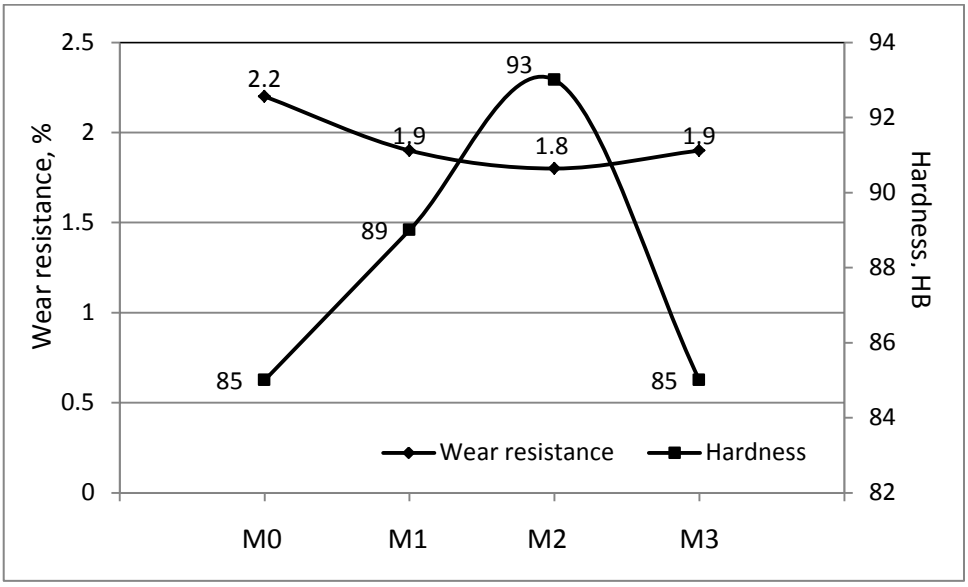

Figure 4.11 Hardness and wear resistance of tested alloys before and after refinement.

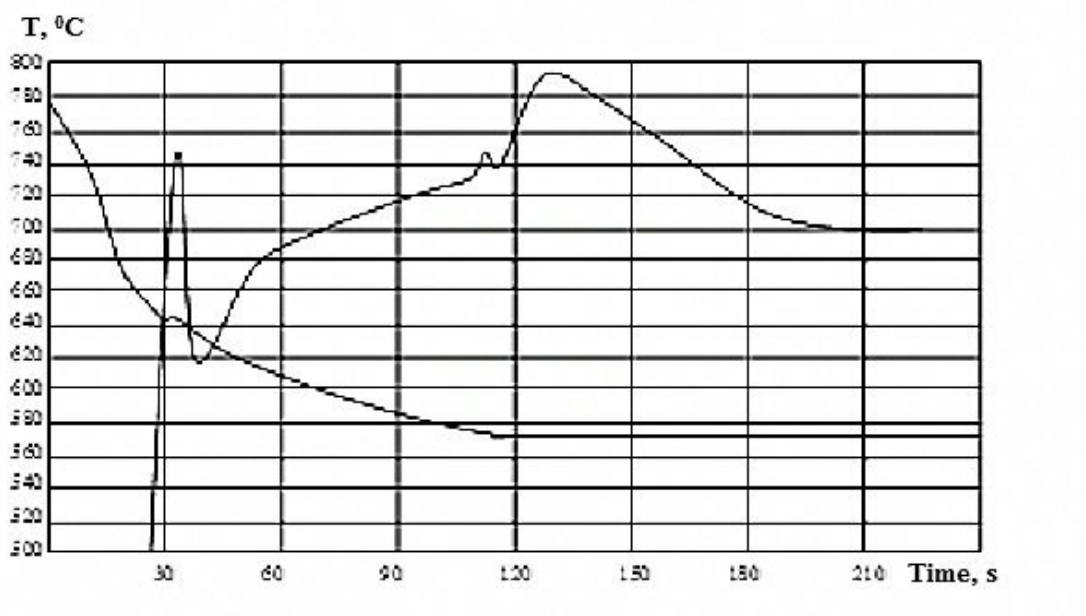

Figure 4.12 Diagram of thermal analysis DTA plotted for tested alloys after refinement with 2 wt. % sodium compound, 0.02 wt. % phosphorus and 1.5 wt. % AlTi5B master alloys.

Figure 4.12 shows the results of thermal analysis DTA of M2 sample. Two exothermic effects were occurred on cooling curve. The first effect takes place at 640 ^{0}C, and the second effect takes place at 577 ^{0}C. When this result was compared with equilibrium phase diagram of aluminum silicon alloys, eutectic temperature is 570 ^{0}C, the first effect occurs at higher temperature range. This temperature range was called proeutectic. And it was the exothermic effect of crystalline reaction of primary silicon. The second effect occurs at the approximate temperature of eutectic. This effect might relate to crystalline reaction of solid solution α-Al in eutectic, under influence of AlTiB master alloys.

Conclusion:

- Both of primary and eutectic silicon can be refined by using two kinds of refiner: sodium compound and Al-CuP master alloys. The order of refiner addition to melt does not affect to particle size of primary silicon. It means that sodium only adsorbs on the surface of silicon particles, not adsorbs on the surface of aluminum phosphides.
- Refinement mechanism was changed when AlTi5B master alloys was added. The second exothermic effect occurs at 570 ^{0}C. It seems to be a crystalline sign of solid solution α-Al in hypereutectic aluminum silicon alloys.

4.2.2 Influence of amount of refiner on refinement quality.

Only Al-CuP master alloys were used to investigate the refinement quality. Amount of added phosphorus are as follow table 3.2. Microstructure of samples were showed in figure 4.13 – 4.20. Data of particle size and properties were showed in table 4.3.

Table 4.3 Particle size and mechanical properties of tested samples.

Phosphorus, %	Particle size, µm	Hardness, HB	Wear resistance, %	Tensile strength, MPa	Elongation %
0.001	52.4	-	1.9	112.5	-
0.002	39.7	110	1.8	128.7	-
0.004	39	146	-	153.1	0.33
0.005	37.6	97	1.6	169.1	0.34
0.006	31.5	95.56	1.3	189	0.345
0.015	26.8	85	2.0	236	0.35
0.020	28.7	85	1.7	258	0.36
0.030	29.6	-	-	-	0.348

The effect of phosphorus on the primary silicon of the hypereutectic Al-20Si alloys is shown in figures 4.13 – 4.20. Many coarse block and stripe primary silicon can be found in the unmodified alloy (shown in Figure 4.l3). The addition of phosphorus refines obviously the primary silicon. The particle size of primary silicon decreases with increasing phosphorus content. And their edges and angles are passivated, as shown in figures 4.14 – 4.20. The optimal refinement effect of primary silicon is obtained when the alloy contains 0.006 to 0.015 wt. % phosphorus.

Follow figure 4.17, a little amount of refiner (0.006 wt. %) can prove the refinement effectiveness. However, particle size is quite large, approximate 30 µm. Increasing continuously the phosphorus content can decrease particle size of primary silicon to 25 – 30 µm. But, it can coarsen the primary silicon of the tested alloys, which means that excess phosphorus is unfavorable to the refinement of primary silicon.

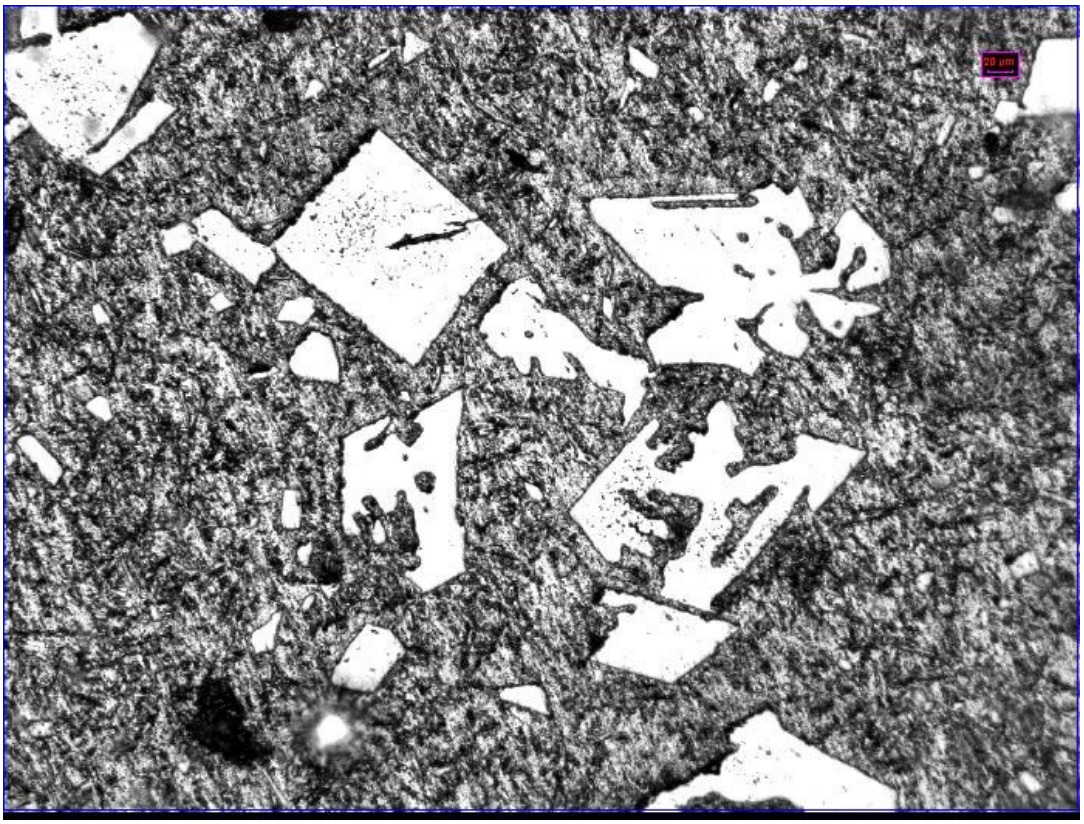

Figure 5.13 Microstructure of non-refined sample (x100)

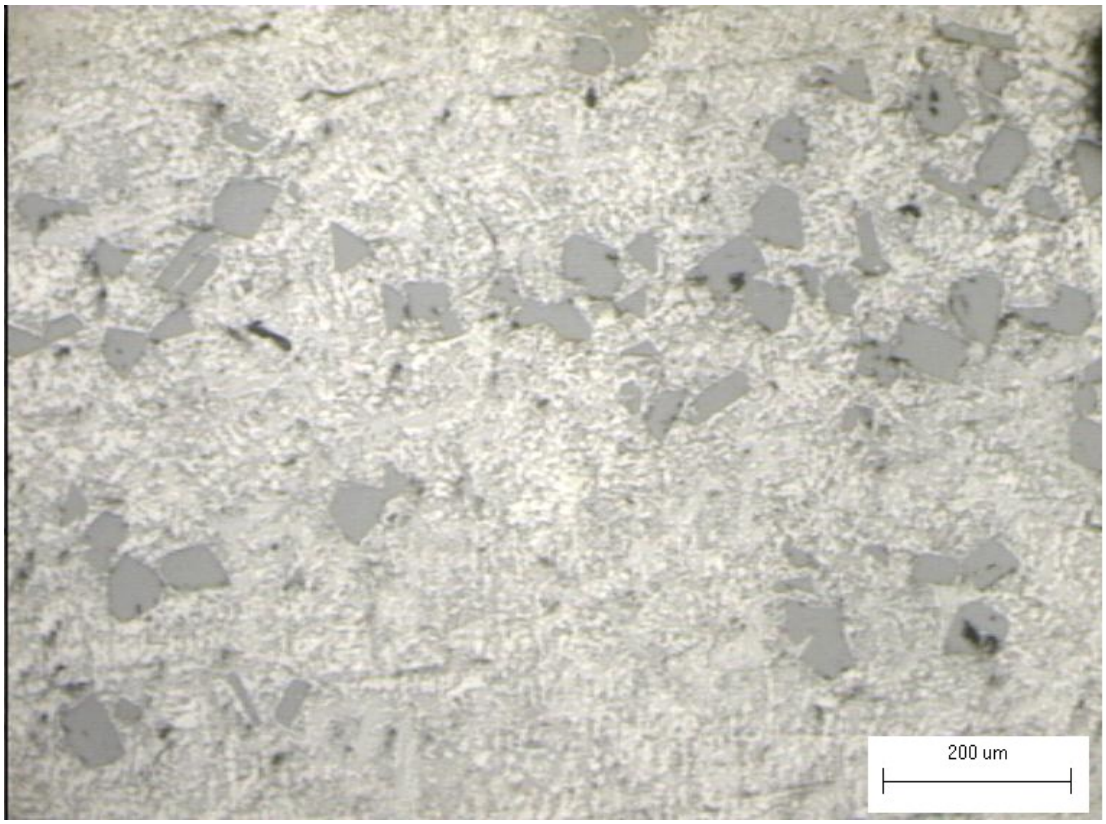

Figure 4.13 Microstructure of sample after refinement with 0.001 wt. % phosphorus.

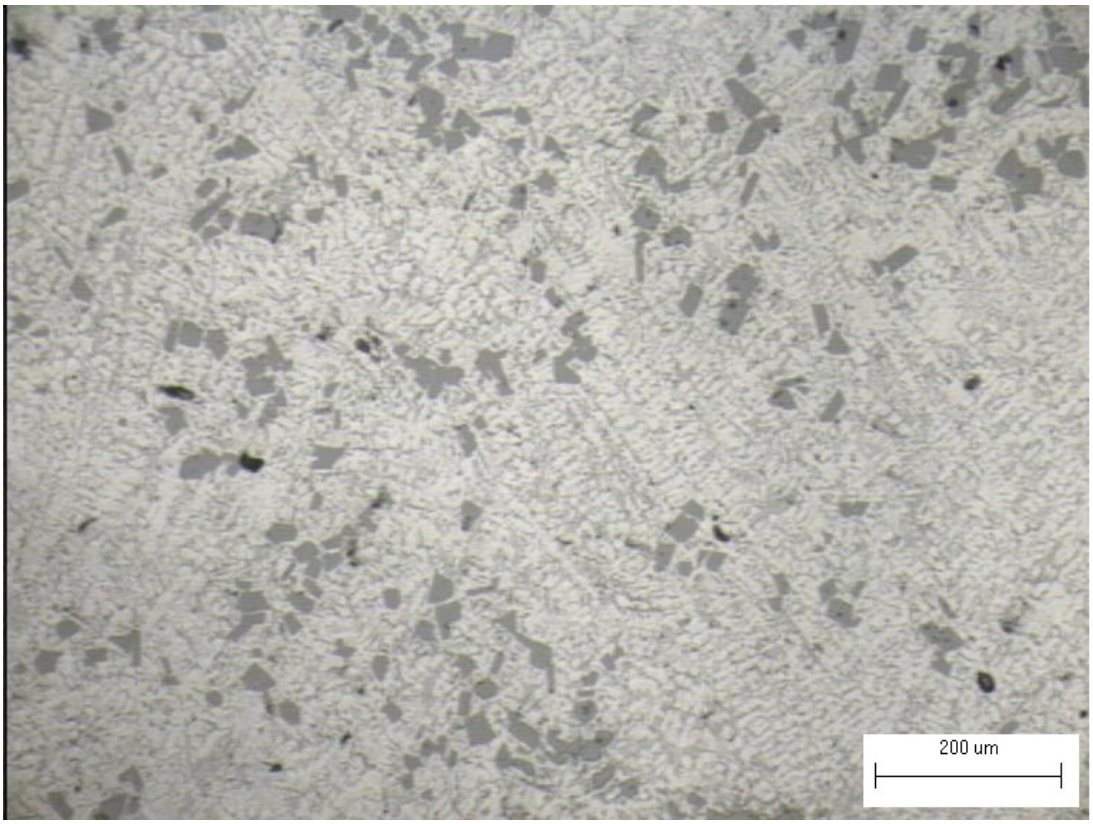

Figure 4.14 Microstructure of sample after refinement with 0.002 wt. % phosphorus

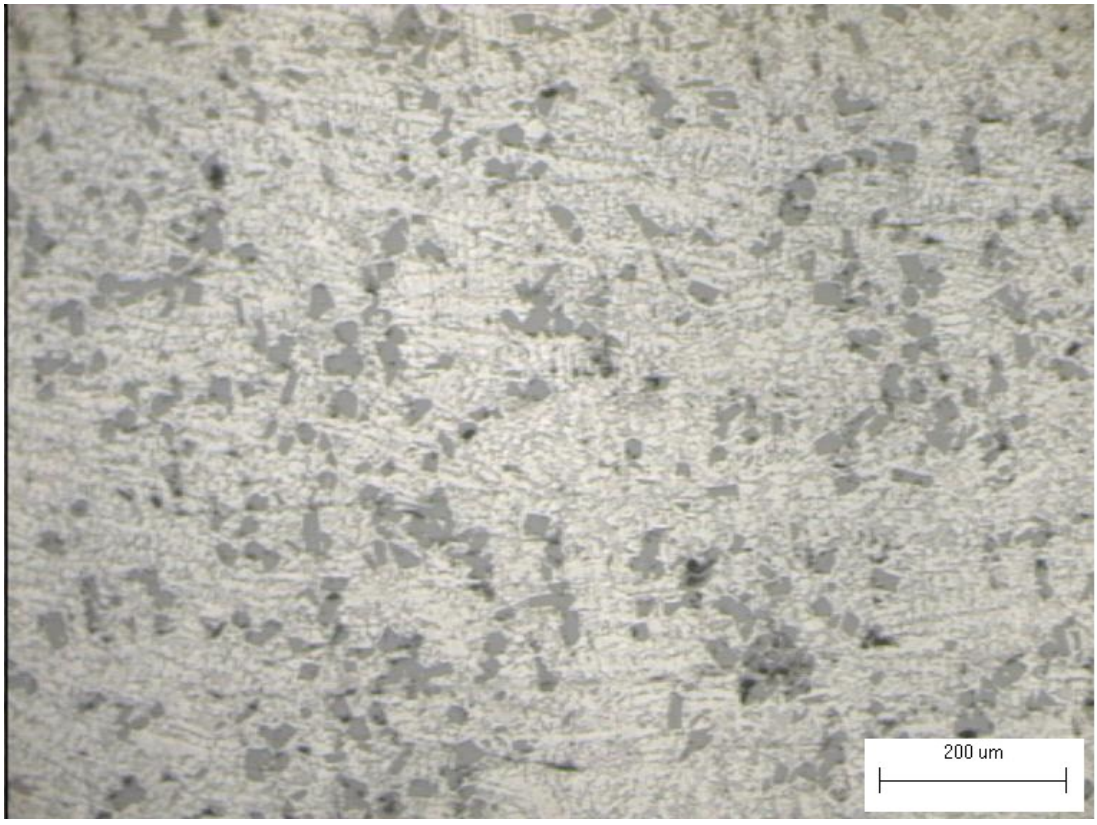

Figure 4.15 Microstructure of sample after refinement with 0.004 wt. % phosphorus.

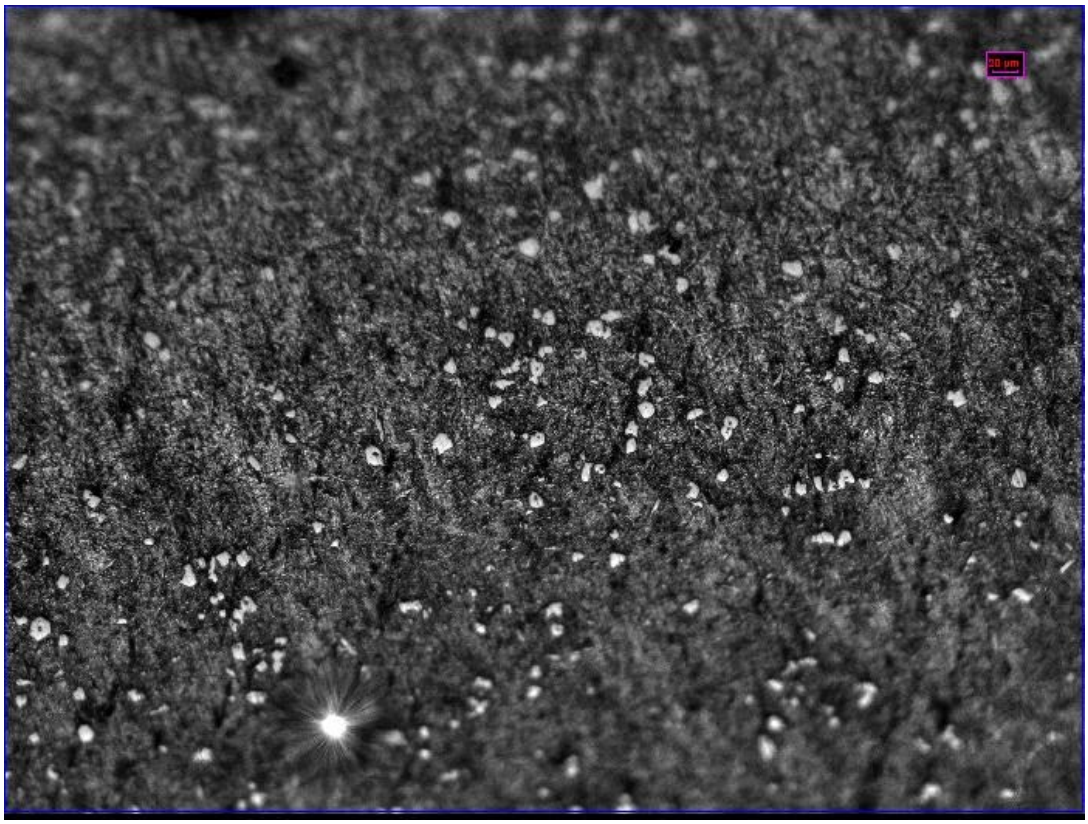

Figure 4.16 Microstructure of sample after refinement with 0.005 wt. % phosphorus.

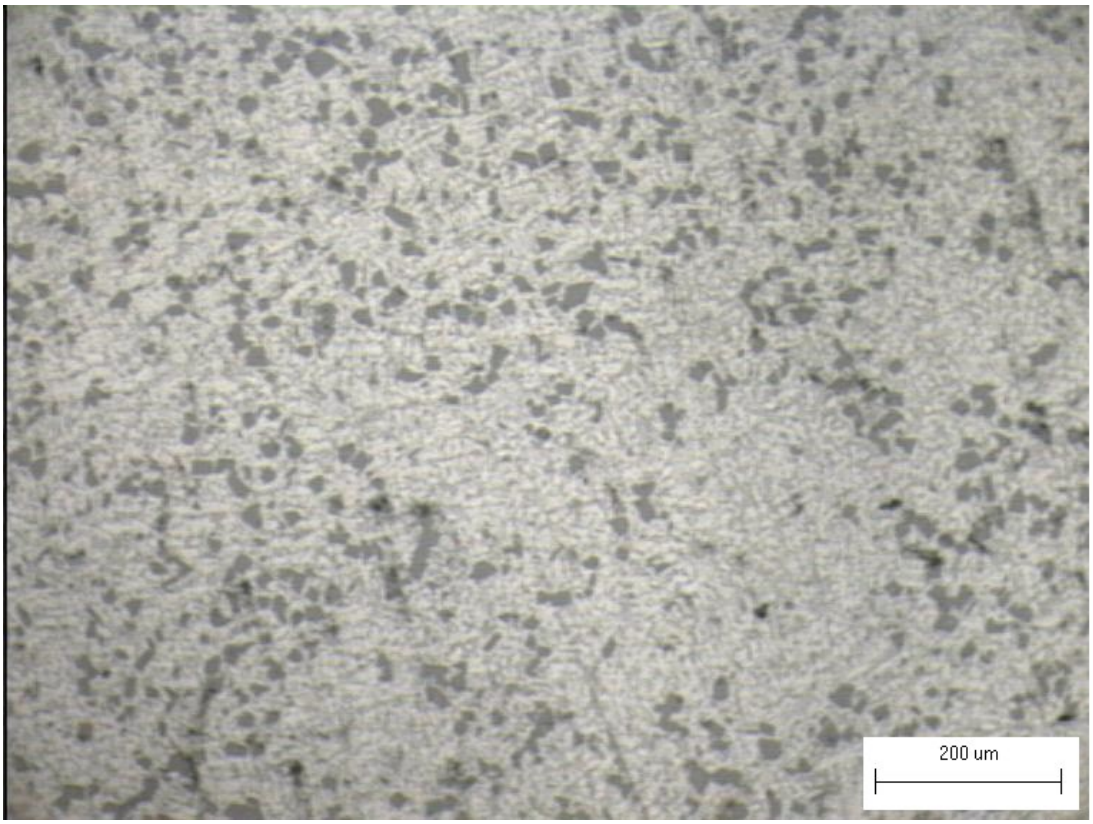

Figure 4.17 Microstructure of sample after refinement with 0.006 wt. % phosphorus.

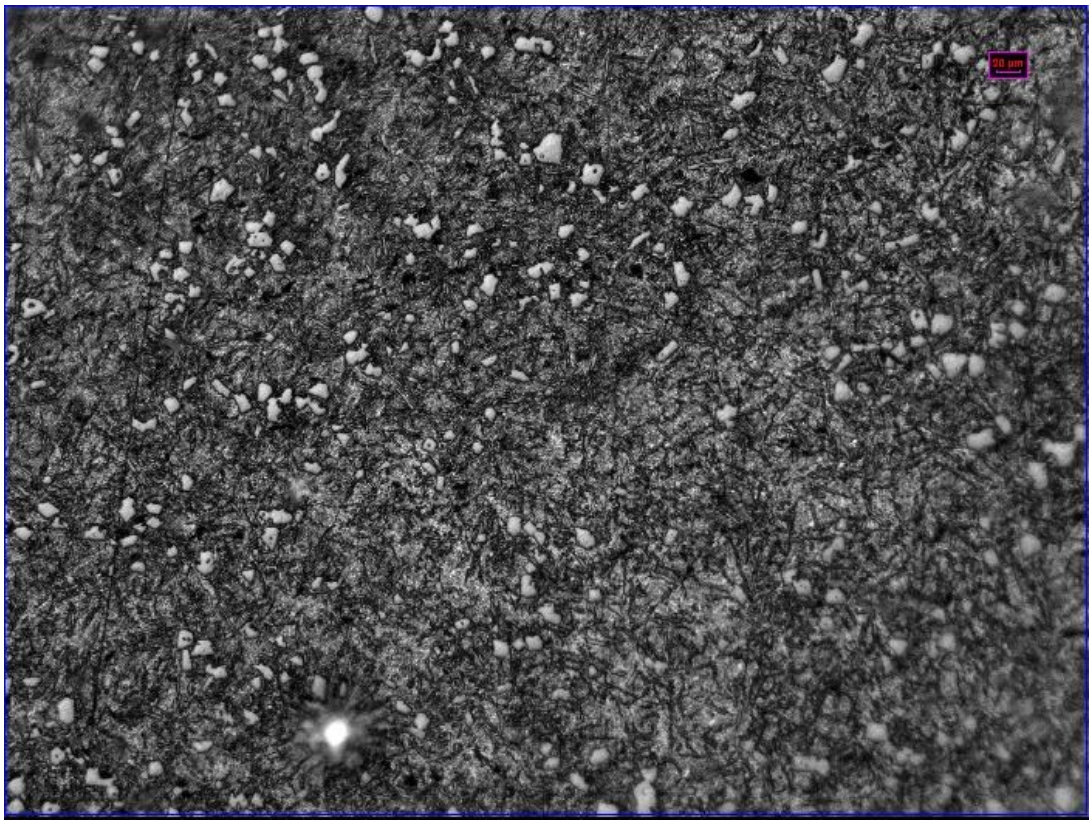

Figure 4.18 Microstructure of sample after refinement with 0.015 wt. % phosphorus.

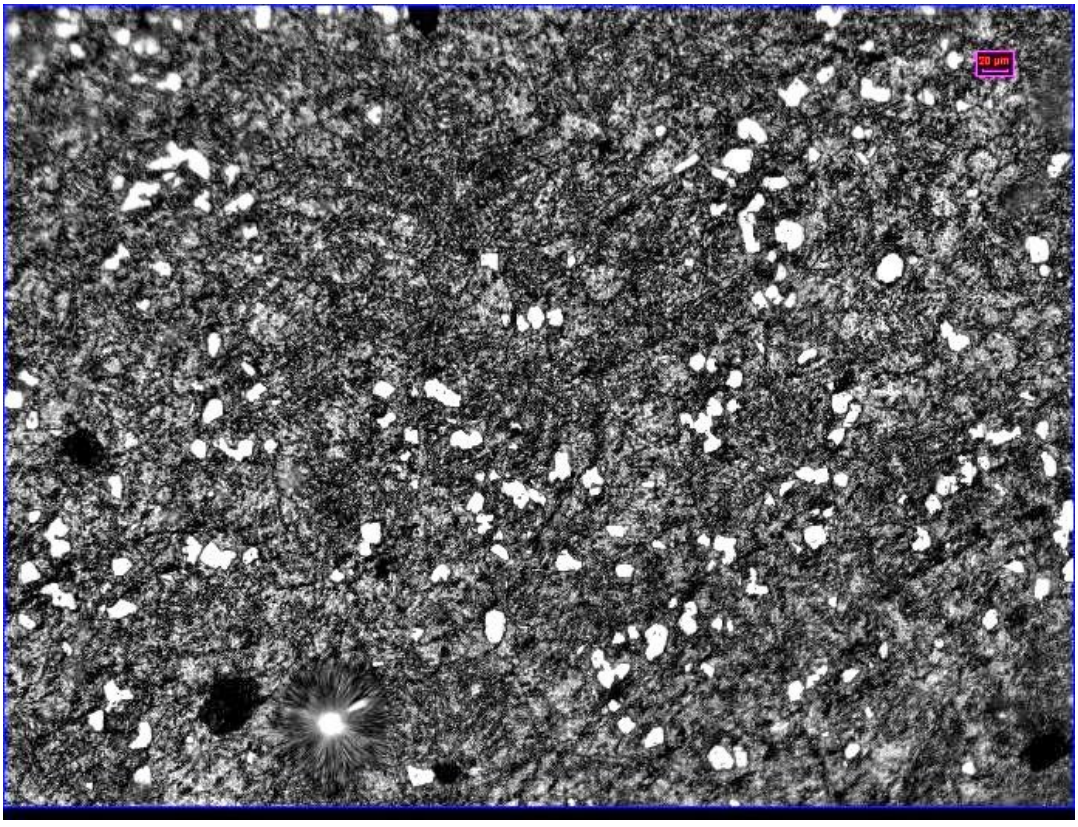

Figure 4.19 Microstructure of sample after refinement with 0.02 wt. % phosphorus.

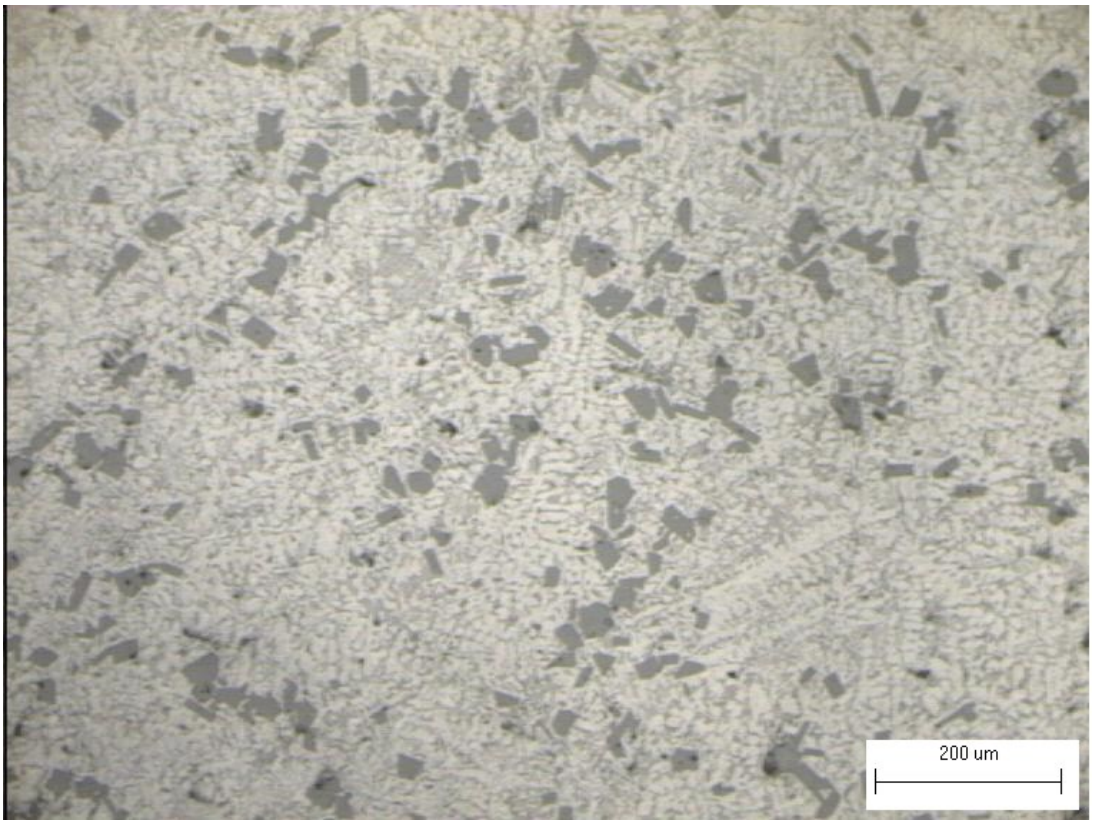

Figure 4.20 Microstructure of sample after refinement with 0.03 wt. % phosphorus.

Result above can be explained by point of view of thermodynamics of dissolving process and mutual interaction between the elements when refined. Follow this point of view, phosphorus solubility is decreased with increasing of silicon content. Silicon "pushes" phosphorus out of solution, and impulses phase formation of phosphorus at the beginning of crystalline process. Copper element increases solubility of phosphorus in melt. It also decreases phase formation of phosphorus. Phosphorus is formed after the melt reached a certain supercooling (ΔT). After being formed from melt, phosphorus immediate be aerosolized at temperature range over 500 ^{0}C. Phosphorus bubbles will be expanded suddenly. The result can make supercooling (ΔT) increases a little. During moving to the surface of melt, phosphorus bubbles will react with aluminum to create aluminum phosphide, nucleation sites of primary silicon. It explains the reason why almost phosphorus concentrated in the surface of cast. Besides, in the area of quite high silicon concentration, a supercooling (ΔT) occurs because of aerosolized phenomenon and expansion effect of phosphorus bubbles. This supercooling impulses formation and growth of particles. In the area of low silicon concentration, amount of phosphorus and its bubble pressure is not enough to create supercooling (ΔT).

As a result, with hypereutectic aluminum silicon alloys, phosphorus well had done its refinement role: creating nucleation sites while decreasing supercooling (ΔT), impulsing formation and growth process of nucleation sites.

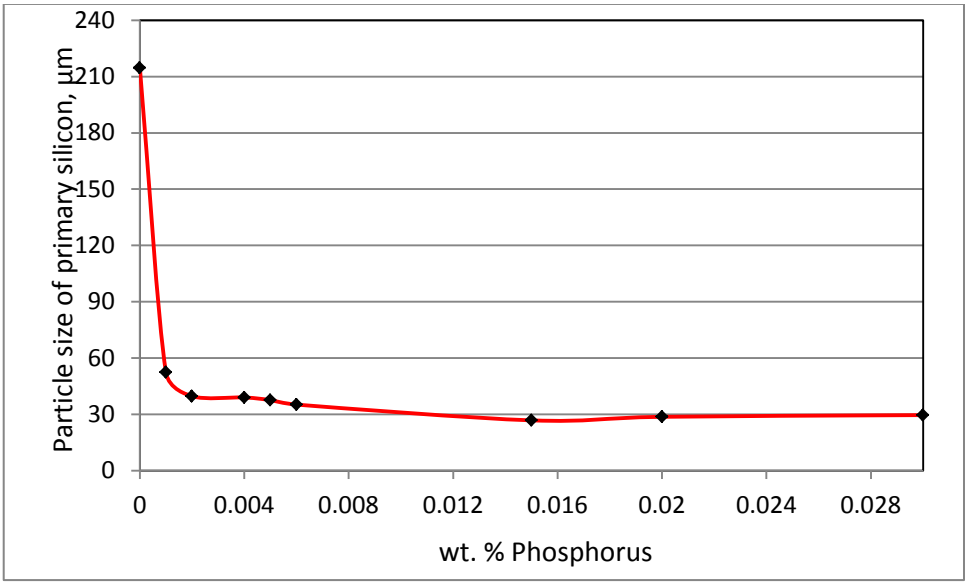

Figure 4.21 Relation between particle sizes of primary silicon and added phosphorus.

Figure 4.22 – 4.25 shows the mechanical properties of hypereutectic AlSi20 alloys with different refiner. The tensile strength and elongation increase with raising phosphorus content. When the tested alloys refined with 0.006 – 0.015 wt. % phosphorus, the optimal combination of strength and plasticity is obtained.

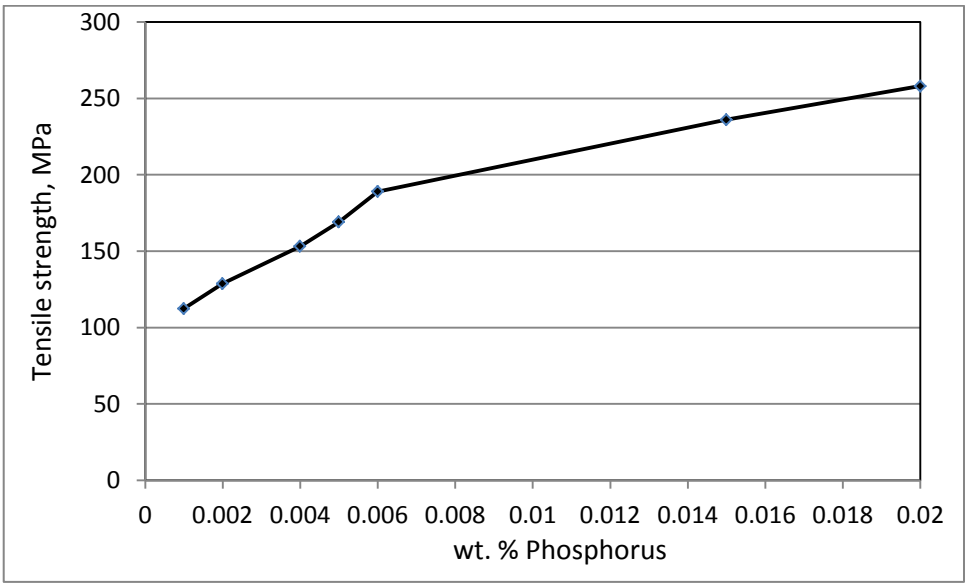

Figure 4.22 Relation between tensile strength and added phosphorus.

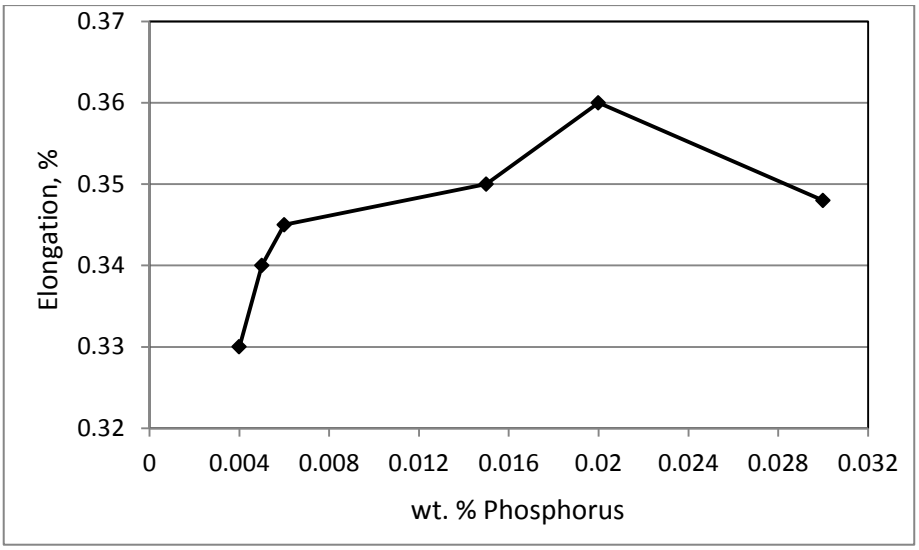

Figure 4.23 Relation between elongation and added phosphorus.

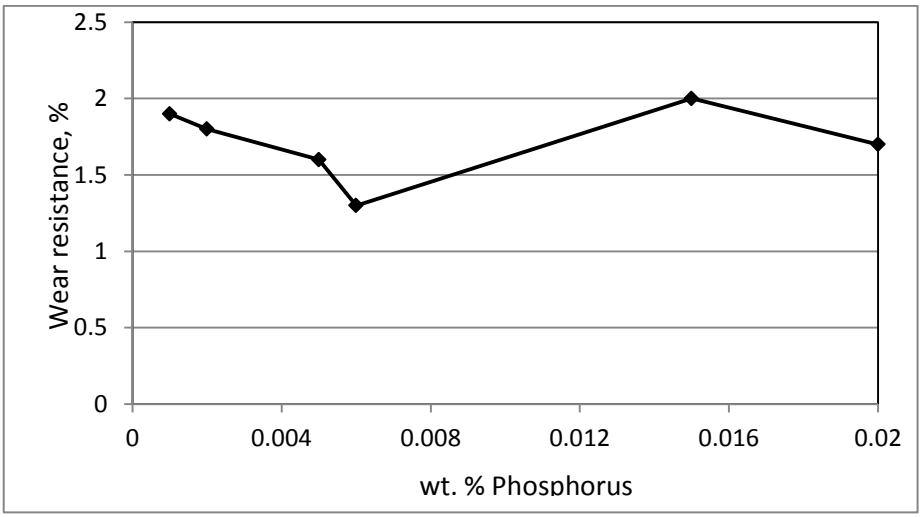

Figure 4.24 Relation between wear resistance and added phosphorus.

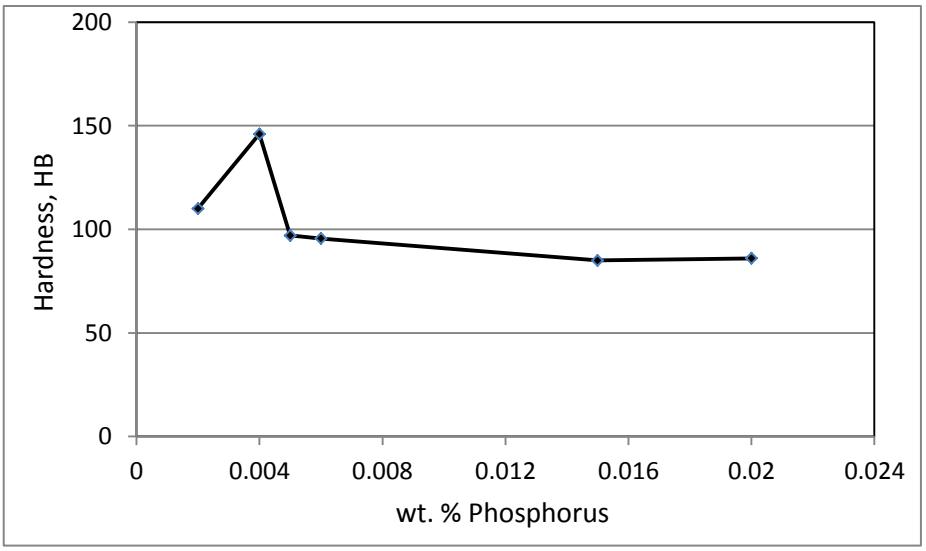

Figure 4.25 Relation between hardness and added phosphorus.

Besides, the hardness strong decreases with raising phosphorus content. When amount of refiner reaches to 0.006 wt. % phosphorus, hardness still decreases but not much. Wear resistance firstly decreases with raising phosphorus content. After tested alloys refined with 0.006 wt. % phosphorus, wear resistance starts to increase with raising phosphorus content. Thereby, the optimal combination of wear resistance and hardness is obtained around 0.006 wt. % phosphorus. It can be say that, the content of phosphorus, which makes the tested alloys has the optimal combination of mechanical properties, is 0.006 – 0.01 wt. % phosphorus.

Figure 4.26 shows the relation between silicon content, amount of refiner and thermal expansion of aluminum silicon alloys in a range of temperature from room temperature to 300 ^{0}C. Of course, thermal expansion of alloys depends on temperature. It will increases with increasing temperature. Thermal expansion of hypereutectic aluminum silicon alloys is significantly lower than eutectic alloys. Refinement of primary silicon helps to decrease thermal expansion of alloys

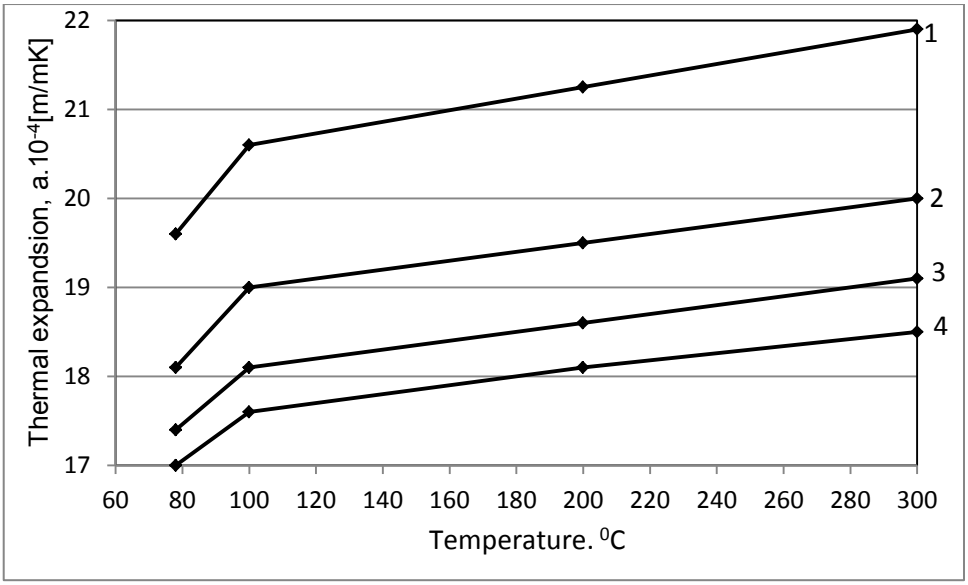

Figure 4.26 Thermal expansion of aluminum silicon alloys; (1) Eutectic alloys; (2) Non-refined hypereutectic alloys; (3) Hypereutectic alloys refined with 0.002 wt. % P; Hypereutectic alloys refined with 0.005 wt. % P.

Conclusion:

- The mechanical properties of hypereutectic aluminum silicon alloys are determined by the primary silicon. The crack always initiate by the brittle fracture of the primary silicon and eutectic silicon particles or deboning of silicon particles from the phase matrix, and then propagate through the α phase matrix and along inter-dendritic

channels during tension. The refinement of primary silicon decreases the probability of crack initiation by premature fracture of primary silicon. The tensile strength and ductility are improved obviously.

- The content of phosphorus, which makes the tested alloys has the optimal combination of mechanical properties, is 0.006 – 0.01 wt. % phosphorus. It is notice that the content of phosphorus that makes the alloys has the optimal combination of mechanical properties is not in correspondence with refinement effect of eutectic silicon. It is because the size of primary silicon is larger than that of eutectic silicon. The probability of crack initiated from primary silicon is larger than that from eutectic silicon. The primary silicon plays a more critical role than the eutectic silicon crystals in determining the mechanical properties.

4.2.3 Influence of refinement temperature.

Influence of temperature was investigated through three values of temperature: 780 ^{0}C, 850 ^{0}C and 950 ^{0}C. Amount of added AlCuP master alloys was constant. Follow the results of head 4.2.1 and 4.2.2, in order to have the optimal combination of mechanical properties all experiments were refined with 0.01 wt. % phosphorus. Sodium compound, which includes 15 wt.% cryolite (Na_3AlF_6), 25 wt. % potassium chloride (KCl) and 60 wt. % sodium chloride (NaCl), was used as slag-forming constituent and covering flux. Refinement quality was appreciated by particle size of primary silicon, hardness and wear resistance.

Table 4.4 Particle size of primary silicon and properties of tested alloys at different temperature.

Temperature, ^{0}C	**Particle size, µm**	**Hardness, HB**	**Wear resistance, g/cm^2.h**
780	25	87	0.090
850	24.9	85	0.105
950	24.5	85	0.099

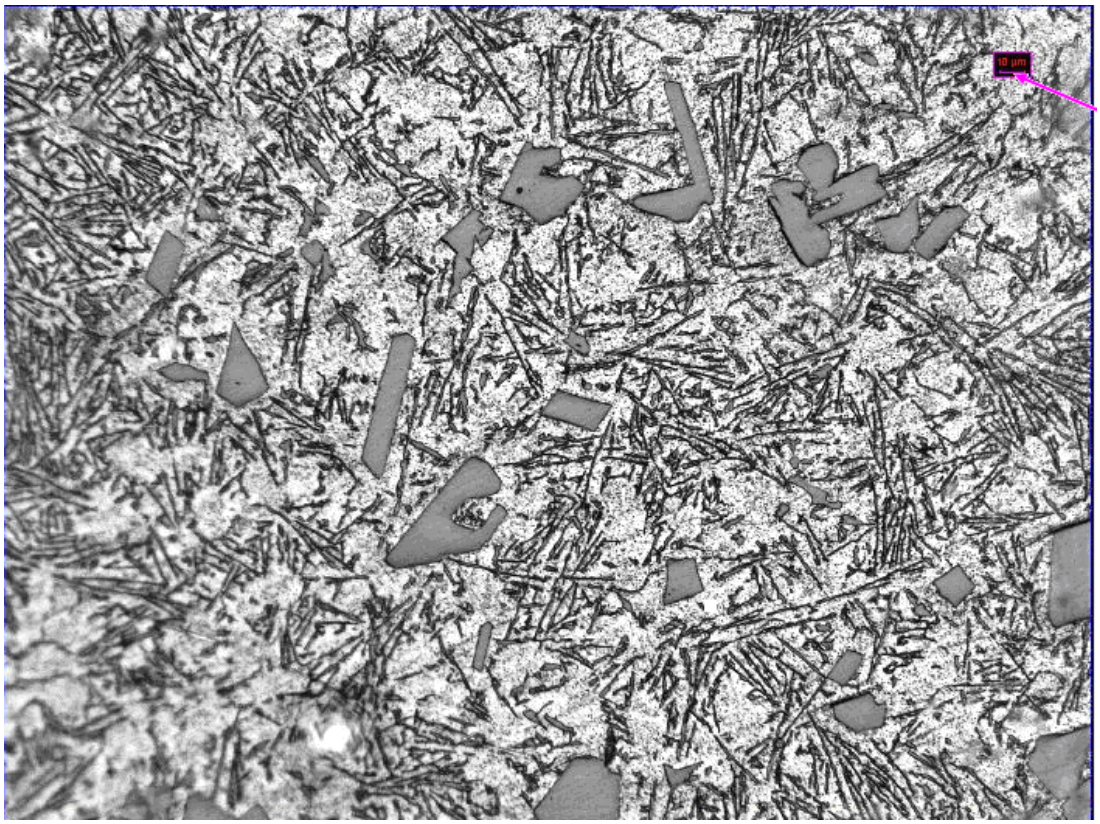

Figure 4.27 Microstructure of sample which refined at 780 0C.

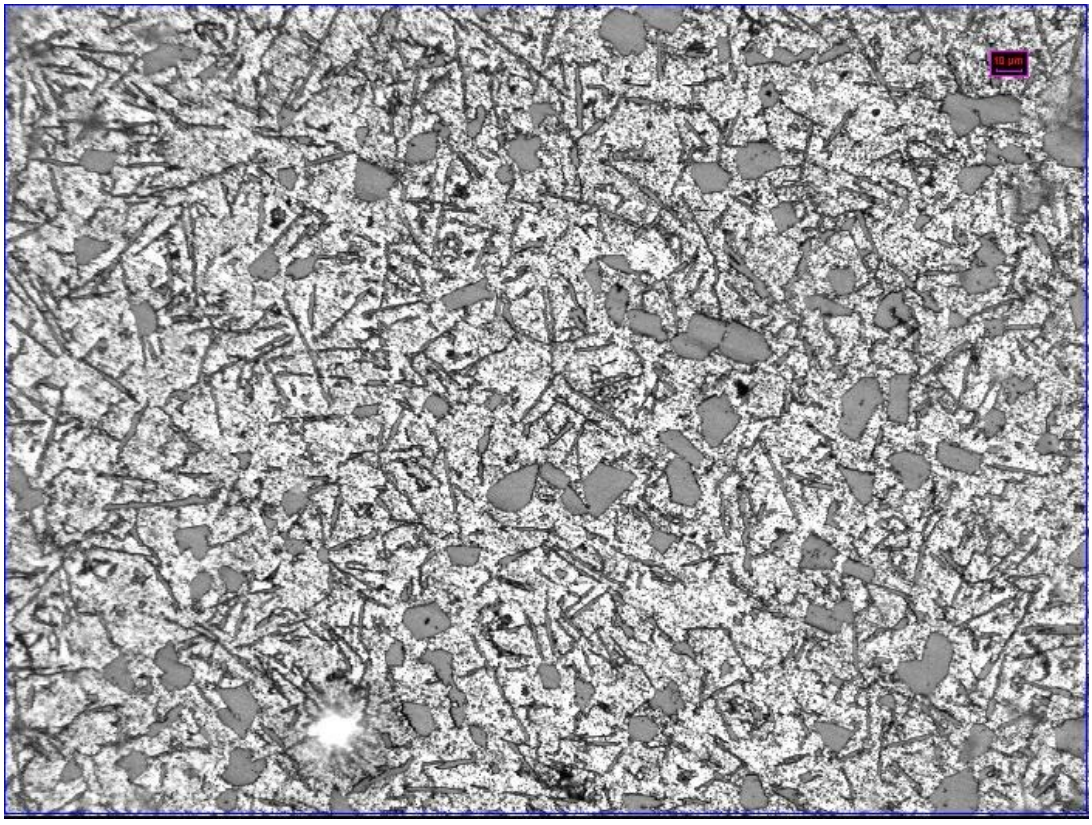

Figure 4.28 Microstructure of sample which refined at 850 ^{0}C.

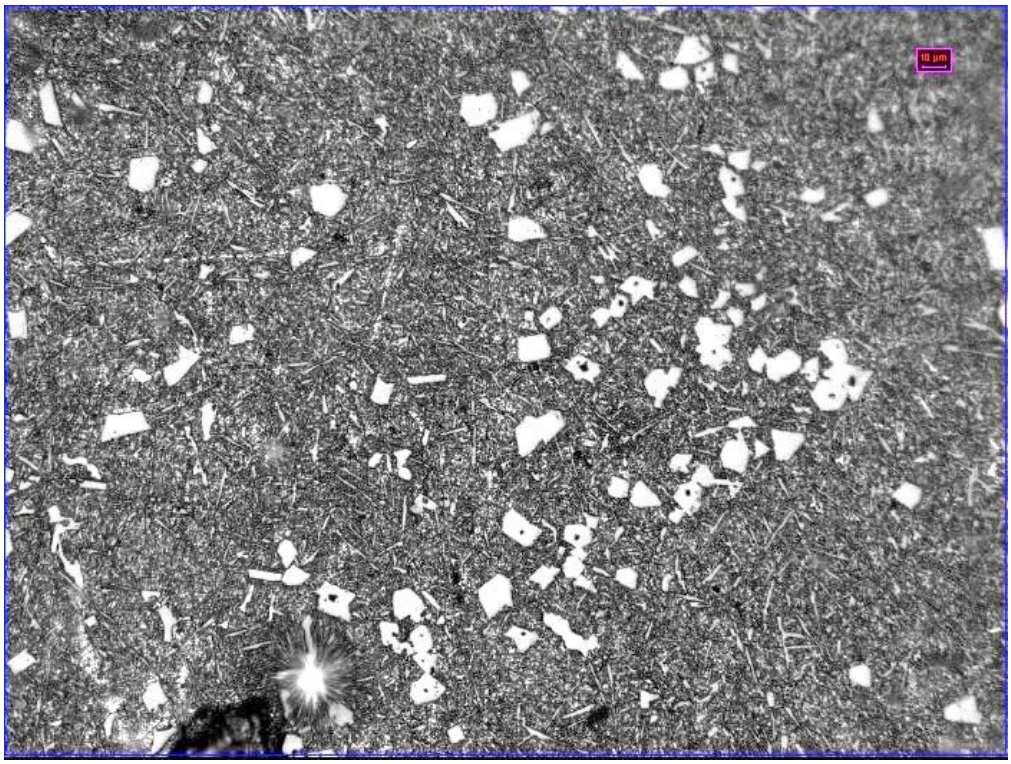

Figure 4.29 Microstructure of sample which refined at 950 0C.

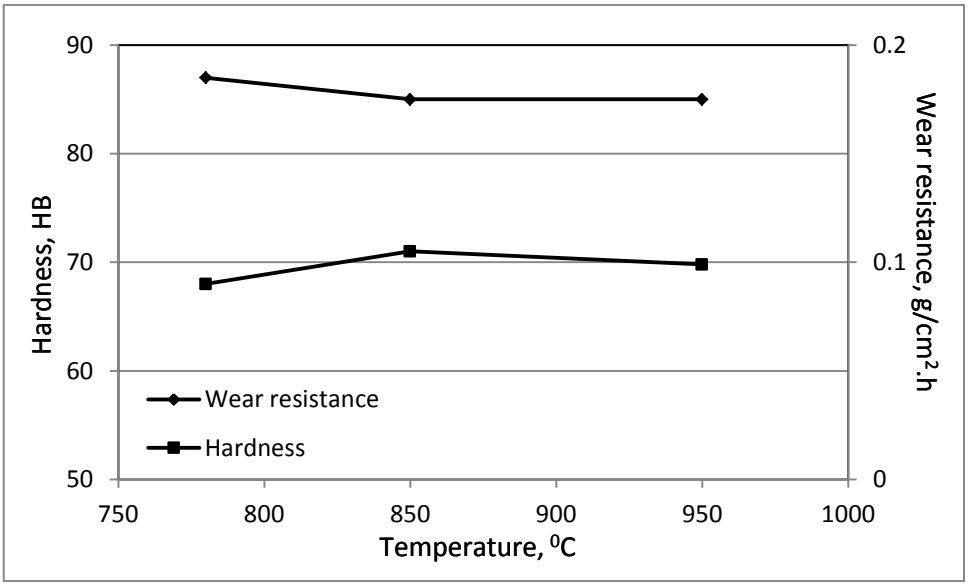

Figure 4.30 Hardness and wear resistance of tested alloys at different refinement temperature.

The change in particle size of primary silicon at different refinement temperature is showed in table 4.4. Higher temperature helps to decrease particle size, but it is insignificant. It seems that shape of silicon particle becomes refiner at higher temperature (figures 4.27 – 4.29). Table 4.4 and figure 4.30 also indicate the change in hardness and wear resistance. Hardness mostly depends on matrix of alloys. In these experiments, only primary silicon was refined, there was any influence on matrix of alloys. Thereby, three samples have the similar hardness reasonably. Wear resistance depends on primary silicon and its distribution on the

matrix. The change of wear resistance is just a bit. Because these experiments have the same refinement process, so they will have the same distribution of primary silicon and their particle size are similar.

Conclusion:

- Temperature is a major factor to determine solubility and loss by burning of master alloys. Solubility of phosphorus in melt increases with increase of temperature. When refinement effectiveness is completely obtained, there is no influence on refinement quality if temperature still increases.
- The optimal combination of particle size and properties is 850 ^{0}C.

4.2.4 Influence of refinement time.

Hypereutectic AlSi20 alloys were used in this experiment. Follow the results of head 4.2.1 – 4.2.3, Al-CuP master alloys were used. Amount of added phosphorus is 0.01 wt. % of charge. Refinement temperature is 850 ^{0}C. Table 4.5 shows results of experiment.

Table 4.5 Influence of refinement time on refinement quality.

	Experiment results					
Time, minute	0	10	17	32	52	62
Tensile strength, MPa		188	135	132	126	120
Particle size, µm	214.4	28	27	25	24	22

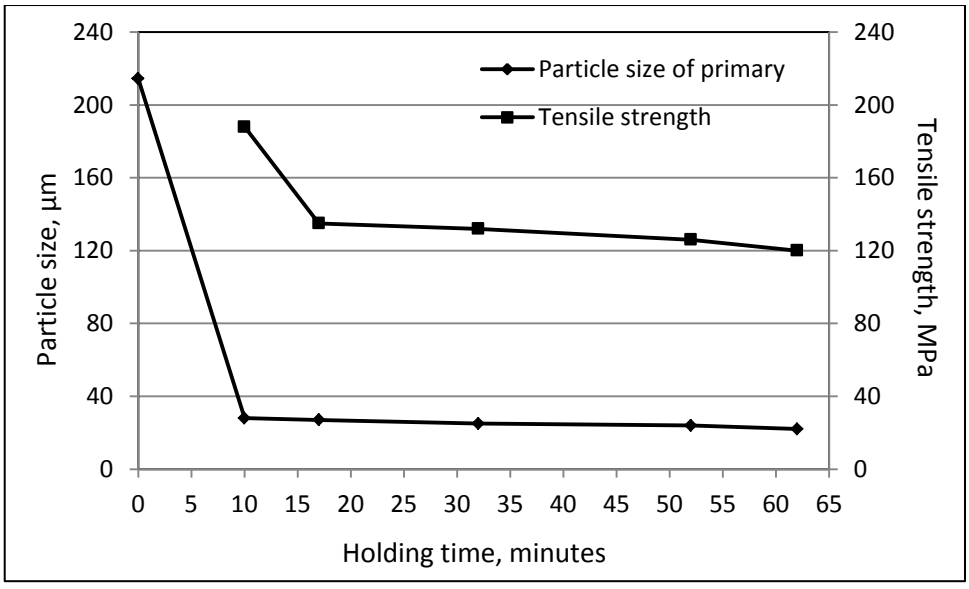

Figure 4.31 Influence of holding time on refinement quality.

Figure 4.31 was build follow data in table 4.4. It indicates particle size of primary silicon decreases with longer holding time. After ten minutes, it obtains the optimal value (28 μm). If continuously keeping holding time, refinement effect still occurs, but change in particle size is insignificant. Because, during produce process, master alloys need to be cooled as fast as possible, there was amount of phosphorus cannot dissolve to melt. This retained phosphorus exists in master alloys and become a reserved source for creating nucleation site of primary silicon.

Otherwise, longer holding time makes negative effect on tensile strength. Tensile strength is decreased with longer holding time. In order to get a good refinement quality, the optimal combination of tensile strength and particle size is from ten to seventeen minutes.

4.2.5 Influence of alloying elements on refinement quality.

The influence of alloying elements on refinement quality of hypereutectic AlSi20 alloys is showed in table 4.6. From this data, figure 4.32 is build. Both of added phosphorus and alloying element influence the wear resistant of tested alloys. Alloying elements was added to alloys to improve its wear resistant.

Table 4.6 Relation between alloying elements and wear resistance.

No.	Alloying elements	Wear resistance, g/cm^2·h
1	Non-refined	0.038
2	0.001 wt. % phosphorus	0.0253
3	0.0045 wt. % phosphorus	0.0251
4	0.012 wt. % phosphorus	0.0249
5	0.001 wt. % phosphorus, alloyed with Cu, Ni, Mg	0.025
6	0.0045 wt. % phosphorus, alloyed with Cu, Ni, Mg	0.019
7	0.012 wt. % phosphorus, alloyed with Cu, Ni, Mg	0.016

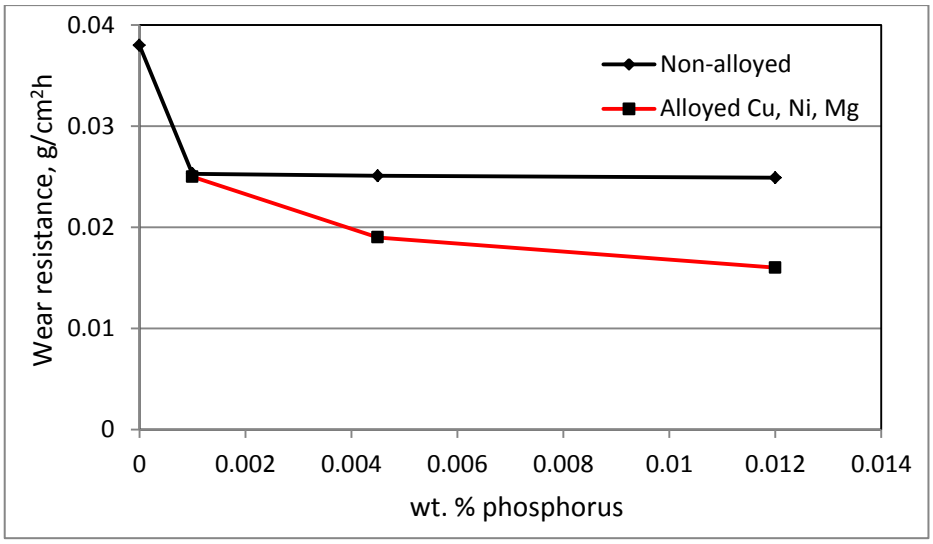

Figure 4.32 Wear resistance comparisons between non-alloyed and alloyed sample.

4.3 Application of present study.

Results of present study were applied to produce piston in Machinery Spare Parts No1 Joint Stock Company, Thainguyen, Vietnam. Composition of materials shows in table 4.7. Mechanical properties of product shows in table 4.8. Microstructure of product shows in figure 4.35. Melting practice is as below:

- Melting temperature: 860 ^{0}C.
- Refinement temperature: 850 ^{0}C.
- Refinement holding time: 10 minutes.
- Pouring time: 50 minutes.
- Refiner: Al-CuP master alloys.
- Amount of refiner: 0.006 and 0.01 wt. % per charge.

Table 4.7 Composition of piston materials.

Al	Si	Cu	Mn	Mg	Ni
73.95 – 74.61	20.58-21.19	2.38 – 2.69	0.61	0.35 – 0.39	0.78 – 0.86

Table 4.8 Mechanical properties of product.

Added phosphorus, %	0.006	0.01
Particle size of primary silicon, µm	28	27
Tensile strength, Mpa	169.06	188
Hardness, HB	86	85
Wear resistance, %	0.123	0.1

Figure 4.33 Die - mold of product.

Figure 4.34 Picture of product.

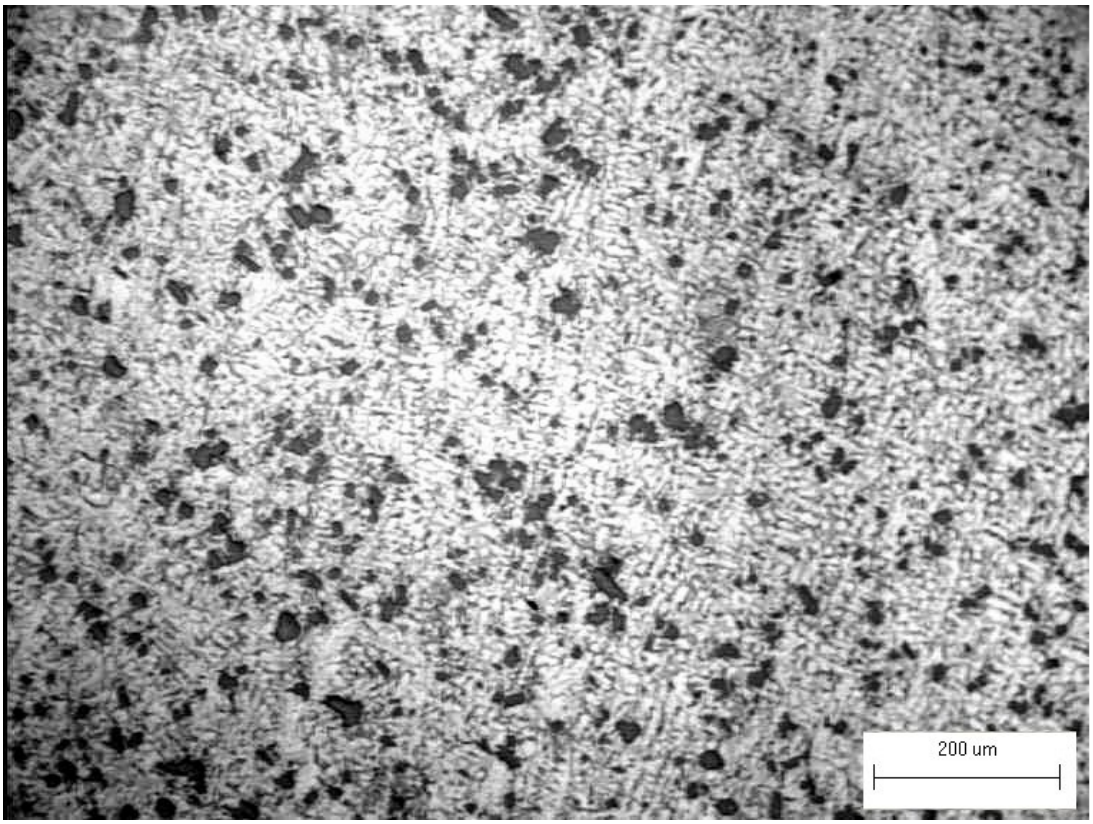

Figure 4.35 Microstructure of product.

5. Conclusion

It is my contribution to the scientific knowledge of metallurgical technology and material science. The aim object of study is refinement technology of hypereutectic aluminum silicon alloys with 20 wt. % silicon content. Master alloys (Al-CuP) has been successful produced in present study. Its composition includes 0.72 – 1 wt. % phosphorus; 18 wt. % copper and the rest is aluminum. The results of experiments affirm again that phosphorus still be the main refining element for primary silicon in hypereutectic aluminum silicon alloys. The limit of phosphorus solubility in melt depends on silicon content. At a constant temperature, various silicon content has a constant phosphorus solunility to form aluminum phosphide(AlP). These aluminum phosphide easy dissolves to melt to formed nucleation sites for primary silicon which crystalline later. Besides, there is amount of retained phosphorus that exists in master alloys. It can continuous combine with aluminum to increase the number of aluminum phosphide (AlP) during refinement process. It can be say that Al-CuP master alloys seems to be better than CuP master alloys. It has lower refinement temperature, sorter refinement time and more nucleation sites. Thereby, using AlCuP master alloys has lower loss by burning of element, better economic effectiveness and better refinement quality.

The refinement effect becomes better with higher refinement temperature and appropriate refinement time. The refinement mechanism of primary silicon according to principle of peritectic reaction below.

$$L + AlP \rightarrow L + AlP + \text{Primary silicon.}$$

Added sodium compound can help to refine both of primary and eutectic silicon. The order of refiner addition to melt does not affect to particle size of primary silicon. It means that sodium only adsorbs on the surface of silicon particles, not adsorbs on the surface of aluminum phosphides. Besides, refinement mechanism was changed when AlTi5B master alloys was added. The second exothermic effect occurs at 570 ^{0}C. It seems to be a crystalline sign of solid solution α-Al in hypereutectic aluminum silicon alloys.

The mechanical properties of hypereutectic aluminum silicon alloys are determined by the primary silicon. The crack always initiate by the brittle fracture of the primary silicon and eutectic silicon particles or deboning of silicon particles from the phase matrix, and then propagate through the α phase matrix and along inter-dendritic channels during tension. The refinement of primary silicon decreases the probability of crack initiation by premature fracture of primary silicon. The tensile strength and ductility are improved obviously.

The optimal refinement technology for hypereutectic aluminum silicon alloys with 20 wt. % silicon content are as below.

- Refiner: AlCuP master alloys with 0.72 – 1 wt. % phosphorus.
- Refinement temperature: 850 ^{0}C.
- Refinement time: 10 – 15 minutes.
- Amount of added phosphorus, which makes alloys has the optimal combination of properties, is 0.006 – 0.01 wt. %. It is notice that the content of phosphorus that makes the alloys has the optimal combination of mechanical properties is not in correspondence with refinement effect of eutectic silicon. It is because the size of primary silicon is larger than that of eutectic silicon. The probability of crack initiated from primary silicon is larger than that from eutectic silicon. The primary silicon plays a more critical role than the eutectic silicon crystals in determining the mechanical properties.

The present study has a practical benefit for practice because results of present study were successful applied in Machinery Spare Parts No1 Joint Stoke Company, Vietnam. Mechanical properties of product are well accepted follow Vietnamese Standard. The

successful production of AlCuP master alloys will promote study and application of hypereutectic aluminum silicon alloys in Vietnam. Especially, Vietnam government invested Vietnam Engine and Agricultural Machinery Corporation to research and manufacture automobile of the interior.

6. References

[1] B. K. Prasad, K. Venkateswarlu, O. P. Modi, A. K. Jha, S. Das, and R. Dasgupta, *Sliding Wear Behavior of Some Al-Si Alloys: Role of Shape and Size of Si Particles and Test Conditions*, Metallurgical and Materials Transactions A, Nov. 1998, vol. 29, p. 2747-2752.

[2] D. K. Dwivedi, *Wear behavior of cast hypereutectic aluminum silicon alloys*, Materials & Design, Jan. 2006, vol. 27, no. 7, p. 610-616.

[3] S. Hegde and K. N. Prabhu, *Modification of eutectic silicon in Al-Si alloys*, Journal of Materials Science, Mar. 2008, vol. 43, no. 9, p.3009-3027.

[4] Malgorzata Warmuzek, *Aluminum-Silicon Casting Alloys: Atlas of Microfractographs*, 2004. ISBN: 0-87170-794-2. SAN: 204-7586.

[5] *A guide to aluminum casting alloys*. www.scribd.comdoc52398544Alum-Casting-Alloys-FEB05

[6] John E. Hatch, *Aluminum Properties and Physical Metallurgy*, Apr 2005, p. 320-350.

[7] W. Vogel, W. Schneider, Giesserei 78 (1991) Nr. 23, S.848-852

[8] T. Onnira, D. Ittipon, T. Umeda, *Grain refinement of Silicon in Hyper-eutectic Al-Si systems.Phosphorus Solubility and a thermodynamic Assessment of the Al-Si-P, Ternary systems.* Proceedings of The Eigth Asian Foundry congress, October 17-20. 2003, Bangkok, Thailand

[9] K T Kashyap, T Chandrashekar, *Effects and mechanisms of grain refinement in aluminium alloys*, Bull. Mater. Sci., Vol. 24, No. 4, August 2001, p. 345–353. © Indian Academy of Sciences.

[10] Misra. A, *Misra technique applied to solidification of cast iron*, Metallurgical transactions A, Feb. 1986, vol. 16, p. 358-360.

[11] X. Liao, Q. Zhai, J. Luo, W. Chen, and Y. Gong, *Refining mechanism of the electric current pulse on the solidification structure of pure aluminum*, Acta Materialia, May 2007, vol. 55, no. 9, p. 3103-3109.

[12] G. Xu, J. Zheng, Y. Liu, and J. Cui, *Effect of electric current on the cast micro-structure of Al-Si alloy,* China Foundry, 2005, Vol. 2, No. 3, p. 171-175.

[13] Granger D A *Proc. int. seminar on refining and alloying of liquid aluminium and ferro-alloys*, 1985 (Norway: Trondheim) p. 231

[14] Granger D A and Liu L 1983 J. Met, pp. 35 54

[15] Labarri L C, James R S, Witters J J, O' Malley R J and Emptage M R 1987 J. Phys. (Orsay) 48 C3 Suppl. 93

[16] Apelian D, Sigworth G K and Whaler K R 1984 Trans. AFS, p.92-297

[17] McCartney D G 1989 Int. Mater. Rev. p. 34-247

[18] CHALMERS, B., 1963, J. Aust. Inst. Metals 8, p.255.

[19] HOLLOMON, J.H., and D. TURNBULL, 1953, *Progress in Met. Phys*., vol. 4, (Interscience, New York), p. 333.

[20] Kurz, W. and D.J. FISHER, *Fundamentals of Solidification*, 1989, 3rd.ed. (Trans. Tech. Publication, Switzerland).

[21] MCCARTNEY, D.G., 1989, Int. Mat. Rev. 34, p.247.

[22] KURZ, W. and R. TRIVEDI, Microstructural Development and Control in Materials Processing, 1989, in: Series M.D., vol. 14, ASM, Metals Park, p. 47.

[23] Alexander Joseph Plotkowski, *Refinement of the Cast Microstructure of Hypereutectic Aluminum-Silicon Alloys with an Applied Electric Potential,* Grand Valley State University. Electric Potential. Masters Theses. 2012, p. 15.

[24] Campbell, J., *Modification of Al-Si alloys*. AFS transactions 2011, p. 171-175.

[25] Campbell. J., Tiryakioglu, M., *Review of effect of P and Sr on modification and porosity development in Al-Si alloys*, Materials science and technology, 2010, vol. 26, no 3, p. 262-268.

[26] Sigworth, G.K, Jorstad, J., Campbell, J., AFS international J Metalcasting, 2008, vol. 3, issue 1, p. 65-77.

[27] H. S. Dai and X. F. Liu, *Optimal holding temperatures and phosphorus additions for primary silicon refinement in Al–high Si alloys,* Materials Science and Technology, Oct. 2009, vol. 25, no. 10, p. 1183-1188.

[28] J. Cisse, G. Bolling, and H. Kerr, *Simultaneous Refinement of Primary and Eutectic Silicon in Hypereutectic AI-Si Alloys,* Metallurgical Transactions B, Mar. 1975, vol. 6, p. 195-197.

[29] P. Shingu and J.-I. Takamura, *Grain-Size Refining of Primary Crystals in Hypereutectic AI-Si and AI-Ge Alloys,* Metallurgical Transactions, Aug. 1970, vol. 1, p. 2339-2340.

[30] CHEN Chong, LIU Zhong-xia, REN Bo, WANG Ming-Xing, WENG Yong-gang, LIU Zhi-yong, *Influences of complex modification of P and RE on microstructure and mechanical properties of hypereutectic Al-20Si alloy*, Transsactions of Nonferrous Metals Society of China 17, 2007, p. 301-306.

[31] Flemings Merton C 1974a *Solidification processing* (eds) M Stephen et al (USA: McGraw-Hill Inc.) ch. 5, p. 135

[32] Stanislav Kores, Livarski vestnick, letnik 56, st. 3/2009, p. 103-111.

[33] Olga Zak, Babette Tonn, Feinung des Primarsiliziums durch kombinierte Zugabe von Phosphor und Tital bzw. Phosphor und Zirkonium, Giesserei-Praxis 9/2009, p. 281-284.

[34] J. Piatkowski, *Proeutectic crystallization in hypereutectic silumins modified with Al-CuP-Me master alloys*, Archives of Foundry engineering, Volume 9, Issue 4/2009, p. 195-198. ISSN 1897-3310.

[35] Nguyen Huu Dung, Nguyen Hong Hai. *Melting technology of casting alloys*. Code 326-2012/CXB/01-17/BKHN. Bachkhoa Publishing House.ISBN 978-604-911-112-9.

[36] www.keytometals.com/Article55.html

[37] E. Fras, *Crystallisation of metals*. WNT 2003, Poland.

[38] S. Pietrowski, *The solidification of metallic materials*. WPL, Lódz 1993, Poland.

[39] J. Sobczak, *Innovations in metalcasting*. IO Kraków 2007, Poland.

[40] Z. Górny, J. Sobczak, *Non-ferrous metals based novel material. In foundry practice*. ZA-PIS Cracow 2005.

[41] K. Nogita, S. D. Mcdonald, and A. Dahle, "*utectic Modification of Al-Si Alloys with Rare Earth Metals,* Materials Transactions, 2004, vol. 45, no. 2, p. 323-326.

[42] N. Abu-Dheir, M. Khraisheh, K. Saito, and A. Male, *Silicon morphology modification in the eutectic Al–Si alloy using mechanical mold vibration,* Materials Science and Engineering: A, Feb. 2005, vol. 393, no. 1–2, p. 109-117.

[43] B. I. Jung, C. H. Jung, T. K. Han, and Y. H. Kim, *Electromagnetic stirring and Sr modification in A356 alloy,* Journal of Materials Processing Technology, 2001, vol. 111, p. 69-73.

[44] D. Lu, Y. Jiang, G. Guan, R. Zhou, Z. Li, and R. Zhou, *Refinement of primary Si in hypereutectic Al–Si alloy by electromagnetic stirring,* Journal of Materials Processing Technology, Jul. 2007, vol. 189, no. 1–3, p. 13-18.

[45] J. Yu, Z. Ren, and K. Deng, *Refinement and migrating behaviors in Al-Si hypereutectic alloys solidified under electromagnetic vibration,* Acta Metallurgica Sinica, 2011, vol. 24, no. 4, p. 301-308.

[46] Radjai. A, K. Miwa, and T. Nishio, *An Investigation of the Effects Caused by Electromagnetic Vibrations in a Hypereutectic Al-Si Alloy Melt,* Metallurgical and Materials Transactions A, May 1998, vol. 29, p. 1477-1484.

[47] Z. Zhang, H.-T. Li, I. C. Stone, and Z. Fan, *Refinement of primary Si in hypereutectic Al-Si alloys by intensive melt shearing,* IOP Conference Series: Materials Science and engineering, Jan. 2012, vol. 27, p. 1-6.

[48] N. S. Barekar, B. K. Dhindaw, and Z. Fan, "Improvement in silicon morphology and mechanical properties of Al–17Si alloy by melt conditioning shear technology," International Journal of Cast Metals Research, Aug. 2010, vol. 23, no. 4, p. 225-230.

[49] H. Choi, H. Konishi, and X. Li, *Al2O3 nanoparticles induced simultaneous refinement and modification of primary and eutectic Si particles in hypereutectic Al–20Si alloy,* Materials Science and Engineering: A, Apr. 2012, vol. 541, p. 159-165.

[50] W. Kasprzak, M. Sahoo, J. Sokolowski, H. Yamagata, and H. Kurita, *The Effect of the Melt Temperature and the Cooling Rate on the Microstructure of the Al-20% Si Alloy Used for Monolithic Engine Blocks,* International Journal of Metalcasting, Summer 2009, p. 55-72.

[51] H. K. Moffatt, *Electromagnetic Stirring,* Physics of Fluids A, May 1991, vol. 3, p. 1336-1343.

[52] J. Angus, D. Ragone, and E. Hucke, *The Effect of an Electric Field on the Segregation of Solute Atoms at a Freezing Interface,* in Metallurgical Society Conference, 1961, p. 833-843.

[53] J. Verhoeven, *The Effect of an Electric Field upon the Solidification of Bismuth-Tin Alloys,* Transactions of the Metallurgical Society of AIME, Jun. 1965, vol. 233, p. 1156-1163.

[54] X. Liao, Q. Zhai, J. Luo, W. Chen, and Y. Gong, *Refining mechanism of the electric current pulse on the solidification structure of pure aluminum,* Acta Materialia, May 2007, vol. 55, no. 9, p. 3103-3109.

[55] D. Hongsheng, Z. Yong, J. Sanyong, C. Ruirun, and Z. Zhilong, *Influences of pulse electric current treatment on solidification microstructures and mechanical properties of Al-Si piston alloys,* China Foundry, 2008, vol. 6, no. 1, p. 24-31.

7. List of publications

[1] Nguyen Van Thai, Nguyen Hong Hai, Nguyen Anh Son, *Modification of silicon crystal on hypereutectic aluminum silicon alloys*, Journal of Science and Technology, Vietnam, Vol. 1, 2003.

[2] Nguyen Hong Hai, Nguyen Van Thai, Nguyen Anh Son. *Refinement of Silicon Particles on Hyper-Eutectic Aluminum Silicon Alloys* , Proceeding of 9th Asian Foundry Congress (AFC-9), 9/2005, p. 57-63.

[3] Nguyen Hong Hai. *Refinement of silicon particles on hyper-eutectic aluminum silicon alloys*, Chvorinov's Colloquium, 2009, p. 32; ISBN 978-80-248-2056-9.

[4] Nguyen Hong Hai. *The effect of phosphorus on modification of hyper-eutectic silumins*, Day of doctoral FMMI, 2009, p. 25. ISBN 978-80-248-2129-0.

[5] Nguyen Hong Hai *The modification mechanism of hyper-eutectic aluminum silicon alloys,* In 47. slévárenské dny s doprovodnou výstavou a 7. mezinárodní PhD konferencí, Brno : Česká slévárenská společnost, 2010,[CD]. ISBN 978-80-904020-6-5

[6] Nguyen Huu Dung, Nguyen Hong Hai, Tran Duc Huy, Nguyen Van Thai. *Modification of Sillicon in Hypereutectic Aluminum Sillicon Alloys*. In the 1st International Conference on Materials Engineering and the 3nd AUN/SEED-Net Regional Conference on Materials, Yogyakarta, Indonesia, 2011, p. 369. ISBN 978-979-97986-5-7.

[7] Nguyen Hong Hai, *Grain refinement of hypereutectic aluminum silicon alloys,* Day of doctoral student 2011, FMMI. ISBN 978-80-248-2523-6.

[8] Nguyen Huu Dung, Nguyen Hong Hai, *Melting technology of casting alloys,* Code 326-2012/CXB/01-17/BKHN. Bachkhoa Publishing House. ISBN 978-604-911-112-9.

8. Appendix

8.1 Microstructure of non-refined AlSi20 alloys

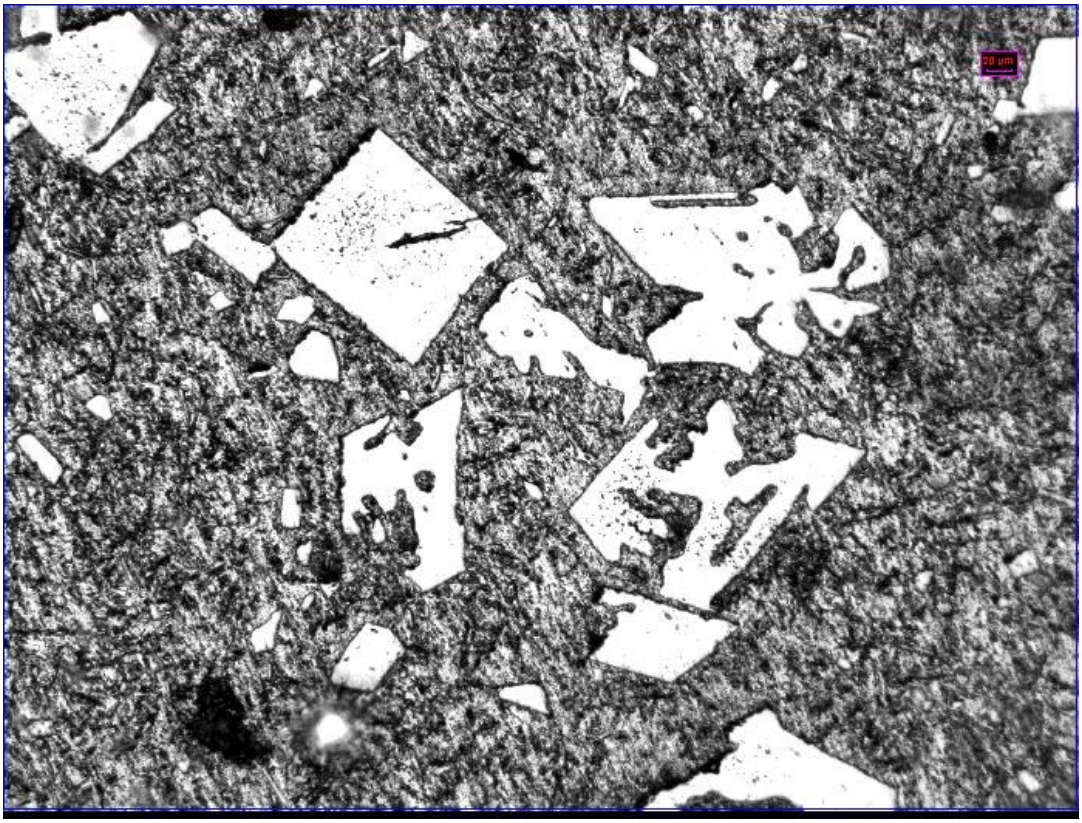

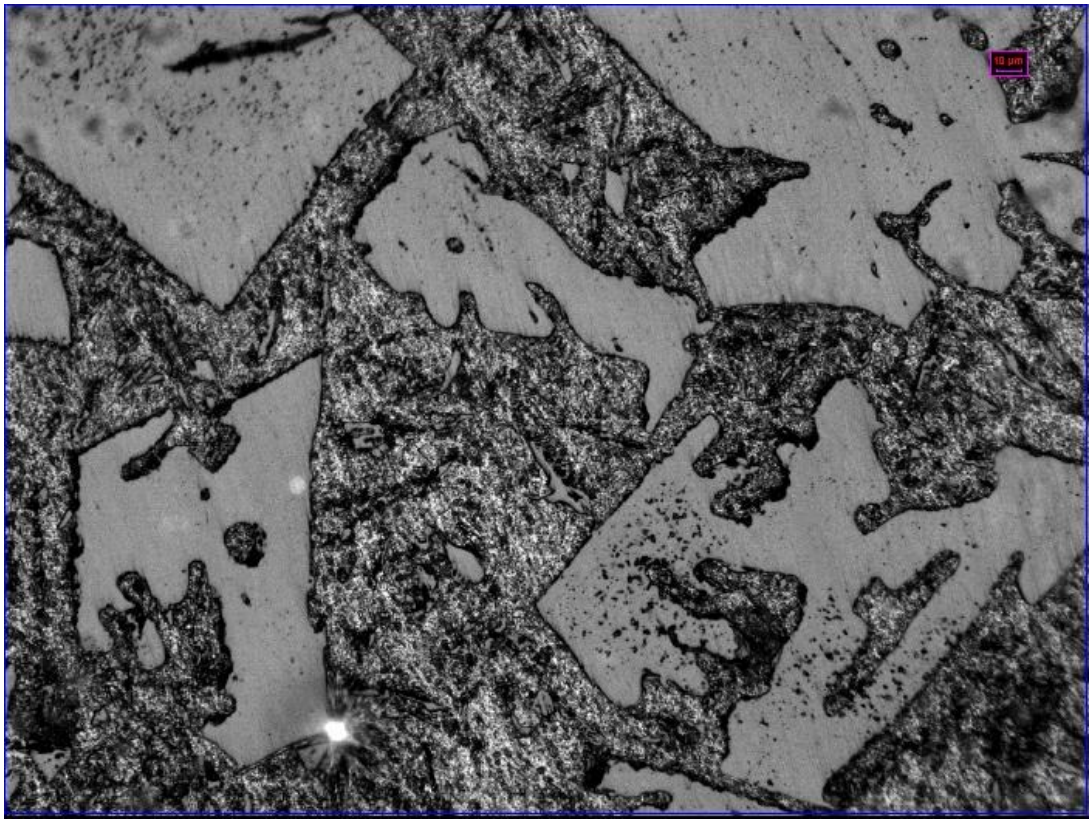

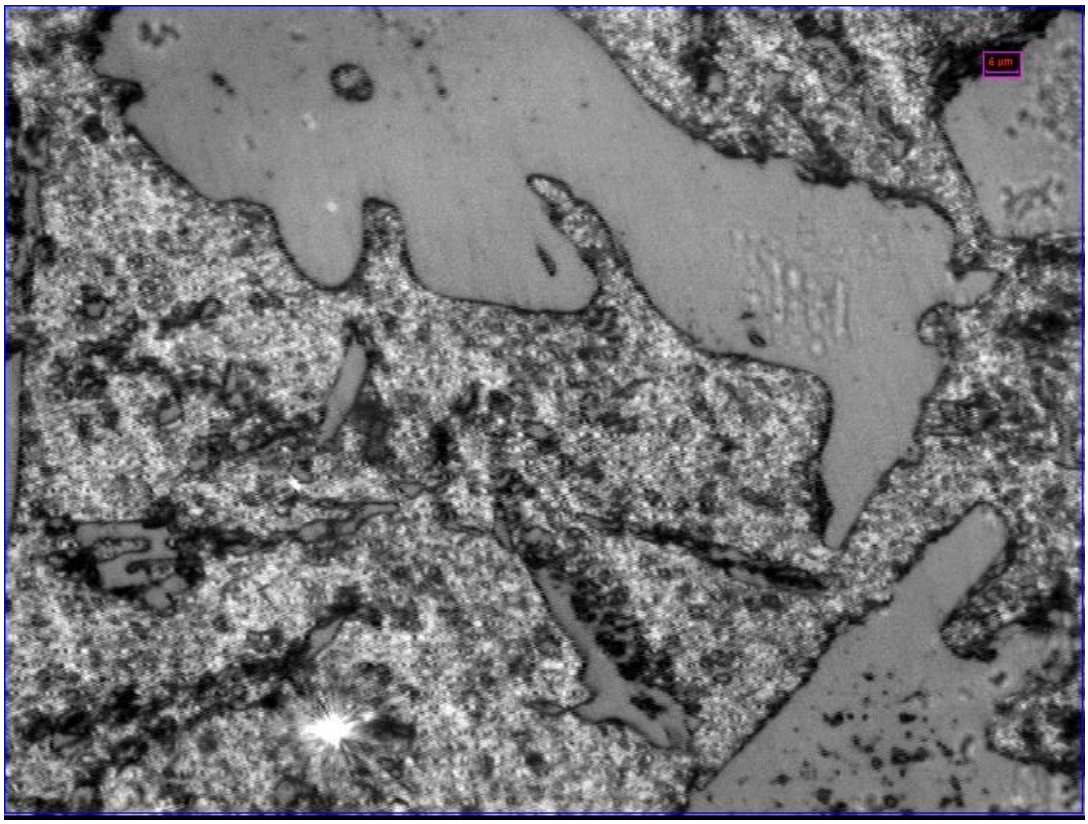

8.2 Microstructure of AlSi20 alloys which was refined with combination of sodium compound, AlTi5B and AlCuP master alloys

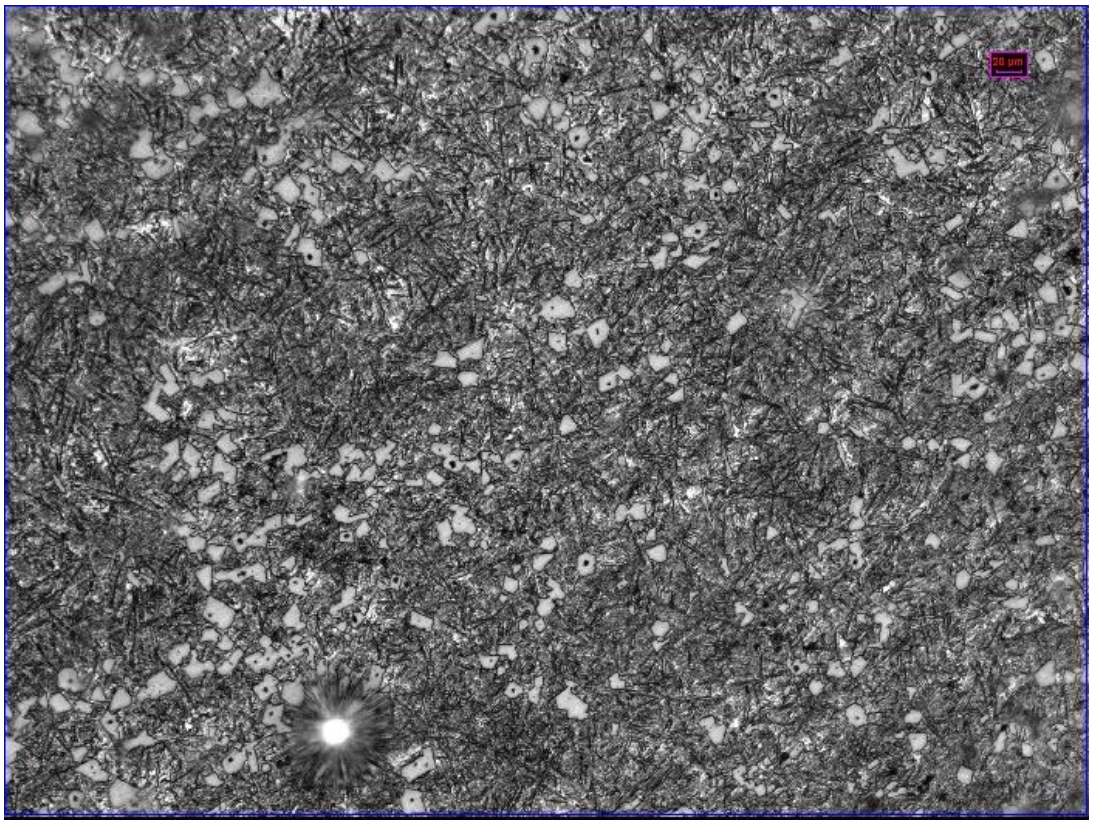

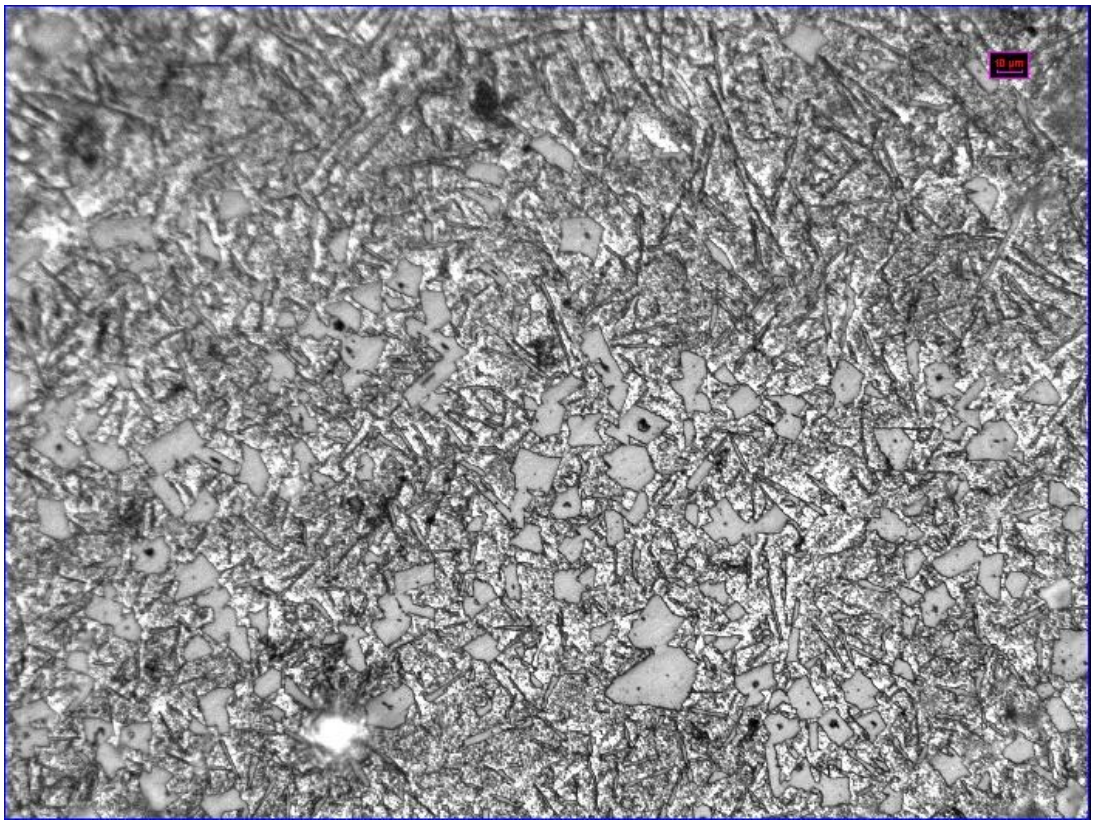
10 µm

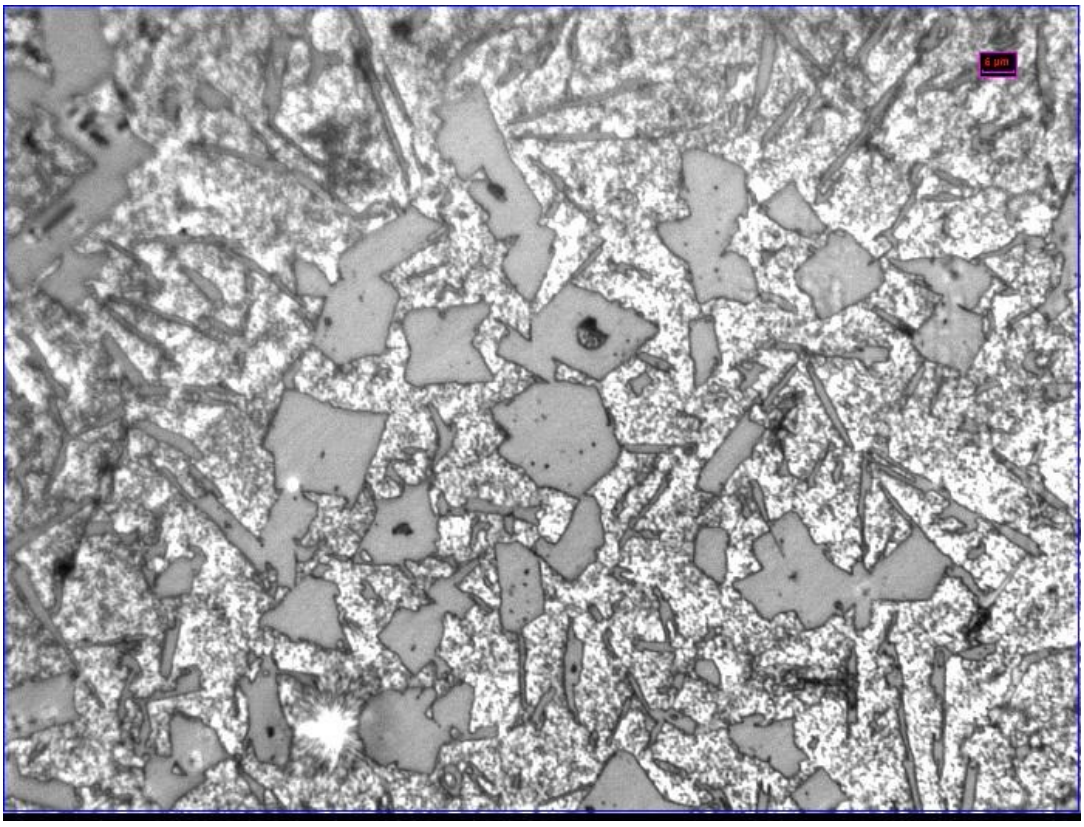
4 µm

8.3 Microstructure of AlSi20 alloys which was refined with different amount of refiner

8.3.1 Microstructure of AlSi20 alloys which was refined with 0.005 wt. % phosphorus

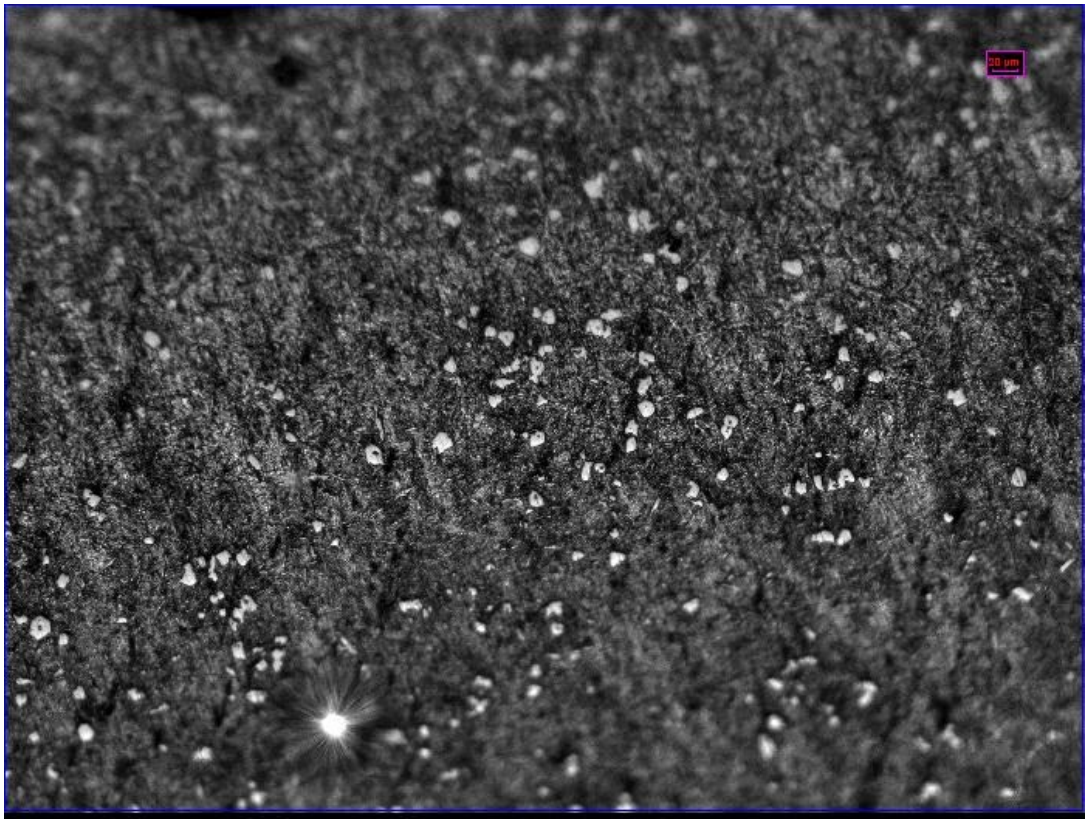

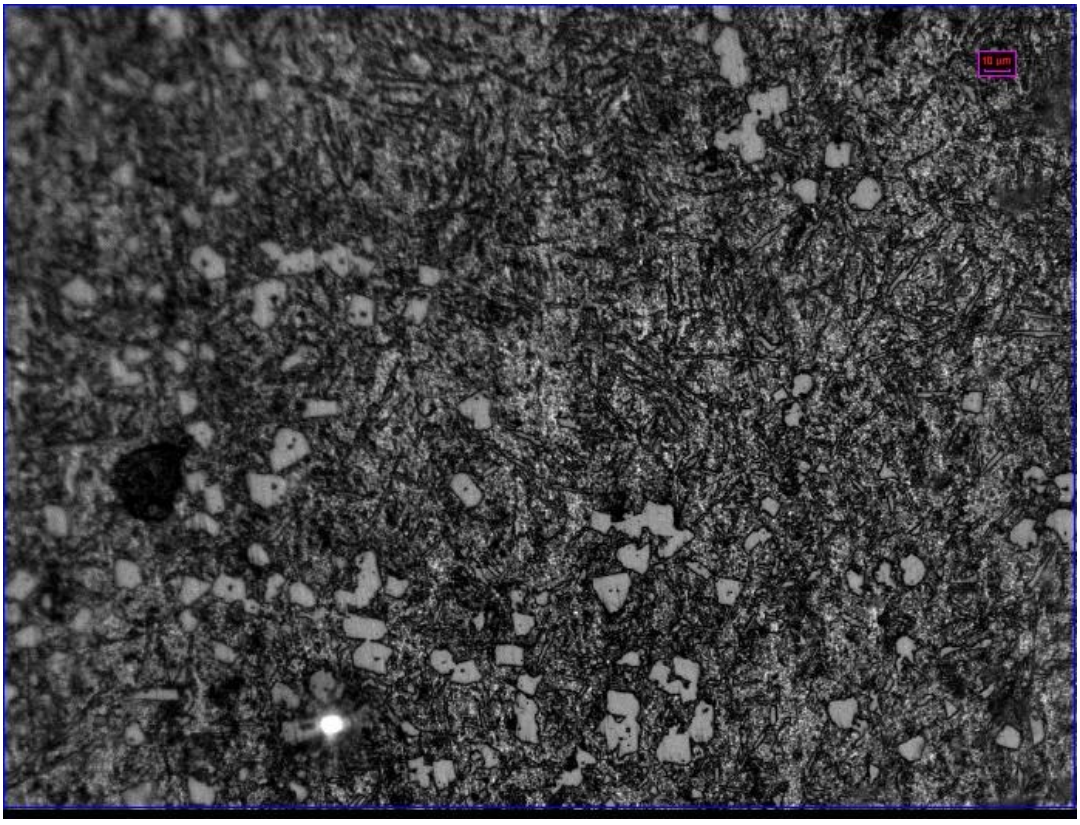

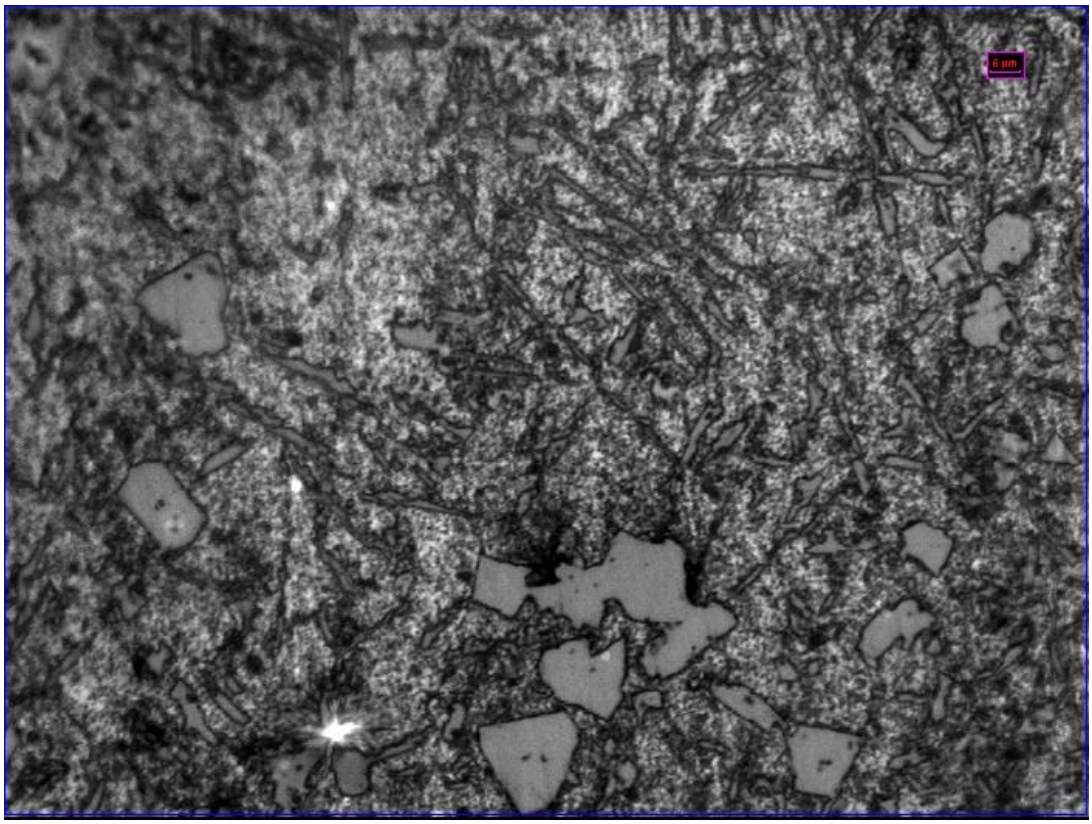

8.3.2 Microstructure of AlSi20 alloys which was refined with 0.01 wt. % phosphorus

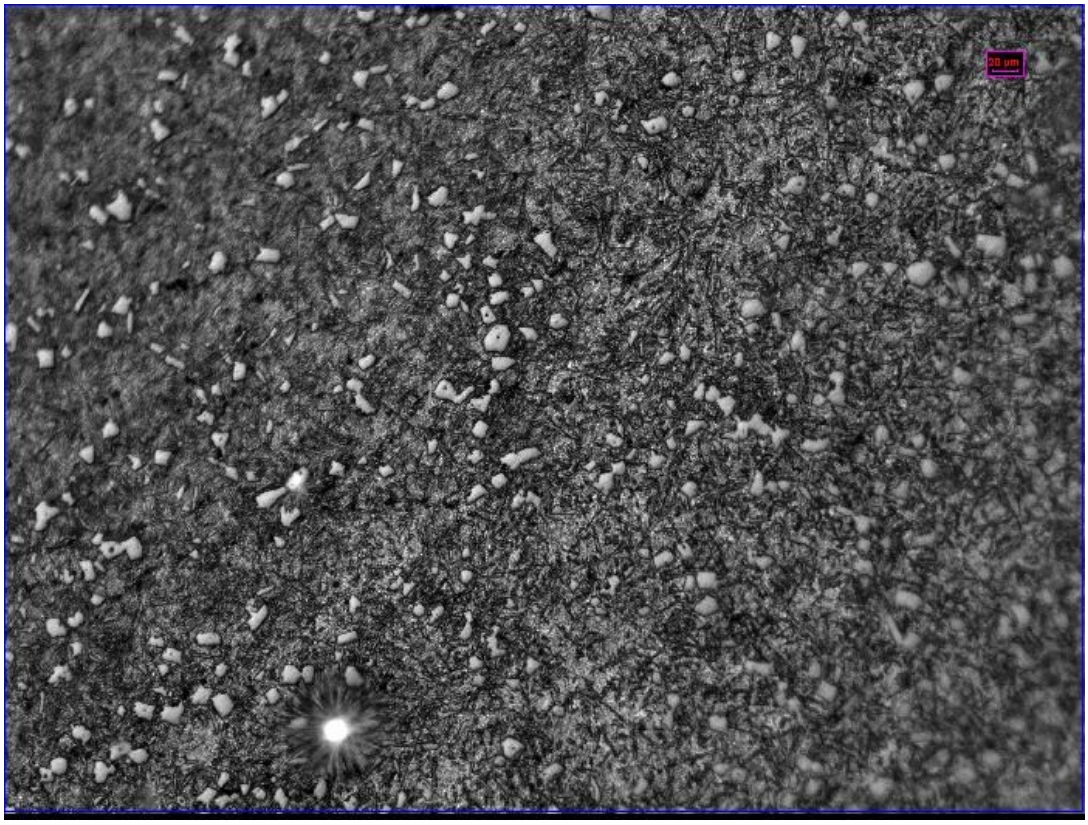

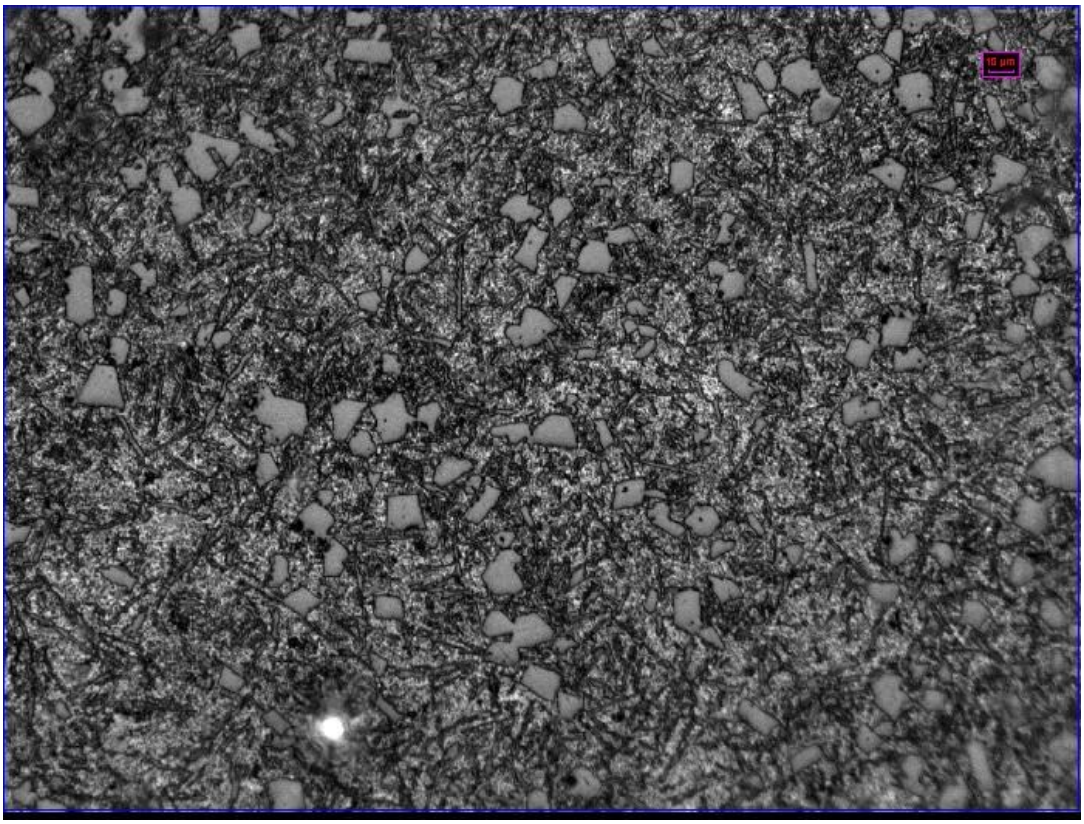
10 µm

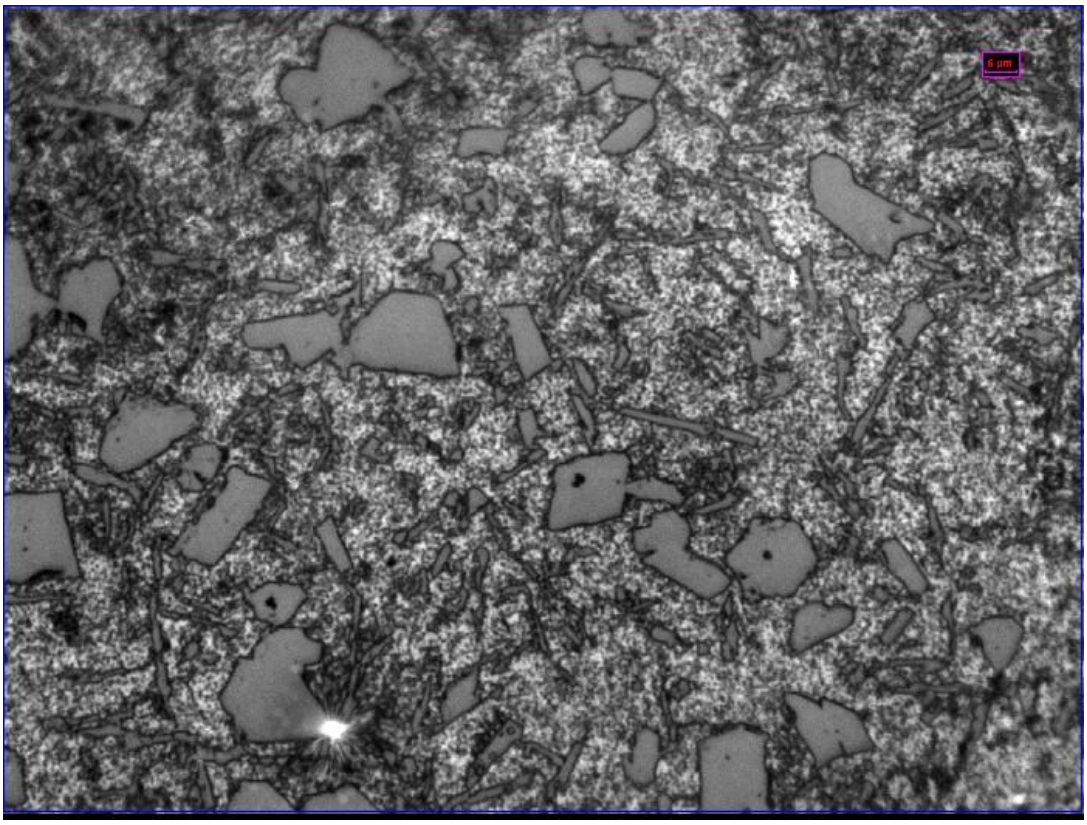
5 µm

8.3.3 Microstructure of AlSi20 alloys which was refined with 0.02 wt. % phosphorus

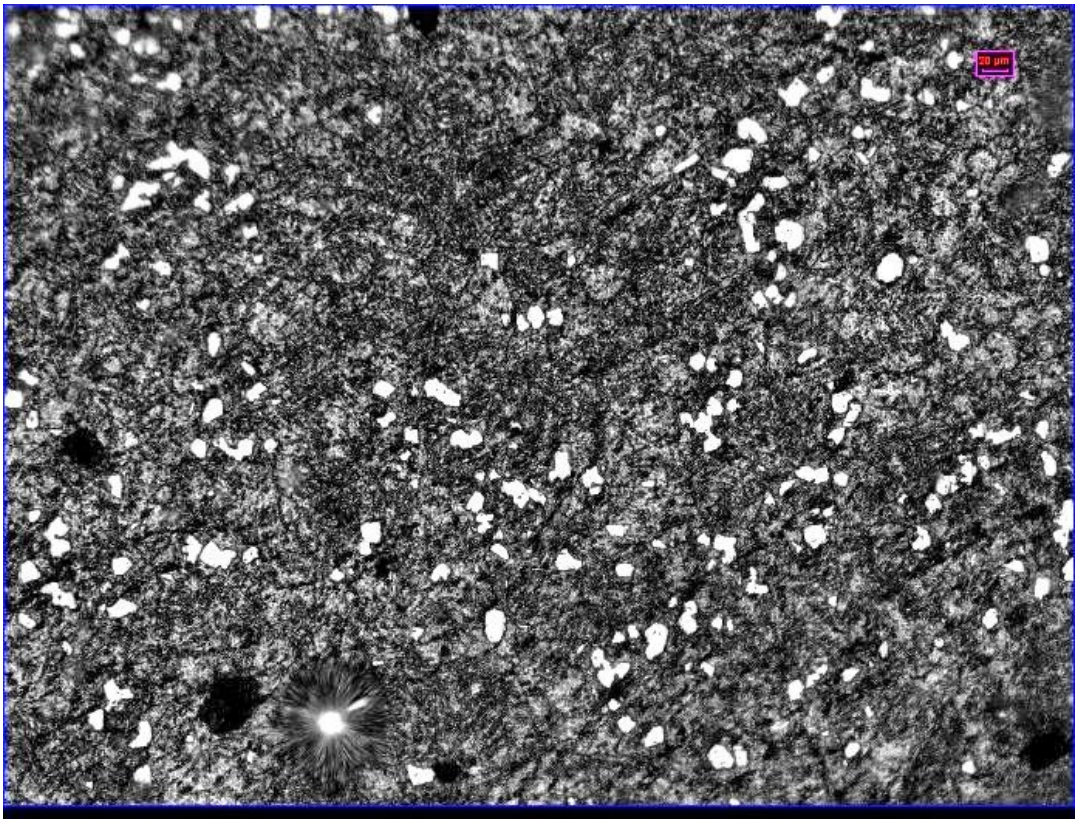

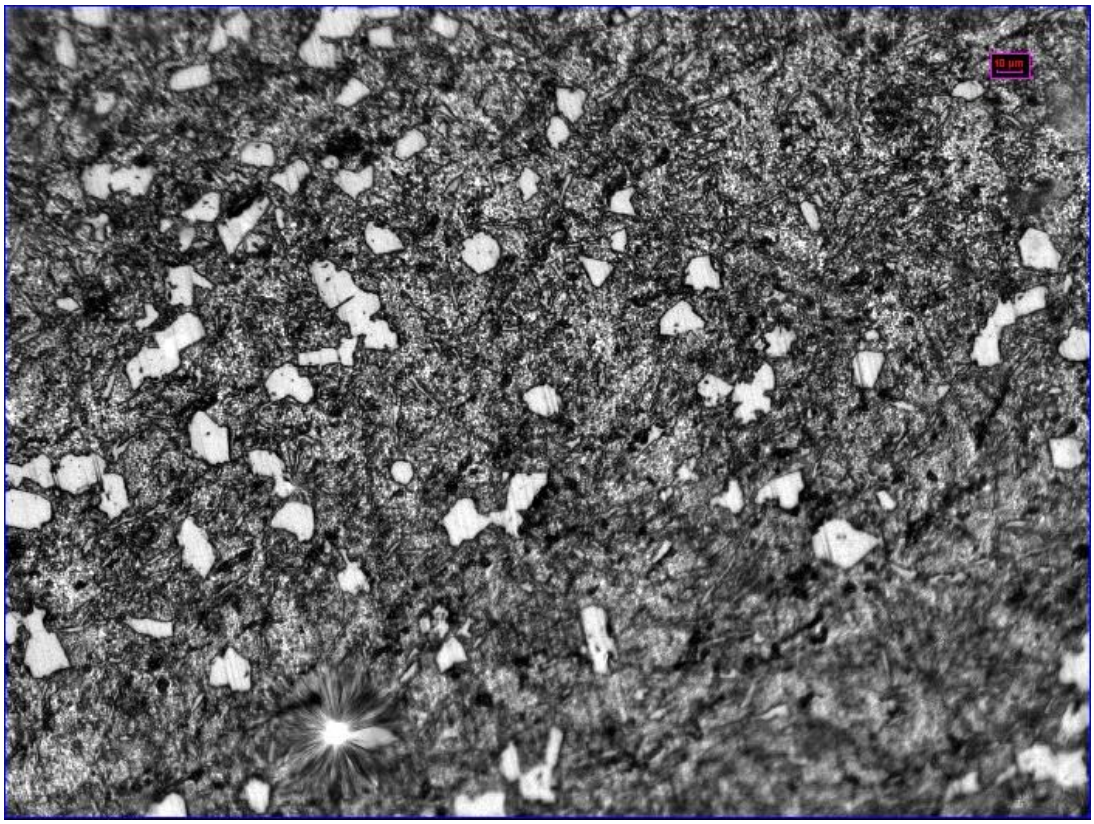

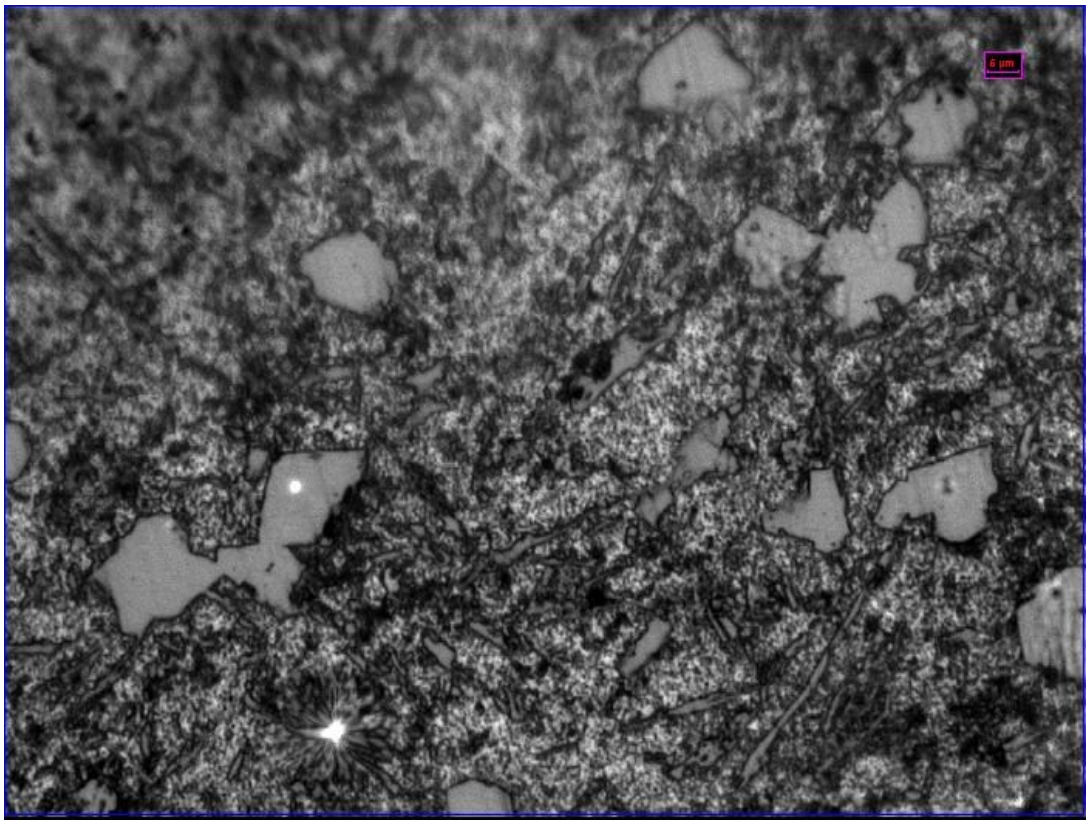

8.4 Microstructure of AlSi20 alloys with different refinement temperature.

8.4.1 Microstructure of AlSi20 alloys which was refined at 780 ^{0}C

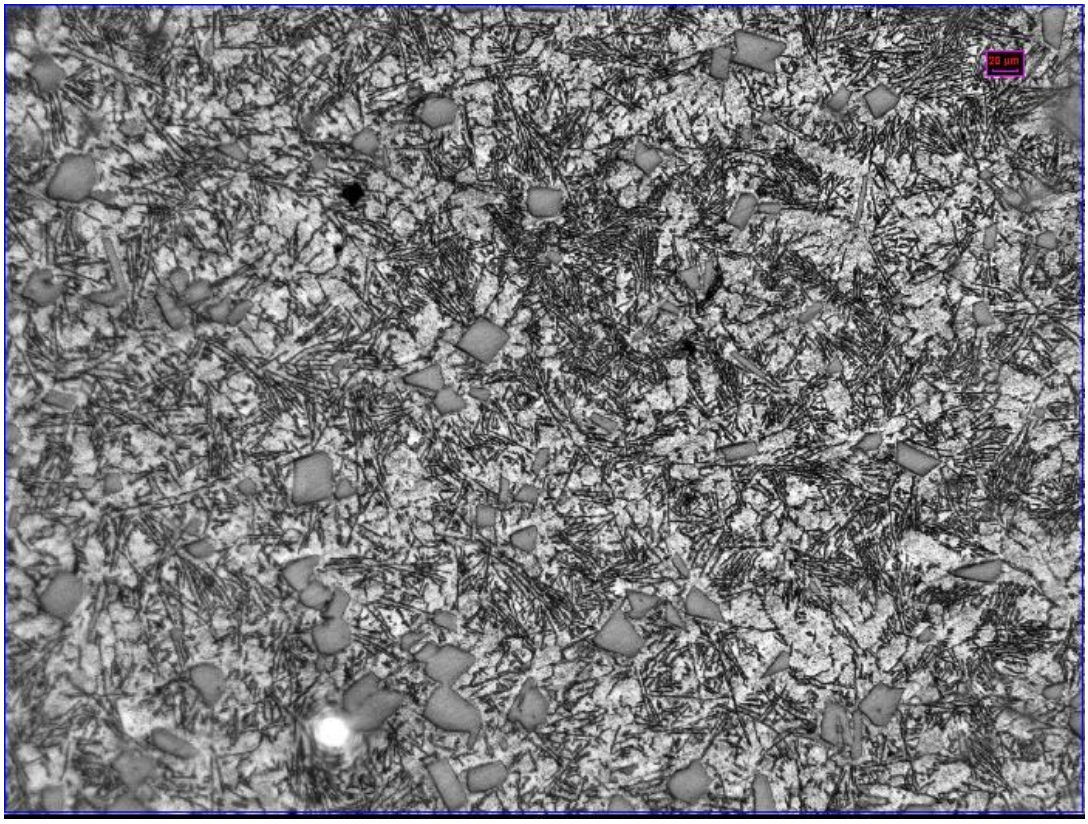

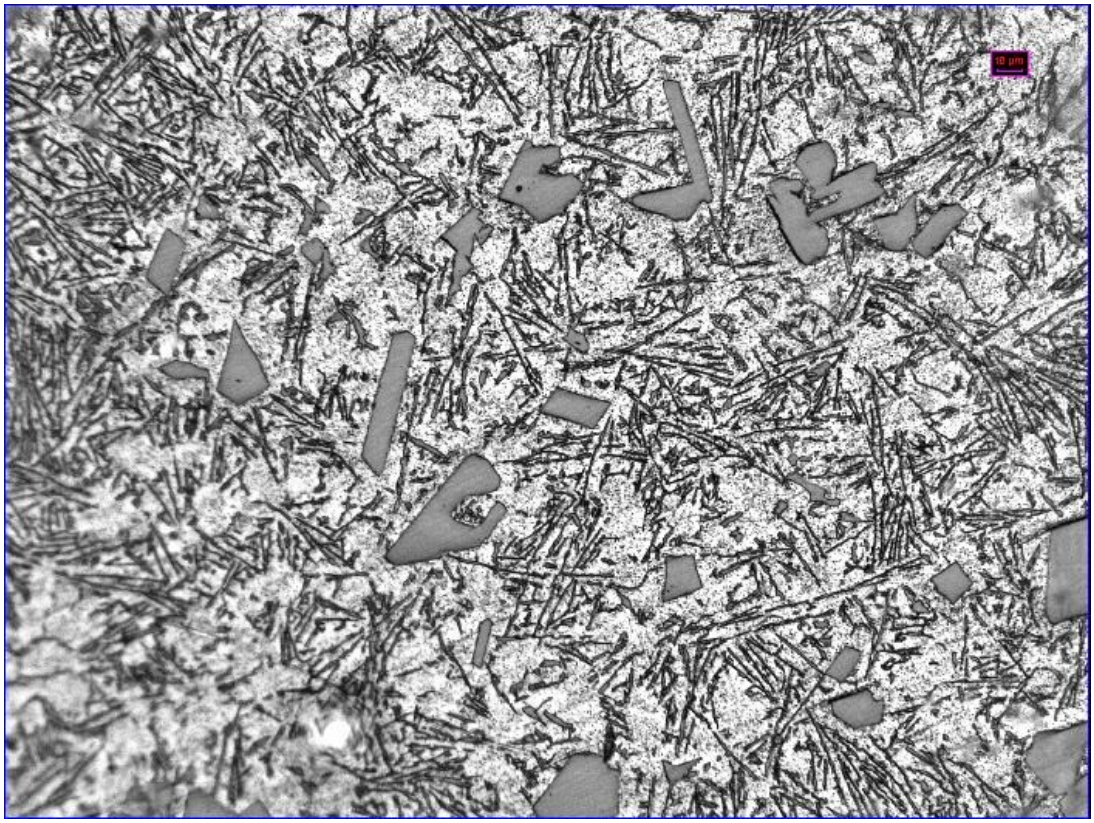
10 µm

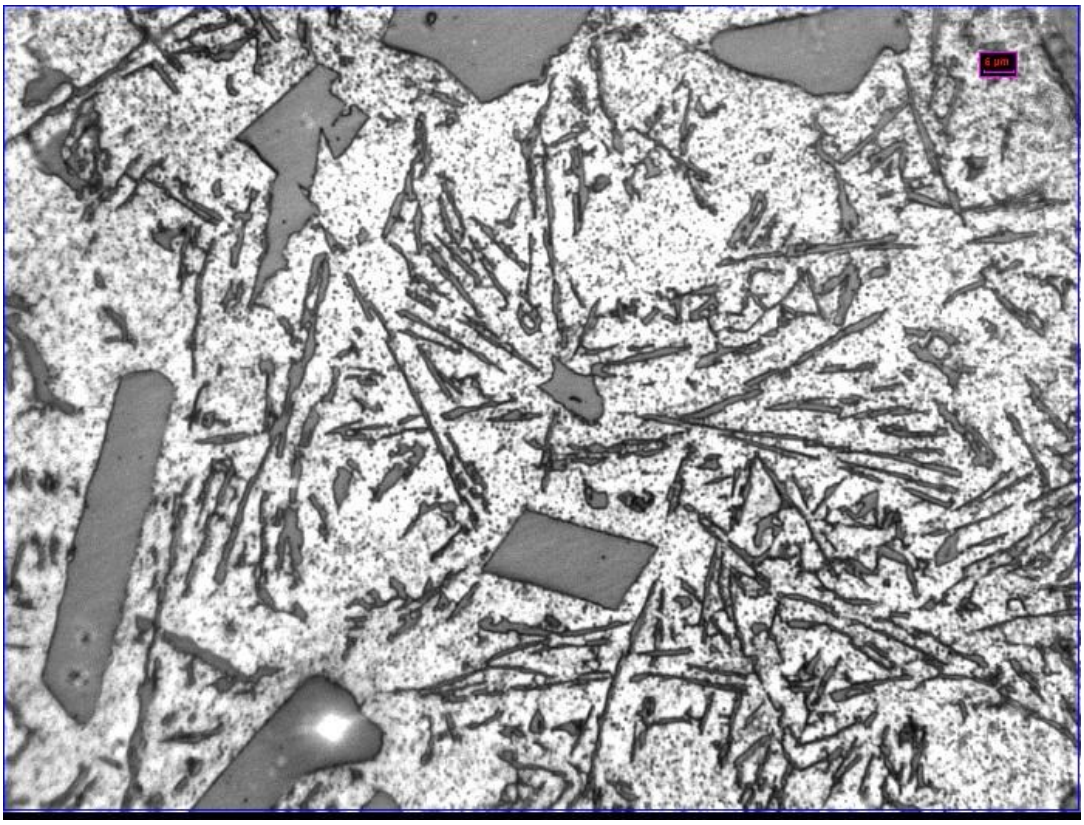
6 µm

8.4.2 Microstructure of AlSi20 alloys which was refined at 850 ^{0}C

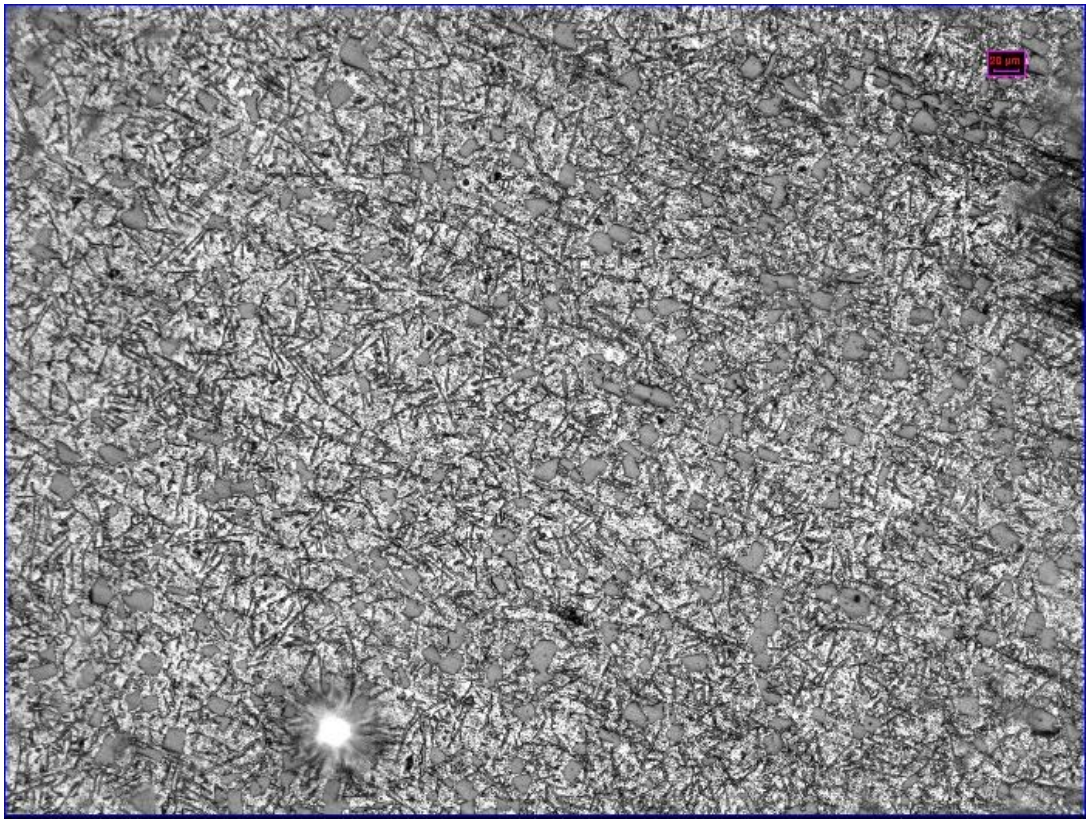

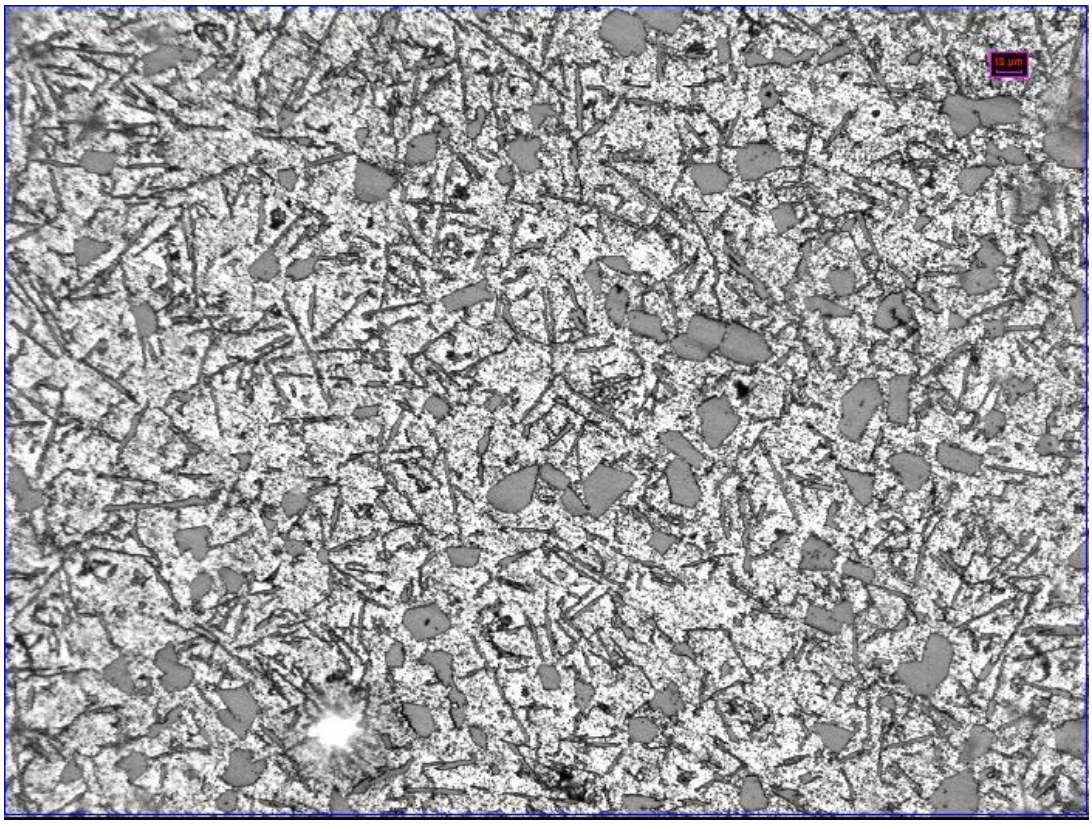

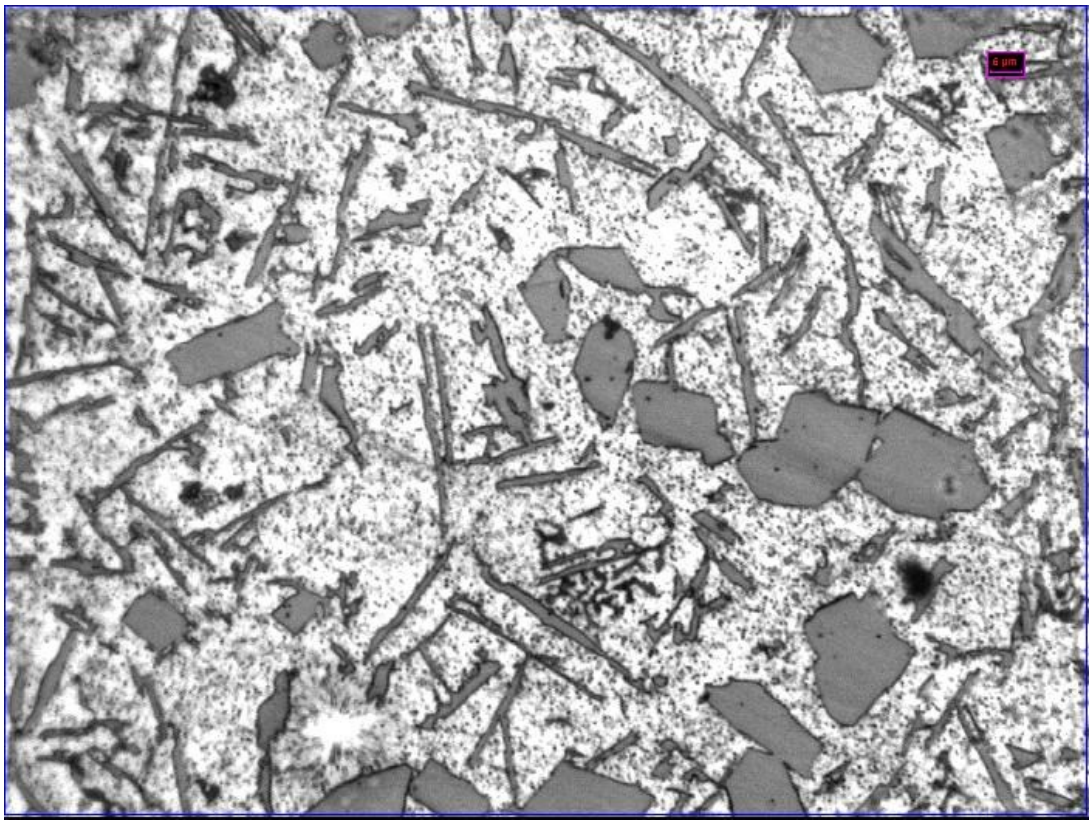

8.4.3 Microstructure of AlSi20 alloys which was refined at 950 ^{0}C

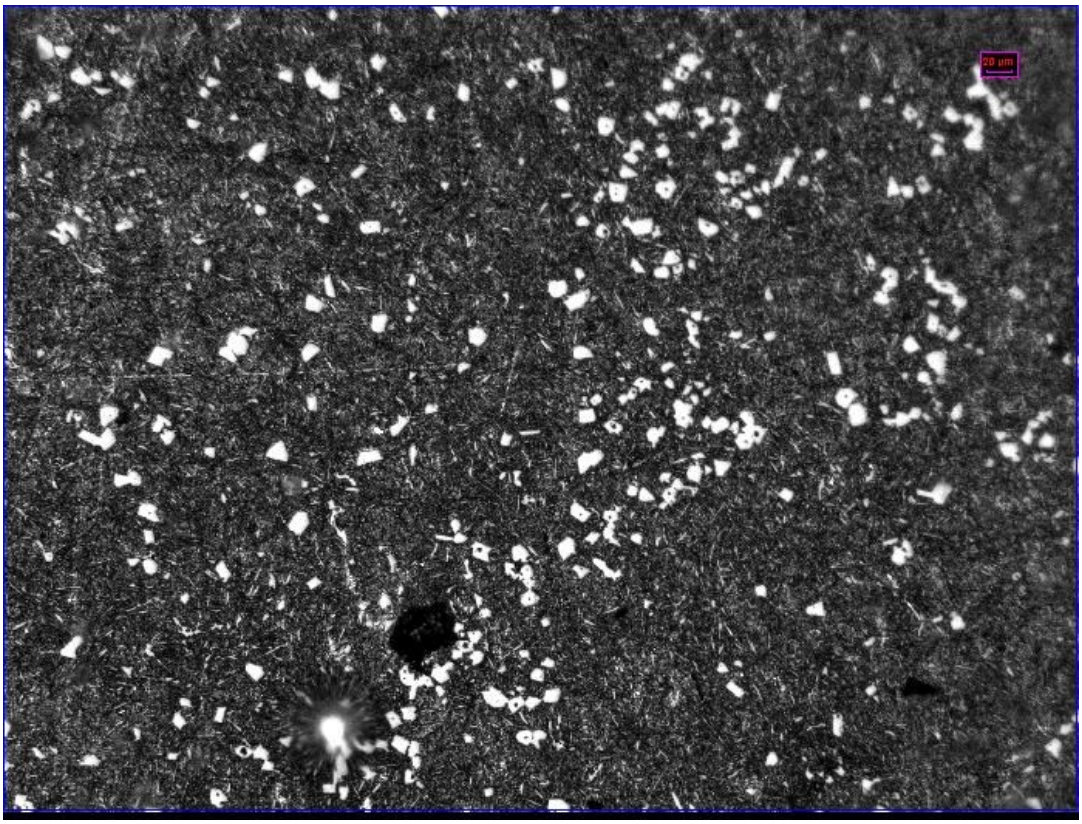

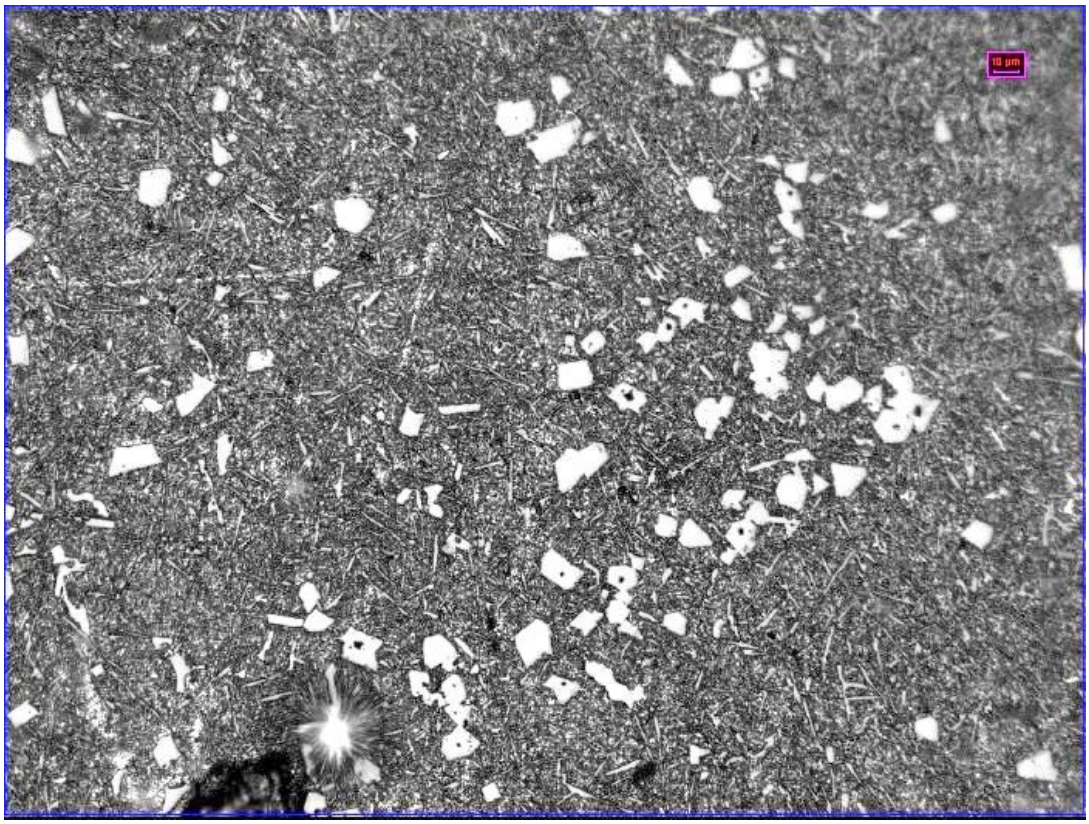
10 µm

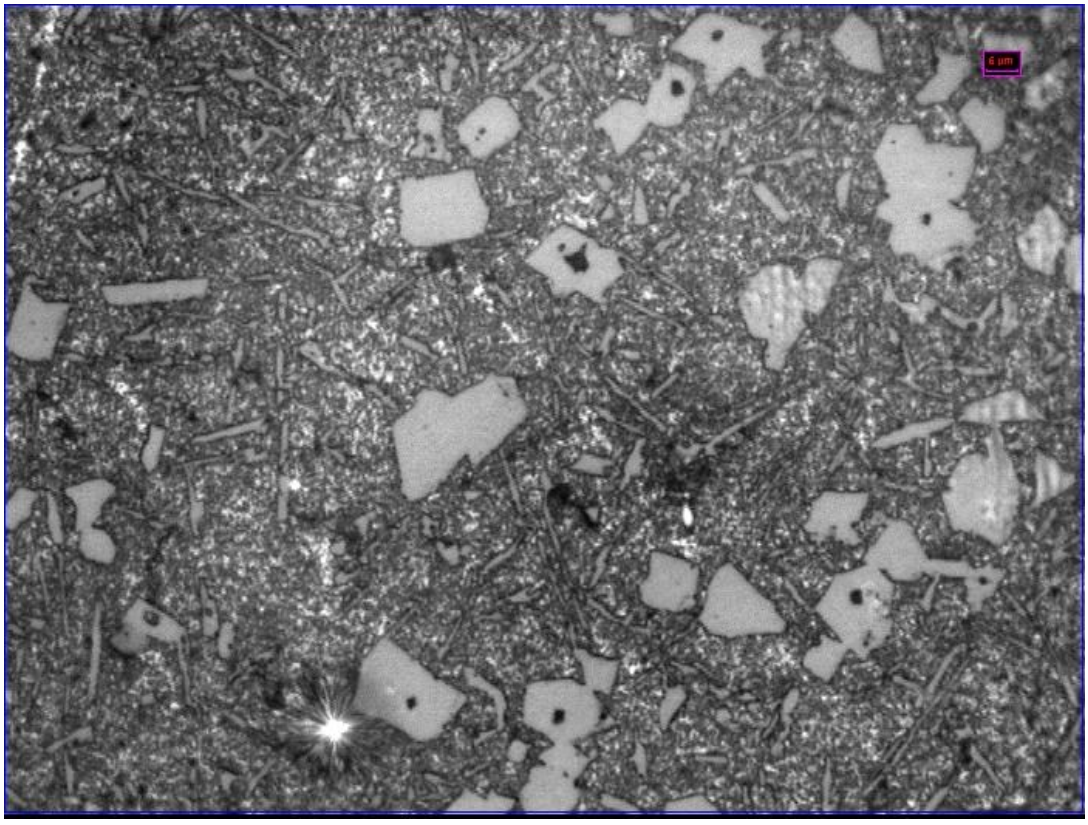
6 µm

8.5 Pictures of piston which was produced in present study.